OKLAHOMA TRANSPORTATION CENTER

ECONOMIC ENHANCEMENT THROUGH INFRASTRUCTURE STEWARDSHIP

EFFECT OF SUCTION HYSTERESIS ON RESILIENT MODULUS OF FINE-GRAINED COHESIONLESS SOIL

CHARBEL N. KHOURY,PH.D.
GERALD A. MILLER, PH.D.
YOUNANE N. ABOUSLEIMAN, PH.D.

OTCREOS7.1-27-F

Oklahoma Transportation Center
2601 Liberty Parkway, Suite 110
Midwest City, Oklahoma 73110

Phone: 405.732.6580
Fax: 405.732.6586
www.oktc.org

DISCLAIMER

The contents of this report reflect the views of the authors, who are responsible for the facts and accuracy of the information presented herein. This document is disseminated under the sponsorship of the Department of Transportation University Transportation Centers Program, in the interest of information exchange. The U.S. Government assumes no liability for the contents or use thereof.

TECHNICAL REPORT DOCUMENTATION PAGE

1. REPORT NO.	2. GOVERNMENT ACCESSION NO.	3. RECIPIENTS CATALOG NO.
OTCREOS7.1-27-F		

4. TITLE AND SUBTITLE	5. REPORT DATE
Effect of Suction Hysteresis on Resilient Modulus of Fine-Grained Cohesionless Soil	July 31, 2010
	6. PERFORMING ORGANIZATION CODE
7. AUTHOR(S)	8. PERFORMING ORGANIZATION REPORT
Charbel N. Khoury, Gerald A. Miller, Younane N. Abousleiman	
9. PERFORMING ORGANIZATION NAME AND ADDRESS	**10. WORK UNIT NO.**
The University of Oklahoma School of Civil Engineering and Environmental Science 202 W. Boyd St., Rm. 334, Norman, OK 73072	**11. CONTRACT OR GRANT NO.** DTRT-06-G-0016
12. SPONSORING AGENCY NAME AND ADDRESS The Oklahoma Transportation Center (Fiscal) 201 ATRC Stillwater, OK 74078 (Technical) 2601 Liberty Parkway, Suite 110 Midwest City, OK 73110	**13. TYPE OF REPORT AND PERIOD COVERED** Final: August 2008 –July 2010
	14. SPONSORING AGENCY CODE

15. SUPPLEMENTARY NOTES
University Transportation Center

16. ABSTRACT

The mechanical behavior of subgrade soil is influenced by the seasonal variations in moisture content. To better understand this behavior, it is crucial to study the relationship between soil moisture content and matric suction known as the Soil Water Characteristic Curve (SWCC). This relationship is hysteretic, i.e., at a given suction the moisture content differs depending on the drying and wetting paths. Research described in this report represents the beginning effort to understand the relationship of the SWCC to resilient modulus of subgrades.

The behavior of the SWCC has been widely studied and various models have been developed to capture this hysteretic behavior, but limited experimental data are available under different applied stresses. The lack of SWCC experimental data is due to the long testing time required for unsaturated soils. A new procedure was developed to shorten equilibrium time and obtain SWCC data as fast as possible. This new approach was used and SWCC tests under different stress states on silty soil specimens under drying, wetting, secondary drying, and along scanning curves were performed. Results from this study helped improve and validate existing models briefly described in this report.

The primary focus of this study was the effect of hydraulic hysteresis on the resilient modulus (M_r) of a cohesionless silty soil. Suction-controlled M_r tests were performed on compacted samples along the primary drying and wetting, secondary drying and wetting paths. A relationship between resilient modulus (M_r) and matric suction identified as the resilient modulus characteristic curve (MRCC) was developed. MRCC results indicated that M_r increased with suction along the drying curve. On the other hand, results of tests along the primary wetting curve indicated higher M_r than along the primary drying and the secondary drying curves. A new model to predict the MRCC results during drying and wetting (i.e., hydraulic hysteresis) is proposed based on the SWCC hysteresis. The model predicted favorably the drying and then the wetting results using the SWCC at all stress levels.

17. KEY WORDS	18. DISTRIBUTION STATEMENT
Resilient Modulus, Suction, Hysteresis	No restrictions. This publication is available at www.oktc.org and from NTIS

19. SECURITY CLASSIF. (OF THIS REPORT)	20. SECURITY CLASSIF. (OF THIS PAGE)	21. NO. OF PAGES	22. PRICE
Unclassified	Unclassified	**100 + covers**	

ACKNOWLEDGEMENTS

The authors are grateful for the financial support of the Oklahoma Transportation Center and U.S. Department of Transportation University Research Centers Program. The authors thank Michael Schmitz of the School of Civil Engineering and Environmental Science for his work in fabricating the specialized equipment needed for this project. In addition, the authors are grateful to Dr. Naji Khoury of Temple University for his technical support and research guidance.

SI (METRIC) CONVERSION FACTORS

Approximate Conversions to SI Units

Symbol	When you know	Multiply by	To Find	Symbol
	LENGTH			
in	inches	25.40	millimeters	mm
ft	feet	0.3048	meters	m
yd	yards	0.9144	meters	m
mi	miles	1.609	kilometers	km
	AREA			
in^2	square inches	645.2	square millimeters	mm
ft^2	square feet	0.0929	square meters	m^2
yd^2	square yards	0.8361	square meters	m^2
ac	acres	0.4047	hectares	ha
mi^2	square miles	2.590	square kilometers	km^2
	VOLUME			
fl oz	fluid ounces	29.57	milliliters	mL
gal	gallons	3.785	liters	L
ft^3	cubic feet	0.0283	cubic meters	m^3
yd^3	cubic yards	0.7645	cubic meters	m^3
	MASS			
oz	ounces	28.35	grams	g
lb	pounds	0.4536	kilograms	kg
T	short tons (2000 lb)	0.907	megagrams	Mg
	TEMPERATURE (exact)			
°F	degrees Fahrenheit	(°F-32)/1.8	degrees Celsius	°C
	FORCE and PRESSURE or STRESS			
lbf	poundforce	4.448	Newtons	N
lbf/in^2	poundforce per square inch	6.895	kilopascals	kPa

Approximate Conversions from SI Units

Symbol	When you know	Multiply by	To Find	Symbol
	LENGTH			
mm	millimeters	0.0394	inches	in
m	meters	3.281	feet	ft
m	meters	1.094	yards	yd
km	kilometers	0.6214	miles	mi
	AREA			
mm^2	square millimeters	0.00155	square inches	in^2
m^2	square meters	10.764	square feet	ft^2
m^2	square meters	1.196	square yards	yd^2
ha	hectares	2.471	acres	ac
km^2	square kilometers	0.3861	square miles	mi^2
	VOLUME			
mL	milliliters	0.0338	fluid ounces	fl oz
L	liters	0.2642	gallons	gal
m^3	cubic meters	35.315	cubic feet	ft^3
m^3	cubic meters	1.308	cubic yards	yd^3
	MASS			
g	grams	0.0353	ounces	oz
kg	kilograms	2.205	pounds	lb
Mg	megagrams	1.1023	short tons (2000 lb)	T
	TEMPERATURE (exact)			
°C	degrees Celsius	9/5+32	degrees Fahrenheit	°F
	FORCE and PRESSURE or STRESS			
N	Newtons	0.2248	poundforce	lbf
kPa	kilopascals	0.1450	poundforce per square inch	lbf/in^2

EFFECT OF SUCTION HYSTERESIS ON RESILIENT MODULUS OF FINE-GRAINED COHESIONLESS SOIL

FINAL REPORT

July 2010

Charbel Khoury and Gerald A. Miller, Ph.D., P.E.
School of Civil Engineering and Environmental Science
Younane N. Abousleiman, Ph.D.
Poromechanics Institute
of
University of Oklahoma
202 West Boyd Street, Room 334
Norman, OK 73019

Oklahoma Transportation Center
Project Number OTCREOS7.1-27
The Oklahoma Transportation Center
201 ARRC
Stillwater, OK 74078

TABLE OF CONTENTS

LIST OF FIGURES

LIST OF TABLES

EXECUTIVE SUMMARY

Unsaturated soils are commonly widespread around the world, especially at shallow depths from the surface as in the case of pavement subgrades. The mechanical behavior of subgrade soil is influenced by the seasonal variations and climatic changes such as rainfall or drought, which in turn may have a detrimental effect on overlying pavement structures. Thus, in order to better understand this behavior, it is crucial to study the complex relationship between soil moisture content and matric suction (a stress state variable defined as pore air pressure minus pore water pressure) known as the Soil Water Characteristic Curve (SWCC). This relationship is hysteretic, i.e., at a given suction the moisture content differs depending on the drying and wetting paths. This hysteretic behavior is also referred to as hydraulic hysteresis. The research described in this report represents the beginning effort to understand the relationship of the SWCC to resilient modulus of subgrades. The natural starting point for this work was to begin with a cohesionless fine-grained soil, which is the focus herein. This important work sets the stage to for continued research on cohesive fine-grained soils, for which the experimental challenges are monumental.

The behavior of the SWCC has been widely studied and various models have been developed to capture this hysteretic behavior, but limited experimental data are available under different applied stresses (or at different void ratios) and do not include secondary drainage or scanning curves (wet-dry cycles). The lack of SWCC experimental data is due to the long testing time required for unsaturated soils. To this end, a new procedure was developed to shorten equilibrium time and obtain SWCC data as practically fast as possible. This new approach was used and SWCC tests under different stress states on silty soil specimens under drying, wetting, secondary drying, and along scanning curves were performed. Results from

this study helped improve and validate existing models such as the elastoplastic constitutive models briefly described in this report.

The study described in this report also explored the effect of hydraulic hysteresis on the resilient modulus (M_r) of a cohesionless silty soil. To this end, suction-controlled M_r tests were performed on compacted samples along the primary drying, wetting, secondary drying and wetting paths. Two test types were performed to check the effect of cyclic deviatoric stress loading history on the results. First, M_r tests were performed on the same sample (stage-loaded sample) at each suction (i.e. 25, 50, 75, 100 kPa) value along all the SWCC paths (drying, wetting etc.). A relationship between resilient modulus (M_r) and matric suction was obtained and identified as the resilient modulus characteristic curve (MRCC). MRCC results indicated that M_r increased with suction along the drying curve. On the other hand, results of tests along the primary wetting curve indicated higher M_r than along the primary drying and the secondary drying curves. The second type of test was performed at selected suctions on samples without previous M_r testing (virgin sample). Results indicated that M_r values from virgin samples compared favorably with stage-loaded samples, which suggests that the cyclic deviatoric stress loading history influence was not as significant as the hydraulic hysteresis (i.e. cyclic suction stress loading). A new model to predict the MRCC results during drying and wetting (i.e., hydraulic hysteresis) is proposed based on the SWCC hysteresis. The model predicted favorably the drying and then the wetting results using the SWCC at all stress levels.

1. INTRODUCTION

1.1 Problem

It is well recognized that the economic vitality and development of a State is directly linked to the quality of the infrastructure and transportation system (AASHTO 2007, OTC 2007). The pavement design guide (AASHTO 2007) reported that highways have contributed extensively to the economic growth of the nation. However, this economic growth requires significant investment to build and maintain the highway infrastructure. For example, the cost for rehabilitating and maintaining these pavements in Oklahoma has exceeded $50 million per year, as indicated by ASCE (2007). Therefore, there is great incentive to undertake measures that increase pavement performance and decelerate the increase in expenditures on new pavement construction, maintenance and rehabilitation. This is a primary focus of the new AASHTO Mechanistic-Empirical Pavement Design Guide (MEPDG) and the driving motivation for the work described herein. According to DOTs and highway agencies, improvements in pavement design and material properties can have tremendous influence on reducing the cost of constructing and maintaining pavements. To this end, AASHTO has been trying to provide the highway community with an improved practical tool for the design of new and rehabilitated pavement structures; that is the Mechanistic-Empirical Pavement Design Guide (MEPDG).

One important aspect of pavement design that has appropriately received greater attention in the MEPDG, compared to its design predecessors, is the influence of subgrade moisture content on pavement performance. In a pavement structure, changes in moisture content can significantly influence the subgrade layer and hence, its carrying capacity (AASHTO 2007). For this reason the new MEPDG includes provisions to predict the variation of resilient modulus of pavement subgrades with

moisture changes due to seasonal variations. While this is a very important step towards better pavement performance, there is still much research to be done to fully understand the role of moisture content changes in subgrade behavior and pavement performance. Improving this understanding, and ultimately our ability to design better pavements, is the focus of the preliminary worked described in this report.

1.2 Purpose

As pavement subgrade soils are unsaturated mostly all the time, their mechanical behavior is largely dictated by the matric suction (e.g. capillary pressure) in the soil. Matric suction is recognized as an important stress state variable for unsaturated soils and is known to increase with decreasing water content and decrease with increasing water content. This phenomenon is in part responsible for subgrade weakening that occurs with increasing moisture content. The new MEPDG recognizes that to properly design a pavement, the correct moisture condition, and hence matric suction, must be selected for design. However, what is not well understood is the importance of wetting and drying cycles on the subgrade performance. It is fairly well established that the relationship of moisture content to matric suction is not unique; this relationship exhibits hysteresis and depends on whether the soil is being dried or wetted. Since the suction is an important stress state variable that controls unsaturated soil behavior it is important that engineers understand this behavior in order to properly design efficient pavement structures. Currently, there is a dearth of experimental information on which to build and validate new and existing theories being developed to address this problem. This is largely because unsaturated soil testing is very time consuming and requires considerable skill to perform properly. The purpose of work described in this report is to begin the process of filling this knowledge void through a laboratory study conducted in the University of Oklahoma Unsaturated Soil Mechanics Laboratory. The research

addresses a topic of critical importance to pavement subgrade performance and has resulted in an improved analytical model (e.g. enhanced version of the model recommended by the new MEPDG) to address this vital aspect of soil behavior in the design process. While this model is still in its infancy, it provides a foundation for building a systematic approach to address cyclic drying and wetting effects on resilient modulus.

1.3 Scope and Objectives

The emphasis of this study is the influence of matric suction hysteresis on resilient modulus (Mr) of subgrade soil. Resilient modulus, one of the important parameters used in pavement design, is sensitive to the state of stress within the subgrade layer. Pavement subgrades are unsaturated nearly all of the time and experience cyclic variations in moisture content due to temporal climate changes. These moisture content variations cause changes in matric suction leading to changes in the mechanical behavior of the soil. The matric suction, however, is not uniquely dependent on the moisture content and will be different for different moisture contents depending on whether the soil is being dried or wetted. That is, the relationship between moisture content and matric suction is hysteretic. Since the mechanical properties of fine-grained soils are strongly dependent on the matric suction it is crucial to understand the influence of suction and its hysteretic behavior on Mr. There is currently movement among transportation agencies in the U.S. and in Oklahoma towards the use of the new AASHTO Mechanistic-Empirical Pavement Design Guide (MEPDG) including provisions to address the influence of variations in moisture content (and matric suction) in the unsaturated pavement subgrade. To this end, this preliminary one-year study was conducted to assess the effect of soil suction hysteresis on the resilient modulus of a subgrade soil. Results were used to enhance the model recommended by the new MEPDG that intends to predict the variation of resilient modulus with seasonal changes in

moisture content. Findings from the proposed study also add useful information to the database of resilient modulus changes with matric suction of soil, which will help pavement engineers to design new long-lasting pavements at higher design levels, i.e., Level 1 and 2, as recommended by the new design guide. In this study, advanced testing of Mr under suction control was performed.

The core objective of the proposed study is to evaluate the effect of drying and wetting (hysteresis including primary drying and wetting, and secondary drying and wetting) on the resilient modulus of one cohesionless fine-grained soil. This was achieved through the following:

- Excessively long periods have been necessary to produce experimental data for unsaturated soils, particularly if wetting and drying cycles were involved. Thus, for this study one soil that allowed more rapid testing and better control over soil properties was selected.
- Determined soil classification parameters, moisture-density relationships, and other relevant properties for the test soil, in accordance with ASTM standards.
- Studied and obtained the soil-water characteristic curve (SWCC) (i.e., moisture content vs. matric suction) behavior for the test soil. In addition, obtained a set of SWCC experimental results for the test soil with hysteretic behavior including primary drying and wetting, secondary drying and scanning curves, under different net normal stresses.
- Evaluated the hysteresis effect on Mr results under suction control for the test soil. The axis translation technique was used to apply target suction; Mr was tested at the same suction value, however, following a different path (drying/wetting curve).
- Developed a Mr Characteristic Curve (MRCC) Model, which is the relationship between resilient modulus and soil suction to illustrate the

effect of suction hysteresis on the results. The MRCC includes primary drying and wetting, secondary drying and scanning curves.

- Building on existing models, such as in the AASHTO MEPDG, developed an enhanced predictive model for capturing the influence of suction hysteresis on Mr.

2. BACKGROUND

2.1 Soil Water Characteristic Curve

The soil water characteristic curve (SWCC) is defined as the relationship between soil suction and water content (typically gravimetric or volumetric). This curve represents basic characteristics of unsaturated soils, from which many engineering properties (e.g. hydraulic conductivity, shear strength) have been determined. Thus, to fully understand unsaturated soil behavior, it is crucial to accurately obtain the SWCC of a given soil under different conditions. While major progress has been made to measure the SWCC, there are limited experimental data available on hysteretic behavior of the SWCC under different stress states. The lack of SWCC hysteresis results (i.e. beyond primary drying and wetting curves) is largely due to the enormous testing time requirements for unsaturated soils. In this study, a new approach was developed and used to evade this problem to some extent by using an artificial soil and reducing the sample height of the soil sample to shorten equilibrium time as much as possible. First, a series of tests was conducted to optimize the testing geometry while shortening the equilibrium time. Then, laboratory tests of SWCCs at different stresses and initial conditions (i.e. initially saturated and as compacted) under drying, wetting, secondary drying, and along scanning curves were performed on the silty soil. Some existing functional form models were used to fit experimental data; the fitting model parameters obtained are key parameters used to predict the shear strength of unsaturated soils and interfaces with suction.

In addition, the SWCC hysteresis results from this study were used to validate the elastoplastic constitutive model reported by Miller et al. (2008). The experimental approach and data obtained demonstrate the significant contribution to the forward progression of constitutive modeling (e.g. by using the results to validate existing models).

2.1.1 Matric Suction

Before discussing the importance and complexity of the SWCC, it is instructive to take a look at a simple physical explanation of matric suction. Matric suction is associated with air-water menisci, which develops due to capillary action of water in the unsaturated soil pores. The interaction between solid particles, air, and water results in a thin layer (i.e. contractile skin) at the air-water interface. Due to the difference in pressure between air and water (i.e. u_a-u_w, defined as matric suction) and the presence of surface tension, the contractile skin is curved and forms a meniscus, as shown in

Figure 2.1.

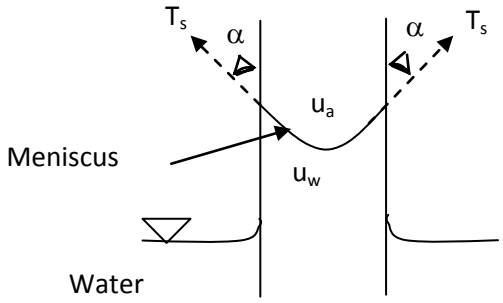

Figure 2.1- Illustration of a Capillary Tube Immersed in Water

As shown in

Figure 2.1, water rises in a capillary tube immersed in water, similarly to the air and water in pores of the soil, where the pressure difference across the meniscus results in the following relation:

$$(u_a - u_w) = 2T_s / R \qquad \textbf{(2.1)}$$

where, u_a = air pressure; u_w = water pressure; T_s = surface tension of water, R = r/cos α = radius of curvature of meniscus, r = radius of tube (similar to radius of pores in soil), and α = contact angle.

This phenomenon is analogous to water in soil pores where R is a function of pores shape and size. The smaller the pore radius, the higher the soil suction. This indicates that the SWCC relation differs from one soil to another. The smaller voids in clayey soils are one of the reasons for higher suction than in granular soils. As the soil de-saturates, the radius of curvature (R) of the meniscus reduces, and thus leads to an increase in matric suction. Similarly, water content increases when suction decreases.

2.1.2 Aspects of the Soil Water Characteristic Curve

A typical SWCC is shown in Figure 2.2, from which it is clear that this relationship is not unique even for the same soil; for a given suction value the moisture content varies depending on the drying and wetting paths (hysteresis behavior). The reasons for SWCC hysteresis have been investigated by many researchers (e.g. Bear, 1972, Adamson, 1990, Lu and Likos, 2004). Several factors contribute to the SWCC hysteresis such as a) contact angle variation during the wetting and drying process, b) non-uniformity of pore size in soil (Ink Bottle Effect), and c) entrapped air in soil. During wetting the contact angle (θ_1) is larger than the one (θ_2) during drying as shown in Figure 2.3. Contact angle (θ_1) is known as the advancing contact angle moving on a surface during wetting while θ_2 is the receding contact angle. The difference in the contact angle may contribute to the SWCC hysteresis where the suction, according to Equation (2.1), is higher during drying (lower contact angle θ_1) than wetting (larger contact angle) at a given water content. The ink bottle effect is explained by the non-uniformity of pore size in soils. Pores are usually larger than their openings, as shown in Figure 2.4 (Marshal et al. 1996). During wetting, which is an

upward capillary flow, the capillary rise is controlled by the pore opening size. However, during drying, which is the case where the capillary tube is initially filled with water, the capillary rise is beyond the larger pore radius. The capillary rise represents suction and is related to pore radius as presented by Equation (2.1). On this basis, at a given suction (capillary rise) the water content during drying exceeds that of the wetting as seen in Figure 2.3 and Figure 2.4.

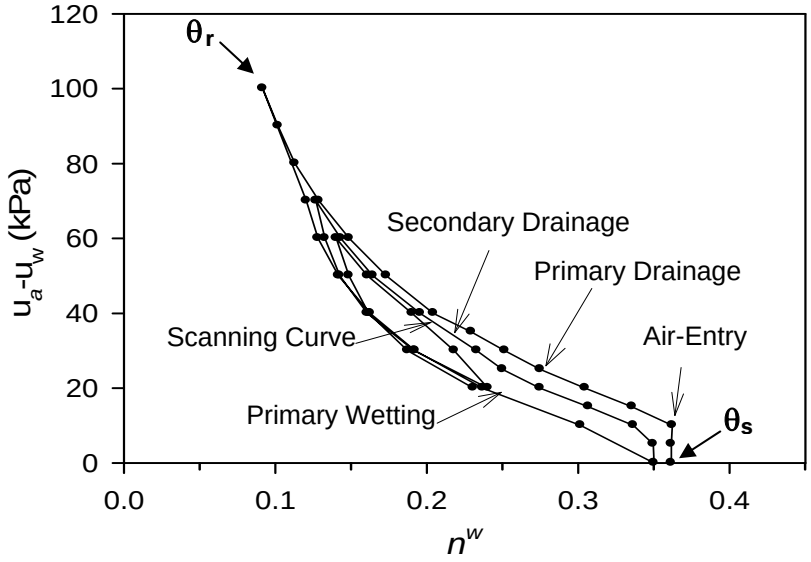

Figure 2.2- Typical Soil Water Characteristic Curve

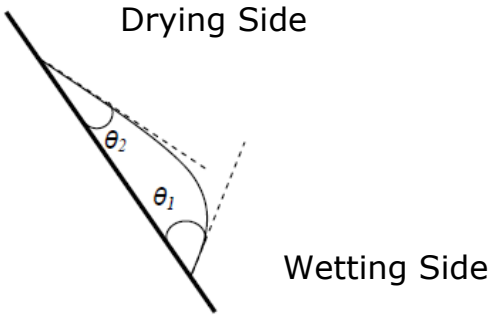

Figure 2.3- Illustration of Contact Angle for Advancing (θ_1, wetting) and Receding (θ_2, drying) Meniscus

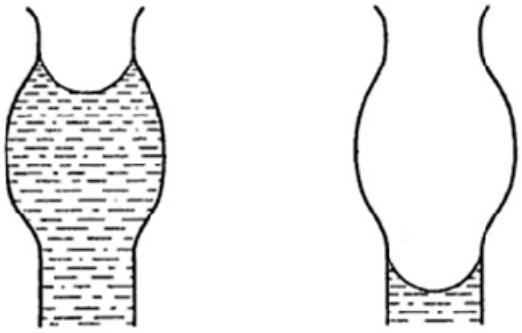

Figure 2.4- Illustration of Pore Non-Uniformity Effect on SWCC Hysteresis (After Marshal et al. 1996)

The different paths on the SWCC (Figure 2.2) are defined as the primary drying, primary wetting, secondary drying, secondary wetting curves, and the scanning curves, which are the curves that initiate inside the primary wetting and the secondary drying curves. Another important parameter shown in Figure 2.2 is the air entry value which is defined as the pressure (i.e. suction) after which air starts to fully penetrate into the pores of the soil during initial drainage.

The SWCC has been extensively studied (e.g. Fredlund and Xing 1994, Barbour 1998, Leong and Rahardjo 1997, Feng and Fredlund 1999, Vanapalli et al. 2001) and has been used as a basic function to predict, for example, the shear strength, and hydraulic conductivity of unsaturated soils (Fredlund et al. 1994, Vanapalli et al. 1996, 1999). But since the SWCC is hysteretic, recent studies have been conducted to capture such behavior and incorporate it into mathematical models (e.g. Wheeler et al. 2003, Gallipoli et al. 2003, Yang et al. 2004, Pham et al. 2005, Wei and Dewoolkar 2006, Li 2007a&b, Sun et al. 2007, Kohgo 2008, Muraleetharan et al. 2008, and Miller et al. 2008 among others). There are limited experimental data available on the hysteretic behavior of SWCCs under different externally applied stress or different void ratios (e.g. Romero et al. 1999, Karube and Kawai 2001, Tarantino and Tombolato 2005, Ho et al. 2006). Data from these studies reveal that samples were prepared at different initial void

ratios and thus, differences in behavior may originate from variations in fabric/structure caused during sample preparation and not variations in void ratio caused by externally applied stress. In addition, SWCC data typically include results of primary drying and wetting curves (i.e. no secondary drainage/wetting or scanning curves), which is largely due to the long time requirements for unsaturated soil testing (a problem that was reduced to an extent in this study as discussed in later sections). SWCC tests (following the primary drying/wetting, secondary drying and scanning curves) were thus obtained in this study for different stress histories (i.e. under different normal stresses) and were used to validate an existing model as shown by Miller et al. (2008).

2.2 Resilient Modulus

Resilient Modulus (M_r), a key parameter for the design of pavements, is influenced by different variables such as the dry density, moisture content, and stress states among others. Numerous research projects have been conducted to study the effect of those factors on M_r, but there is still much research needed to fully understand the role of moisture content changes (e.g. suction hysteresis) in subgrade behavior and pavement performance. Therefore, this study aimed at assessing the effect of soil suction hysteresis on the resilient modulus (M_r) of a subgrade soil. To this end, suction-controlled M_r tests along the drying and wetting (hysteresis) curves of the SWCC were performed on the same test soil used to study the SWCC. A relationship between resilient modulus and matric suction herein called the resilient modulus characteristic curve (MRCC) is presented. In addition, a new model related to the SWCC is proposed to predict the M_r results during drying and wetting (due to suction hysteresis).

2.2.1 Some Relevant Work on Resilient Modulus

Resilient modulus (M_r) of subgrade soil was introduced as an important parameter in the 1986 AASHTO Guide for Design of Pavements, and is treated as such in the revised 1993 and 2002 AASHTO Guides. Although AASHTO and DOTs have made major investments in resilient modulus studies over the past years, little research has been conducted to address the effect of suction hysteresis on resilient modulus of subgrade soils.

A number of studies have been undertaken previously to evaluate changes in moisture condition and soil suction with resilient modulus. For example, Khoury and Khoury (2009) and Khoury et al. (2009) studied the variation of moisture content on the behavior of M_r; results showed that the M_r-moisture content relationship exhibits a hysteretic behavior due to wetting and drying. Liang et al. (2007) proposed a new predictive equation for the resilient modulus of cohesive soils using the concept of soil suction. Yang et al. (2008) conducted suction controlled M_r tests using the axis translation technique on clayey soils. Their study indicates that M_r increases with an increase in suction. Kung et al. (2006) studied the variations of M_r and plastic strains with the post-construction moisture content and soil suction for cohesive subgrade soils. Results indicated that M_r increased with increasing suction and decreased with increasing deviator stress, while plastic strains decreased with increase in suction. Yang et al. (2005) also used the filter paper technique to study the effect of matric and total suction on M_r. In their study, matric suction was the key parameter for predicting the mechanical behavior of subgrade soil. Yuan and Nazarian (2003) investigated the effect of wetting and drying on the seismic modulus of compacted base and subgrade specimens. Ceratti et al. (2004) conducted both in-situ and laboratory tests to determine the effect of seasonal variation on subgrade resilient modulus of soils from southern Brazil. They reported that wetting after drying can lower the resilient modulus up to four times

compared to drying only. Khoury and Zaman (2004) used the filter paper technique to evaluate the variation of resilient modulus with post-compaction moisture content and suction for a selected clayey subgrade soil in Oklahoma and found that M_r-moisture content relationships exhibit a hysteretic behavior due to wetting and drying and that M_r and suction were influenced by the compacted moisture content. Drumm et al. (1997) examined the effect of post-compaction moisture variation on the resilient modulus of subgrade soils in Tennessee. Resilient modulus for all subgrade soils exhibited a decrease with increase in degree of saturation. The authors are not aware of any other significant studies that address the effect of suction hysteresis on the M_r of subgrade soil, especially with regard to primary drying and wetting, secondary drying and states on the scanning curves. The aforementioned studies have used the filter paper method to study the effect of suction on M_r, except Yang et al. (2008). In their study Yang et al. (2008) controlled the pore air (u_a) and pore water (u_w) pressures during testing. However, the limitations associated with the low hydraulic conductivity (e.g. unsaturated fine-grained soils) leads to very long equilibrium times associated with suction changes during testing.

2.2.2 Relevant Resilient Modulus Models

The generalized universal model adopted by the mechanistic-empirical pavement design guide (MEPDG) M_r-Stress Model is presented below:

$$M_r = k_1 p_a \times \frac{\theta}{p_a}^{k_2} \times (\frac{\tau}{p_a} + 1)^{k_3} \qquad \textbf{(2.2)}$$

In this model, the resilient modulus (M_r) is expressed as a function of, θ = bulk stress = $\sigma_1+\sigma_2+\sigma_3$ where σ_1, σ_2, and σ_3 are the three principal stresses, and τ = octahedral stress = $(\sqrt{2}/3)$ $(\sigma_1-\sigma_3)$. The coefficients k_1, k_2, and k_3 are model regression parameters. This model does not take into consideration the variation of moisture content effect. In an attempt to study

the effect of seasonal variation in moisture content in pavement design, AASHTO (2007) presented a new MEPDG model. The MEPDG incorporates the enhanced integrated climatic model using the resilient modulus for the optimum moisture content (Larson and Dempsey 1997). The current model predicts the change of modulus due to a change in degree of saturation of the soils as follows:

$$Log\left(\frac{M_r}{M_{ropt}}\right) = a + \left(\frac{b-a}{1+\exp\left(\ln\frac{-b}{a} + k_m \times \left(S - S_{opt}\right)\right)}\right) \qquad \textbf{(2.3)}$$

where: $M_r/M_{r\text{opt}}$ = resilient modulus ratio, M_r = resilient modulus at a given degree of saturation, $M_{r\text{opt}}$ = resilient modulus at a reference condition, a = minimum of $\log(M_r/M_{r\text{opt}})$, b = maximum of $\log(M_r/M_{r\text{opt}})$, k_m = regression parameter, and $(S-S_{\text{opt}})$ = variation in degree of saturation.

However, the MEPDG equation does not combine the effects of state of stress and water content (Liang et al. 2007). Various relationships between soil suction and resilient modulus (M_r) were presented by Edris and Lytton (1976), Khoury et al. (2003), and Khoury and Zaman (2004) among others. Yang et al. 2005 (TRB), presented a model based on the effective stress concept; their study reflects the effects of seasonal variation of moisture content on the resilient modulus of subgrade soils in a deviator stress-matric suction model. Kung et al. (2006) also presented a model including the effect of moisture content variations on M_r; the model is the same as presented by Yang et al. 2005, which is based on the effective stress concept of unsaturated soil. The latter model explicitly includes the effect of stress and suction. In this model, the regression parameters must be calibrated at each water content in order to predict resilient modulus.

Yang et al. (2005) used the effective stress approach (Bishop 1959) and explicitly incorporated the effect of externally applied stress and matric suction in a prediction model for M_r, as shown below:

$$M_r = k_1\left(\sigma_d + \chi_m \psi_m\right)^{K_2} \quad \textbf{(2.4)}$$

where: χ_m = Bishop's parameter, k_1 and k_2 are model regression parameters

Liang et al. (2007), proposed the following model for predicting the effect of moisture variations on M_r, using the effective stress (Bishop 1959) concept and assuming the pore air pressure equal to zero (u_a=0):

$$M_r = K_1 \times P_a \times \left(\frac{\theta + \chi_w \cdot \psi_m}{P_a}\right)^{K_2} \left(\frac{\tau_{oct}}{P_a} + 1\right)^{K_3} \quad \textbf{(2.5)}$$

where: θ = bulk stress = $\sigma_1+\sigma_2+\sigma_3$; σ_1, σ_2, and σ_3 are the three principal stresses, τ_{oct} = octahedral shear stress; τ_{oct} = ($\sqrt{2}/3$) ($\sigma_1-\sigma_3$), Ψ_m = matric suction; X_w = Bishop's parameter, P_a= atmospheric pressure, and k_1, k_2, k_3 = regression constants.

Recently Gupta et al. (2007) proposed a new analytical model presented in the following equation:

$$M_r = k_1 p_a \times \left(\frac{\theta - 3k_6}{P_a}\right)^{k_2} \times \left(\frac{\tau}{P_a} + k_7\right)^{k_3} + \alpha_1 \times (u_a - u_w)^{\beta_1} \quad \textbf{(2.6)}$$

where: k_1, k_2, k_3, k_6, k_7, α_1, β_1 are regression parameters and u_a-u_w is the soil matric suction. Gupta et al. (2007) reported that such a model is simple and does not require measurements of both water content and suction to estimate the resilient modulus.

Cary and Zapata (2010) proposed a regression model by incorporating suction as a fundamental variable within the stress state for unsaturated soils, as follows:

$$M_r = k_1^{'} p_a \times \left(\frac{\theta_{net} - 3\Delta u_{w-sat}}{P_a}\right)^{k_2^{'}} \left(\frac{\tau_{oct}}{P_a} + 1\right)^{k_3^{'}} \left(\frac{\left(\psi_{m_0} - \Delta\psi_m\right)}{P_a} + 1\right)^{k_4^{'}} \quad \textbf{(2.7)}$$

where: $\theta_{net} = \theta - 3u_a$ = net bulk stress, Δu_{w-sat} = build up of pore water pressure under saturated conditions, in this case $\Delta\psi_m = 0$, τ_{oct} = octahedral shear stress, ψ_{m_o} = initial matric suction, $\Delta\psi_m$ = relative change of matric

suction with respect to ψ_{m_o} due to build up of pore water pressure under unsaturated conditions, in this case $\Delta u_{w-sat} = 0$. Coefficients k'_1, k'_2, k'_3 and k'_4 are regression parameters.

While the Liang et al. 2007 model may be able to predict M_r due to moisture variations, it doesn't include the effect of suction hysteresis (drying/wetting) on M_r. The Gupta et al. (2007) model predicts M_r values only at a specific suction (as compacted). Also, Cary and Zapata (2010) model predicts M_r based on regression analysis due to changes in matric suction (drying only) without hysteresis. The work described herein provides information to better understand the influence of the suction hysteresis on M_r, and proposes a new model to predict the M_r due to hysteresis for a cohesionless fine-grained soil.

3. MATERIALS AND METHODS – SOIL WATER CHARACTERISTIC CURVE TESTSING

3.1 Soil Material and Sample Preparation

Excessively long periods have been necessary to produce experimental data for unsaturated soils, particularly if wetting and drying cycles (i.e., hysteresis) are involved. Thus, a manufactured soil that provides levels of matric suction consistent with a silty soil, but with considerably greater hydraulic conductivity ($6e^{-5}$ cm/sec) than most natural soils with similar suction ranges is used in this study in order to obtain experimental results in a reasonable amount of time.

The artificial soil used is a mixture of two commercially available manufactured soils, Sil-Co-Sil 250 (SCS), with nominal particle size range of 0.002 to 0.212 mm, manufactured by U.S. Silica Company and Glass Beads, Size BT-9 (nominal particle size range = 0.127 to 0.178 mm), manufactured by Zero Products. The soil mixture consists of 75% ground silica and 25% glass beads. The mixture has a grain size distribution (Figure 3.1) similar to

that of fine sandy silt having about 48% fine sand (0.075-0.25 mm), 46% silt (0.002-0.075 mm), and 6% clay size material ($\leq$0.002 mm). Based on standard compaction tests, the soil mixture has a maximum dry density (γ_d) of 103.6 pcf (16.3 kN/m^3) and optimum moisture content (OMC) of 16.5%.

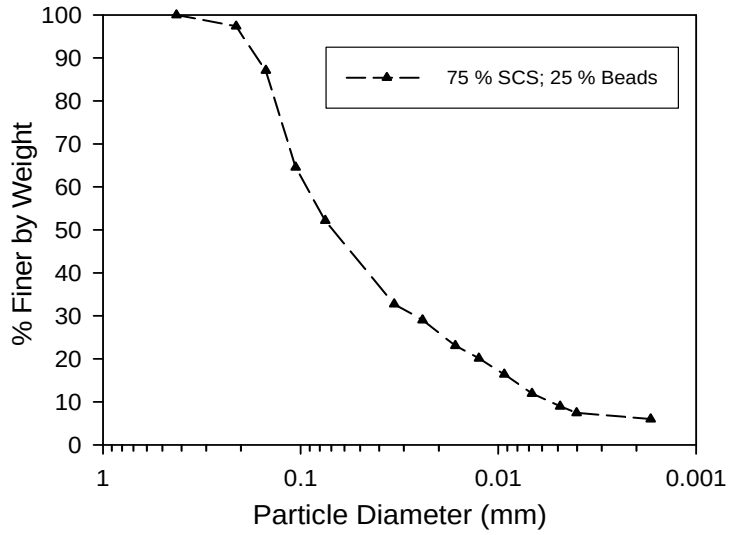

Figure 3.1- Grain size distribution of the soil mixture used in this study

The soil specimens prepared in this study, for all tests, are compacted to an initial dry density of 15.4 kN/m^3 and at a moisture content of 17.2 $\pm$ 1%. Soil is mixed to the desired moisture content and compacted to the required density by moist tamping (i.e. volume-based compaction) inside the test cell device.

3.2 SWCC Testing Device

A custom made test cell was designed and built at the University of Oklahoma to obtain different Soil Water Characteristic Curves (SWCCs). Schematic and photographic views of the test cell are shown in Figure 3.2. The pore-water and pore-air pressures are digitally controlled using two commercially available high precision motorized piston pumps, which can accurately control pressure and volume changes to a resolution on the order

of 1 kPa and 1 mm^3, respectively. The water is transmitted to the soil via a high air entry porous disc (HAEPD) having an air entry value of 3 bar.

The experimental apparatus allows for continuous control and measurement of the pore air pressure (u_a) and pore water pressure (u_w) throughout testing. Different cells were fabricated to obtain SWCCs with and without vertical net normal stress. One test cell was fabricated to fit into a one dimensional consolidation apparatus as shown in Figure3.2b and Figure 3.2c, so that incremental vertical loading can be externally applied while independently controlling u_a and u_w in the soil sample. A vertical normal stress is applied to the sample through a stainless steel piston acting against the rigid top platen above the sample and a linear variable differential transformer (LVDT) is used to measure the vertical deformation of the sample during the test. For the SWCC tests, the LVDT resolution was estimated at approximately 1.68×10^{-4} mm. The experimental apparatus allows for independent control/measurement of suction (i.e. difference between air pressure and water pressure) and vertical net normal stress throughout testing so that a variety of loading sequences can be investigated.

3.3 Experimental Test Methodologies

Soil Water Characteristic Curves (SWCCs) were experimentally determined using the device described previously in Section 3.2. Samples were prepared by moist tamping (i.e. volume-based compaction) the soil directly into the test cell on top of the pre-conditioned high air entry porous disc. The test cell was then placed in the oedometer frame and a seating load (5-35 kPa) was applied to assure a good contact between the top cap and the soil.

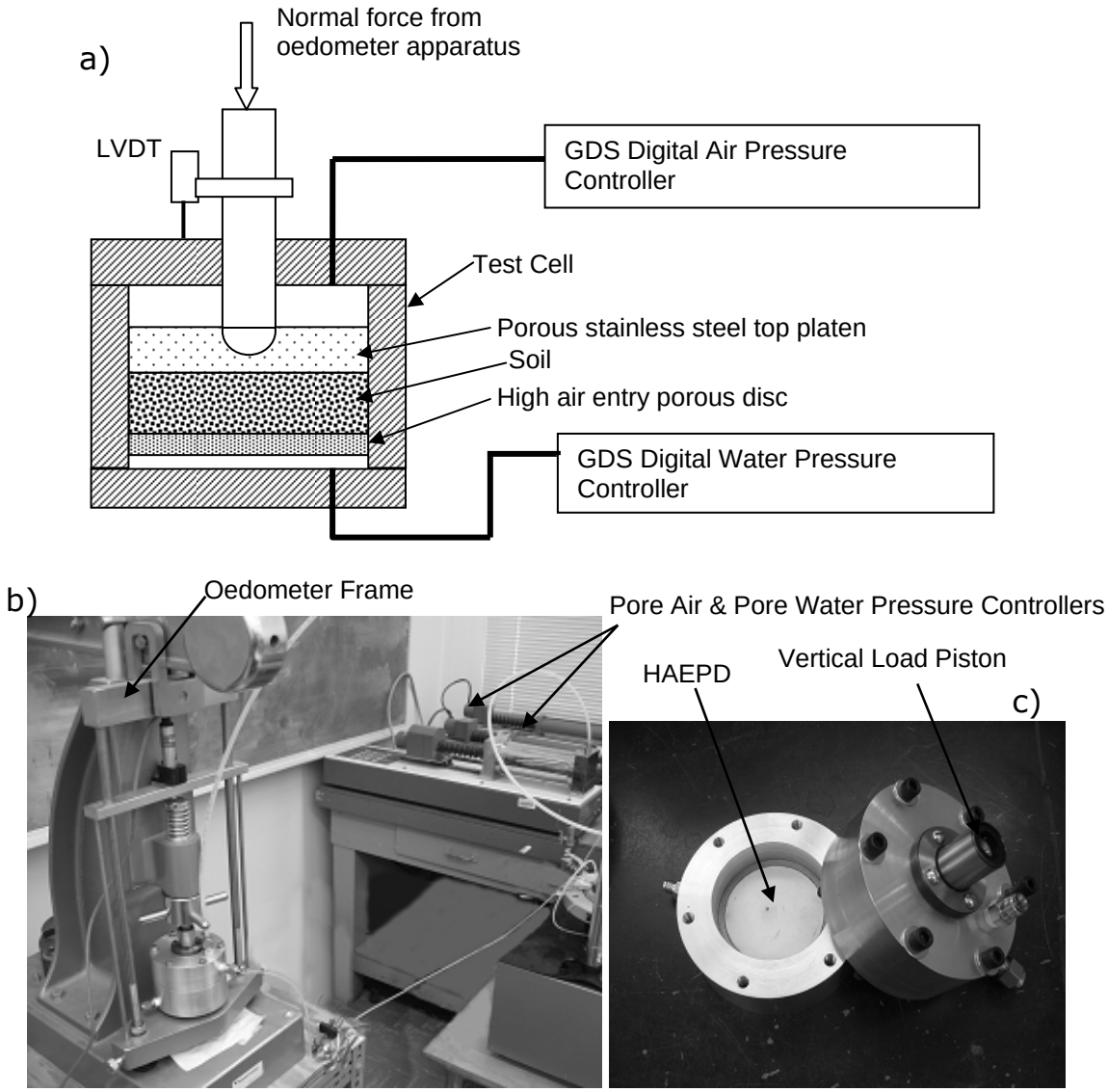

Figure 3.2- a) Schematic of the Test Cell Cross-section and Measurement System, b) Modified Oedometer Setup and c) Photo of Test Cell

Two different types of SWCC tests were performed in this study. The first involved complete saturation of the soil at the beginning of the SWCC test. This type of test was conducted by first filling the cell with water on top of the soil specimen. Water was then forced, under low pressure, through the sample by increasing the air pressure above the water in the cell. This process continues until a minimum of three pore volumes of water flow through the sample to remove the entrapped air in the soil pores. Following saturation, samples were loaded incrementally to the desired vertical normal stress, after which the drying (increase of suction by increasing u_a, air

pressure) and wetting cycles were initiated. The second type of test was performed on samples without saturation; in other words, samples were compacted into the cell (Figure 3.2c) at the target density of 15.4 kN/m^3 and moisture content of 17.2%. Samples were then loaded incrementally to the desired vertical normal stress, as described above, after which drying and wetting cycles for SWCCs were initiated without prior saturation. For this type of test, it is important to obtain the initial (as-compacted) suction value. To this end, a new testing procedure was developed and used. The sample was first compacted on top of the HAEPD in the test cell (Figure 3.2), while the tube connected to the water controller piston is closed with a valve. Then, air pressure (u_a) was applied on top of the sample while maintaining a zero water volume change ($\Delta V_w = 0$) by setting the precision pumps to volume control. After u_a application the water valve connected to the tube was then opened, and the test started by recording the change in pore water pressure (u_w) due to an increase in air pressure, while maintaining a zero water volume change. After reaching equilibrium (i.e. no more change in u_w), initial suction of the sample was thus estimated as the difference between the target u_a and measured u_w values.

Throughout SWCC testing, suction was controlled by using the axis translation method whereby the air pressure was increased while maintaining a constant water pressure of zero kPa or minimal pressure using the precision pumps described in Section 3.2. To maintain constant net normal stress during an increase in air pressure the axial normal force exerted by the oedometer was adjusted slightly to compensate for the air pressure acting on the portion of the axial load piston inside the air chamber.

As previously mentioned, time required for completing the SWCC test may be the main reason for the lack of reported hysteretic data; thus, reducing testing time will encourage more extensive testing to fully define

hysteretic behavior of the SWCC. This was precisely the motivation for an investigation to determine the minimum height of soil sample that could be used while practically achieving results similar to samples with heights more typical of one dimensional testing. The goal was to optimize the testing geometry while shortening the equilibrium time. To this end, a set of experimental results is presented and discussed in Section 5.1.

4. MATERIALS AND METHODS – RESILIENT MODULUS TESTING

4.1 Soil Material and Sample Preparation

The soil described previously for SWCC testing was used to conducted resilient modulus tests. As described, this soil was used because it allowed for more rapid equilibrium time at various levels of suction along the soil water characteristic curve prior to resilient modulus testing. That said, to complete drying and wetting and resilient modulus testing cycles on a single sample required several months.

The soil specimens prepared in this study, for all tests, were compacted to an initial target dry density of 15.4 kN/m^3 and at a target moisture content of 17.2 $\pm$ 1%. Soil was mixed to the desired moisture content and compacted in five layers to the required density by moist tamping (i.e. volume-based compaction) inside the sample preparation split mold.

4.2 Suction-Controlled Resilient Modulus Tests

Figure 4.1 shows an illustration of the suction control M_r test setup. In this study, M_r tests were performed in accordance with the AASHTO T 307-99 test method. M_r tests consisted of applying a cyclic haversine-shaped load with a duration of 0.1 seconds and rest period of 0.9 seconds. For each sequence, the applied load and the vertical displacement for the last five cycles were measured and used to determine M_r. The load was measured by using an internally mounted load cell with a capacity of 2.23 kN (500 lbf).

The vertical displacements were measured using two linear variable differential transformers (LVDTs) fixed to opposite sides and equidistant from the piston rod outside the test chamber (refer to

Figure 4.1). The LVDTs had a maximum stroke length of 5.0 mm (0.2 in). In this study, with a 16-bit data acquisition card, the LVDT resolution used for M_r tests was estimated at approximately $5.0/2^{16} = 7.63 \times 10^{-5}$ mm. The expected M_r displacement for unsaturated soil, in the range of suction (or moisture content) used in this study is generally between 1.4×10^{-2} mm to 3.5 mm. Therefore, the deviation or maximum relative error was approximately in the range of 0.002 to 0.6 %.

M_r tests were conducted on remolded specimens; while soil suction was controlled via an automated system to able to fix air and water pressure in the sample using the axis translation technique (Fredlund and Rahardjo 1993). The pore water pressure (u_w) was digitally controlled using a commercially available, high precision, motorized piston pump and transmitted to the bottom of the soil sample via a high air entry porous disc (HAEPD). A similar pump, having a larger piston volume, was used to control the air pressure (u_a) on top of the sample in order to achieve desired matric suction (u_a-u_w). These pumps can accurately resolve pressure and volume changes on the order of 1 kPa and $1mm^3$, respectively. Air pressure in the chamber (σ_3) above the confining fluid (water) was controlled using a regulator and monitored using a pressure gage with a resolution of about 0.7 kPa.

The procedure and loading patterns used to study the influence of suction hysteresis (i.e. drying, wetting and scanning curves) on Mr are illustrated schematically in Figure 4.2, and summarized as follows:

1. Water was first conditioned in the tubes and pumps. The HAEPD was then saturated by applying water pressure of about 14 kPa (2 psi)

underneath the disk. The water pressure was applied for about 48 hours during which de-aired water was flowing out of the HAEPD.

2. After HAEPD saturation, the compacted soil sample was mounted on top of the HAEPD; the sample was sealed by a membrane and the chamber filled with water. A minimal cell pressure of 14 kPa (2 psi) was applied to hold the sample together while the valves connecting to the pore water pressure were open.

3. The desired net confining stresses and matric suction were applied using the axis translation technique. For this study, pore water pressure (u_w) was held constant at 15 kPa, while increasing the air pressure (u_a) and cell pressure to reach the desired target suction values (25 kPa, 50 kPa, 75 kPa and 100 kPa) and net confining stresses (41 kPa, 28 kPa, and 14 kPa). Basically, the soil sample was dried out by increasing the suction on the drying path (i.e. primary drying) starting from a compacted suction value of approximately 8 kPa.

4. After reaching equilibrium of suction (e.g. 25 kPa), an M_r test was conducted at the three net confining stresses (41 kPa, 28 kPa, and 14 kPa). Equilibrium of suction was assumed when changes in water content became negligible.

5. After the M_r test, suction was increased following the drying path (e.g. suction of 50 kPa, 75 kPa and 100 kPa). At the end of the drying curve, the soil sample was wetted (primary wetting) by decreasing u_a to reach target suctions similar to that of the drying paths. The sample was tested for M_r at each suction value (e.g. 25, 50, 75, and 100 kPa) on the way up (drying) and down (wetting) the SWCC.

6. Step 5 was repeated again so that the secondary drying/wetting and scanning curves were developed, resulting in a relationship between resilient modulus and matric suction called herein the resilient modulus characteristic curve (MRCC).

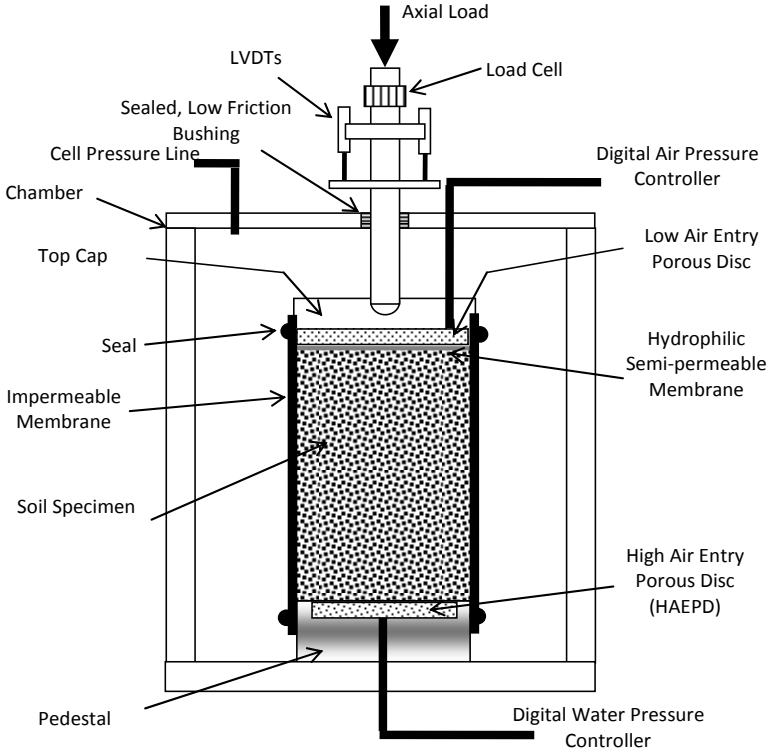

Figure 4.1- Schematic Plot of the Triaxial/Resilient Modulus Testing Cell for Unsaturated Soils (not to scale)

In this study, M_r tests were conducted at different suction values along the primary drying, primary wetting and the secondary drying and wetting curves. Table 4.1 summarizes the cell pressure (σ_3), pore air pressure (u_a), and pore water pressure (u_w) for each target suction (u_a-u_w) and net confining stress (σ_3-u_a). It is noteworthy to emphasize that M_r tests in this aforementioned procedure were performed on the same sample at each target suction value along the drying and wetting paths. In order to check influence of previous M_r loading history on the results, virgin samples were tested at different points on the SWCC without previous M_r testing. For example, virgin samples were tested for M_r at suction along the drying curve without previous M_r testing at lower suction values. Similar virgin samples were also prepared and subjected to drying then wetting and tested on the wetting curve with similar suction of that on the drying curve.

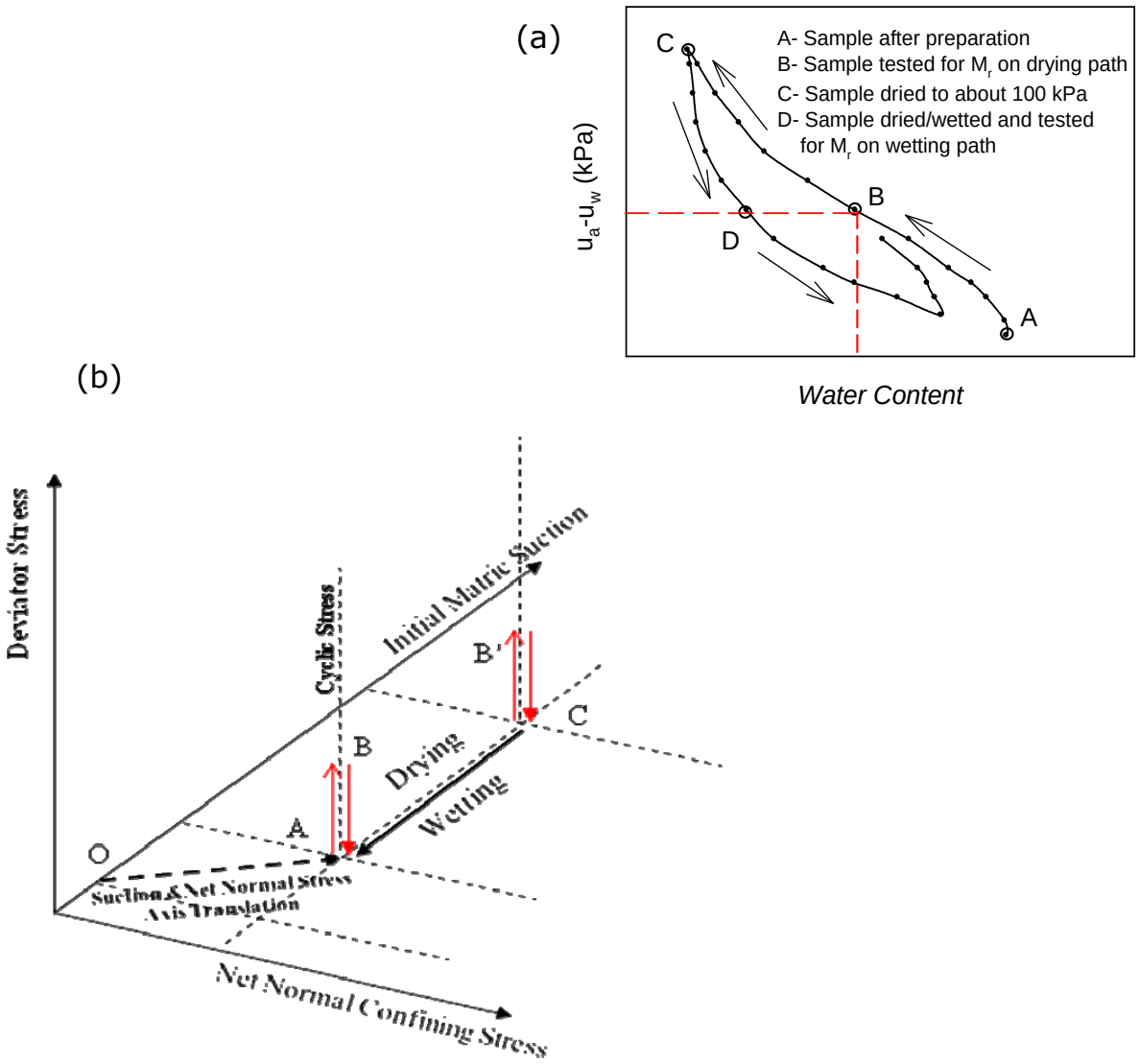

Figure 4.2- Illustration of (a) Suction Hysteresis and Mr Tests, (b) Suction-Stress Path Loading History

Table 4.1- Summary of the Suction Control Test Conditions

Target Suction u_a-u_w (kPa)	Target Net Confining Stress σ_3-u_a (kPa)	Cell Pressure (σ_c)	Pore Water Pressure (u_w)	Pore Air Pressure (u_a)
25	41	81	15	40
	28	68	15	40
	14	54	15	40
50	41	106	15	65
	28	93	15	65
	14	79	15	65
75	41	131	15	90
	28	118	15	90
	14	104	15	90
100	41	156	15	115
	28	143	15	115
	14	129	15	115

5. RESULTS AND DISCUSSION – SOIL WATER CHARACTERISTIC CURVE TESTING

5.1 Influence of Sample Height on the SWCC Equilibrium Time

Mainly SWCC tests were first performed on SCS soil samples (pure silco-sil) with heights of 1" (25.4 mm), then on samples with ¼" (6.35 mm), which was the smallest practical height that could be compacted. Plots of the Soil Water Characteristic Curves (SWCCs, matric suction (u_a-u_w) versus gravimetric water content) for tests having heights of 25.4 mm and 6.35 mm are presented in Figure 5.1 and Figure 5.2, respectively. Each data point in these figures represents an increment of suction and corresponding measurement of water volume change at equilibrium. Equilibrium was assumed to occur when negligible water volume change occurred for each suction increment. In Figure 5.3 an example of water volume change versus time for primary drainage of the 25.4 mm sample height is shown. Water volume changed fairly rapidly after of an increment of suction followed by a more gradual change until equilibrium was observed.

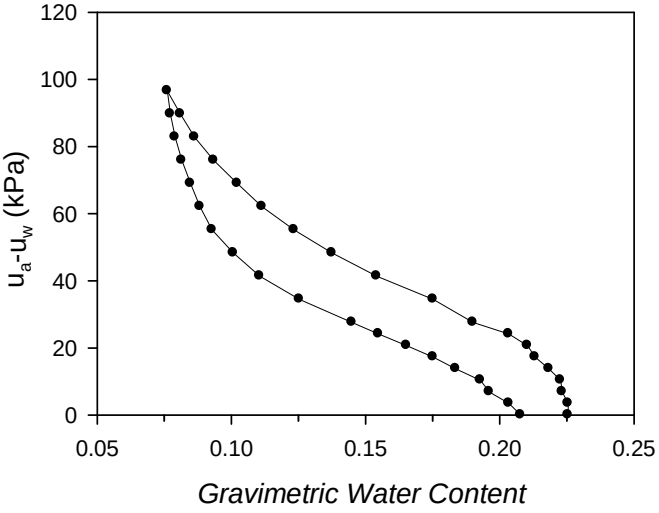

Figure 5.1- SWCC for Sample height of 25.4 mm

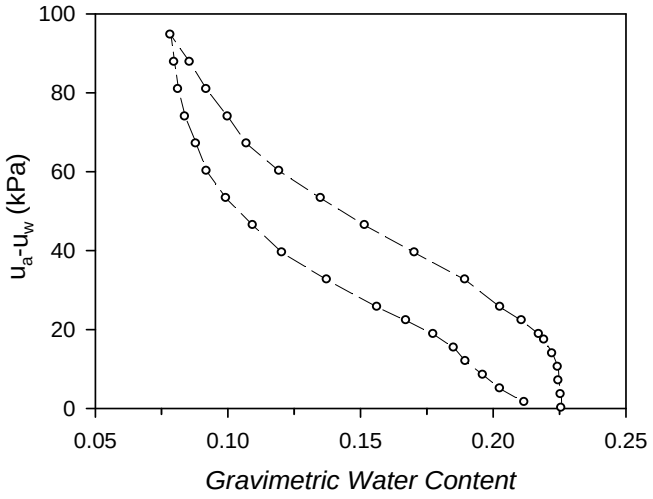

Figure 5.2- SWCC for Sample height of 6.35 mm

In Figure 5.4, a comparison of the primary drainage and primary wetting curves for each (25.4 mm and 6.35 mm sample height) test is shown. In examining Figure 5.4 it is apparent that the SWCCs for both sample heights were practically the same.

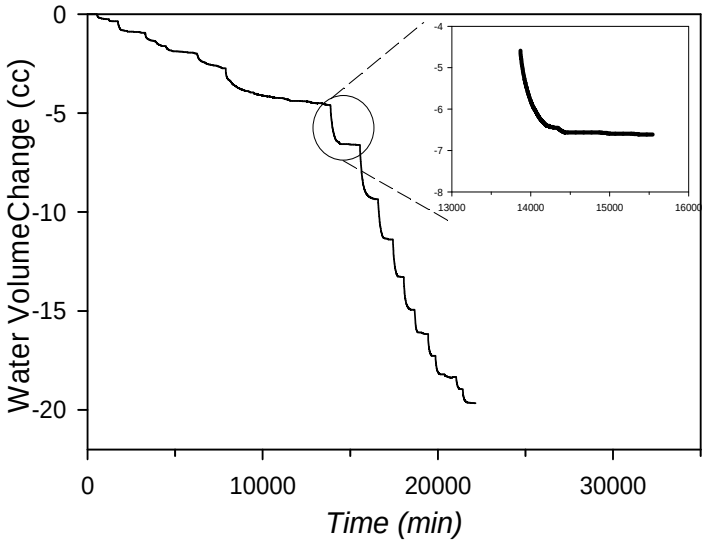

Figure 5.3- Water Volume Change versus Time for Primary Drainage during Testing for 25.4 mm Height

Figure 5.5 shows a comparison of water volume change versus total test time for both sample heights. The total time for testing, including primary drainage and primary wetting curves for the 25.4 mm height was about 25 days compared to 10 days for the reduced sample height (6.35 mm). It can be noted that the time required to complete testing was reduced by more than 50% when the sample height was reduced from 25.4 mm to 6.35 mm. Results indicate that a reduction in sample height can be an effective way of achieving considerably faster equilibrium test times. However, other considerations remain when reducing the test specimen height, such as sample uniformity, and minimum vertical deformations required for accurate measurements on the specimen under vertical loading (i.e. for a given strain shorter heights mean smaller displacements). That said, the vertical deformations measured for the minimum height (6.35 mm) used in this study were acceptable given the accuracy of measurement devices.

In addition, previous to conducting a test on the smaller height sample a repeat test was conducted for the 1” (25.4 mm) sample height to investigate

experimental variability. Figure 5.6 shows the comparison of results from the two nominally identical tests. Results of the duplicate test demonstrate that the SWCC is reproducible to reasonable accuracy.

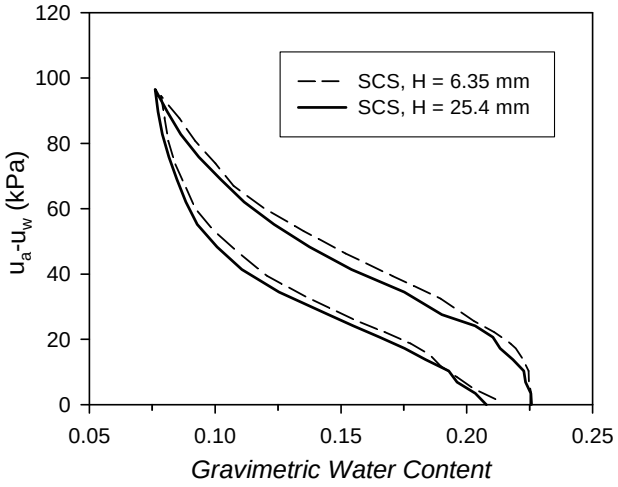

Figure 5.4- SWCC Comparison for the both Sample Heights (25.4 and 6.35 mm)

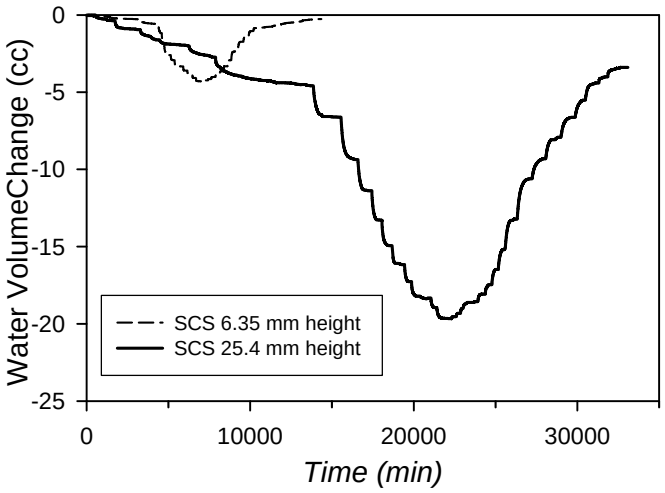

Figure 5.5- Water Volume Change versus Time for both 25.4 mm to 6.35 mm Sample Height

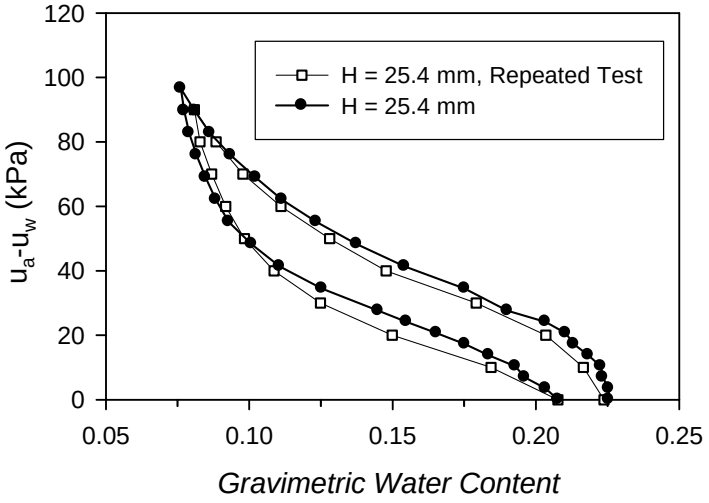

Figure 5.6- Comparison of SWCC Results for Two Nominally Identical Samples with a Height of 25.4 mm

The reduction in testing time gained by reducing the sample height to ¼" (6.35 mm) was a major achievement in that it allowed obtaining, in a reasonable time frame, a complete SWCC including the hysteretic behavior; this included primary drying, primary wetting, secondary drying and scanning curves, which are presented in Sections 5.2 and 5.3.

5.2 Initially Saturated Samples

Results in this section represent tests performed on the soil mixture (75 % SCS and 25 % Glass Beads) with sample height of ¼" (6.35 mm), in which samples were saturated before initiation of Soil Water Characteristic Curve (SWCC) testing. Initially saturated SWCCs, denoted by (IS-SWCC) were conducted under net normal stresses (σ_n-u_a) of 0, 10 and 200 kPa. IS-SWCC results for net normal stresses of 10 and 200 kPa are presented in Figures 5.7 and 5.8, where matric suction is u_a-u_w, and θ_w is the volumetric water content (volume of water/total volume). The data points in these figures represent the increments of suction and corresponding measurements of water volume at equilibrium. Similar to previous tests, equilibrium was also assumed to occur when negligible water volume and total volume change

occurred following application of a new suction increment. In Figure 5.9 an example of water volume change (*w* is gravimetric water content) versus time for primary drainage at 200 kPa normal stress is shown. Based on Figure 5.9, the time to complete primary drainage was about 18 days, which demonstrates the relatively fast equilibrium times that were achieved using the artificial soil and smaller sample heights.

In Figure 5.10, a comparison of the primary drainage and primary wetting curves for each test is shown. Note that for 0 kPa normal stress, only the primary drainage and a portion of the primary wetting curve were obtained because the test had to be terminated prematurely; these are shown for comparison to the 10 and 200 kPa normal stress curves.

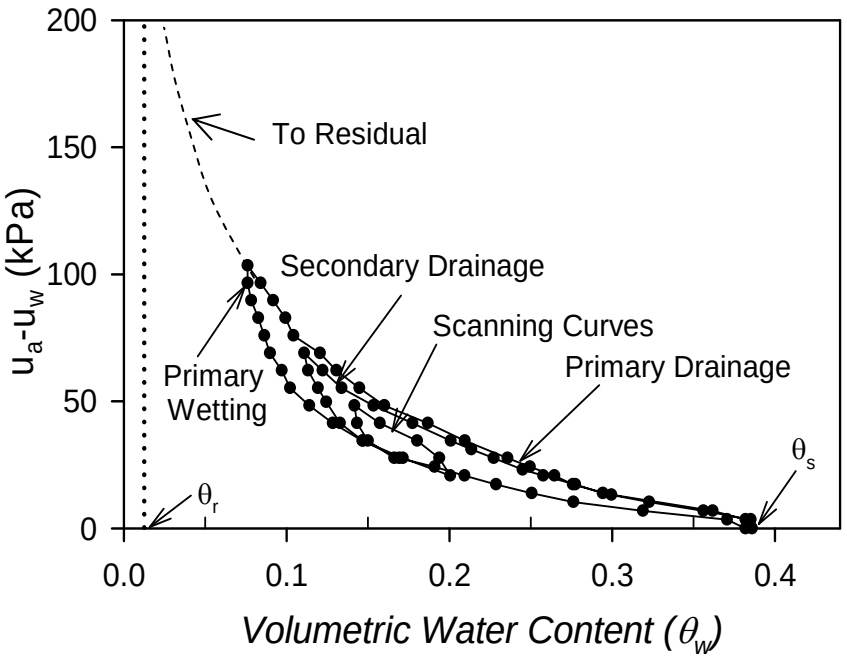

Figure 5.7- SWCC for Net Normal Stress of 10 kPa

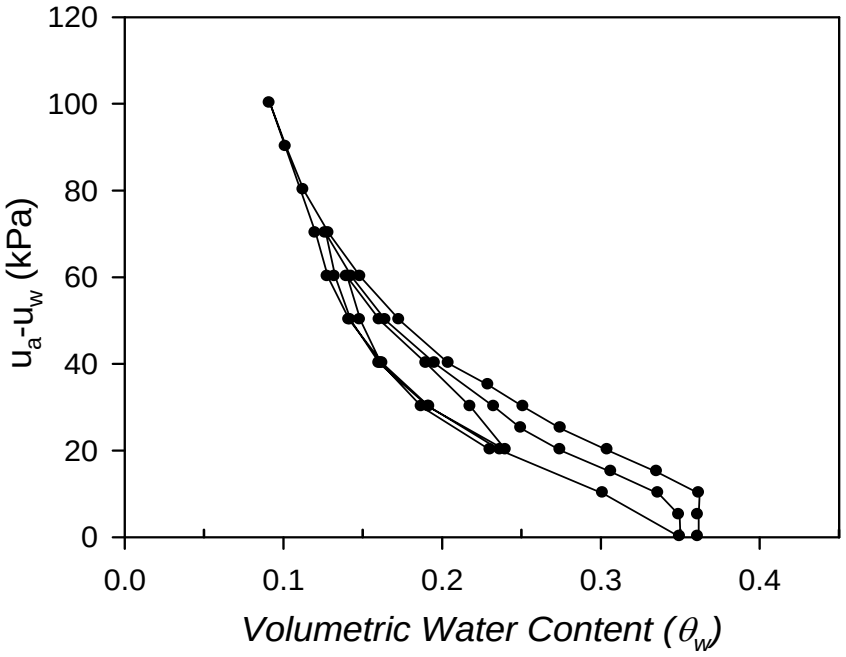

Figure 5.8- SWCC for Net Normal Stress of 200 kPa

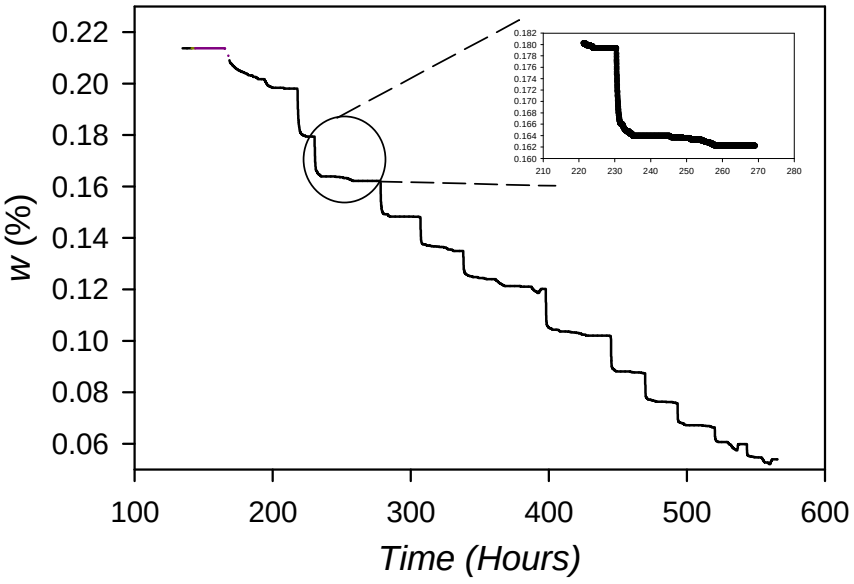

Figure 5.9- Water Volume Change versus Time for Primary Drainage during Testing for Net Normal Stress of 200 kPa

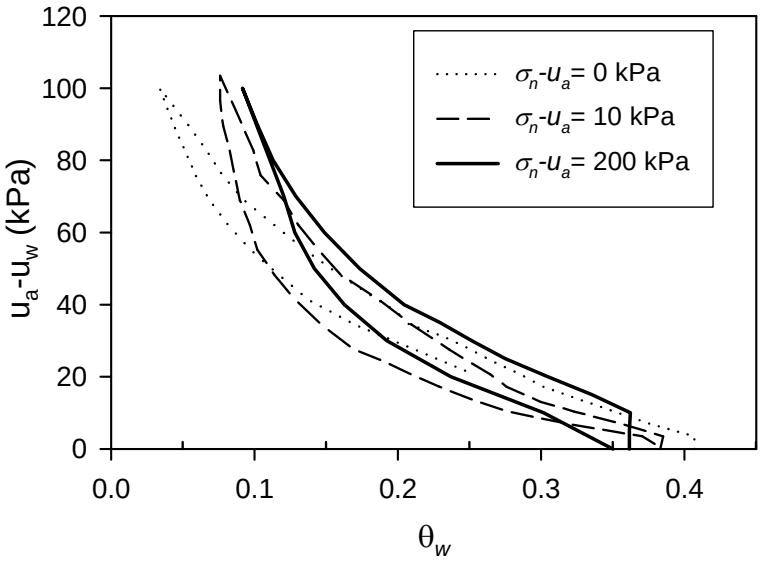

Figure 5.10 - Comparison of SWCCs at Net Normal Stresses of 0, 10 and 200 kPa

In examining Figures 5.7, 5.8 and 5.10 some interesting observations are made:

1) For the 10 and 200 kPa normal stresses, the scanning curves are bounded by the secondary drainage and primary wetting curve.
2) The initial volumetric water content decreases with increasing normal stress as expected since the void ratio decreases more during application of higher normal stress.
3) Generally, the air entry value increases with increasing normal stress, again as expected due to the lower void ratio. However, the difference between the air entry value for 0 and 10 kPa normal stress is negligible, probably because the change in void ratio from 0 to 10 kPa is relatively small compared to the difference between normal stress of 10 and 200 kPa. The air entry value is the matric suction necessary for air to penetrate the void space when the soil is initially saturated.

4) Generally, the slope of the SWCC is flatter at lower normal stress and becomes steeper with increasing normal stress; it is especially apparent as the curves approach the lower residual saturation moisture contents. This observation is reasonable because the pore channels in soil with lower void ratio would be smaller relative to higher void ratio soil. Thus, the lower void ratio soil would generate higher capillary pressure than a higher void ratio (i.e. matric suction) at the same volumetric water content. Also, the residual moisture contents appear to increase with increasing normal stresses.

In addition, the SWCC test at 200 kPa normal stress was repeated to investigate the experimental repeatability. Figure 5.11 shows the comparison of results from the two nominally identical tests. For the repeat test, only the primary drainage and a portion of the primary wetting curve were obtained because the system developed a leak that could not be repaired during testing. Nevertheless, the comparison of the SWCC curves is favorable, as is the volume change behavior represented by specific volume (1+void ratio) data presented in Figure 5.12. While the number of repeat tests was limited, the results for duplicate tests demonstrate that the SWCC is reproducible to reasonable accuracy.

For the 10 and 200 kPa normal stress SWCC tests, vertical displacements were recorded throughout testing beginning with the saturation process and continuing through the saturated compression and SWCC testing. In Figure 5.12, a comparison of specific volume versus normal stress curves is presented. These curves represent compression starting from the compacted state, followed by wetting induced compression during saturation at a constant total stress, and subsequent compression under saturated conditions to reach the starting point of the SWCC tests. Although the curves exhibit some slight differences, they are generally similar and express similar soil behavior. Since samples were prepared in nearly identical

fashion, similar behavior was expected. Interestingly, the samples showed considerable wetting-induced compression under a very low normal stress; the change in specific volume due to wetting represents a volumetric strain of about 1.5%. This collapse may be partly attributed to the relatively loose initial state of the sample following compaction and the significant angularity of the crushed silica particles. Both of these factors contribute to an open soil structure susceptible to collapse.

During incremental loading the samples behaved similarly as evidenced by the similar slopes of each curve. Comparison of the specific volumes at 10 kPa and 200 kPa net normal stresses indicates that significant compression, about 4 to 5% volumetric strain, occurred during incremental loading up to 200 kPa. This accounts for the differences in the initial volumetric water content for corresponding SWCCs.

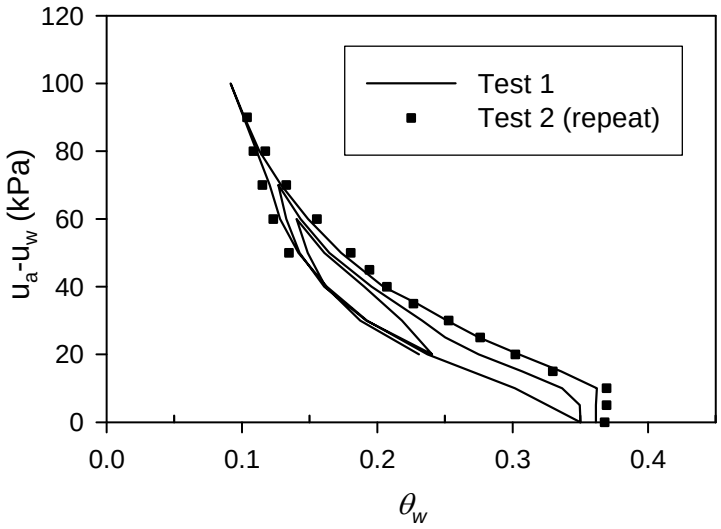

Figure 5.11- Comparison of SWCC Results for Two Nominally Identical Samples at σ_n-u_a of 200 kPa

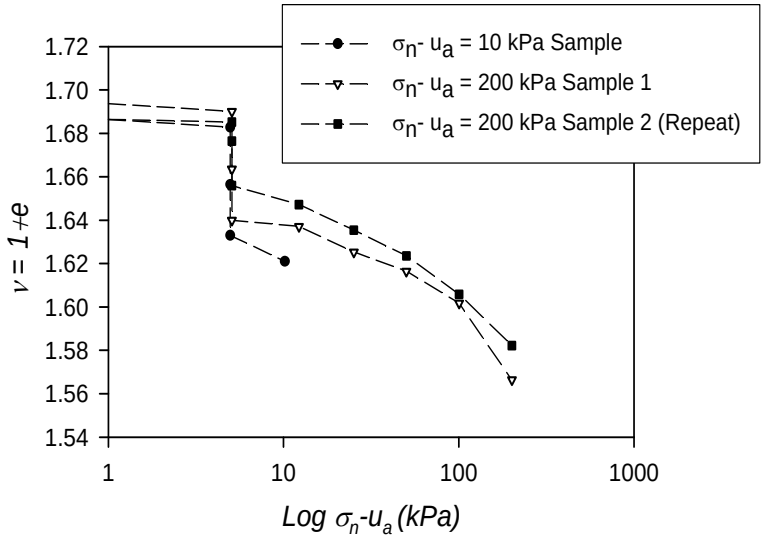

Figure 5.12 - Specific Volume (1+e) versus Net Normal Stress of the Three Identically Prepared SWCC Specimens

Figure 5.13 shows a plot of void ratio (e) versus suction during SWCC drying-wetting cycles. During the SWCC testing, the volume change (or change in void ratio) as determined from LVDT measurements of vertical deformation was practically negligible with a maximum volumetric strain (due to suction change beginning from the start of the SWCC) of about 0.75%, for both the 10 and 200 kPa normal stress specimens. While small, the volume change was included in the computation of volumetric water content. This small volume change due to suction was initially observed during drying, but then ceased during wetting/drying cycles.

5.3 As-Compacted Samples

This type of SWCC (as-compacted) test was performed on samples without initial saturation. Samples were first loaded incrementally (in an oedometer setup, as discussed in Section 3.3) to the desired vertical normal stress after which drying and wetting cycles were initiated.

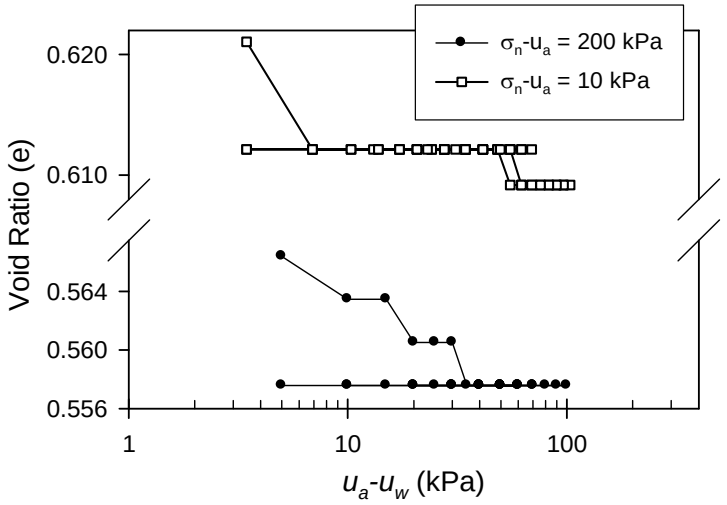

Figure 5.13 - Void Ratio versus Suction during SWCC Drying-Wetting Cycles

This set of SWCCs was used to simulate as close as possible a similar stress path performed for resilient modulus tests conducted in this study. Where, for example, a seating load was first applied to the test samples without saturation, after which suction and net normal stresses were applied and samples were then tested.

The as-compacted SWCC tests were conducted under net normal stresses (σ_n-u_a) of 0 and 150 kPa; results are presented in Figures 5.14 and 5.15, respectively. Note this range of σ_n-u_a (0-150kPa) was selected because it covers the same range that resilient modulus and other tests not discussed in this report were subjected to.

Similar to the initially saturated SWCC (IS-SWCC) test results (Section 0), Figures 5.14, 5.15 and 5.16 showed that: a) the scanning curves are bounded by the secondary drainage and primary wetting curve, b) the initial volumetric water content decreases slightly with increasing normal stress, a behavior, however, not as pronounced as for the IS-SWCC, c) the slope of the SWCC is flatter at 0 kPa normal stress and became steeper at higher normal stress (150 kPa). Again, an expected behavior because the pore channels in soil with lower void ratio (150 kPa net normal stress) would be

smaller relative to higher void ratio soil (0 kPa net normal stress), d) also the residual moisture contents appear to increase with increasing normal stresses, for the same reasoning in c).

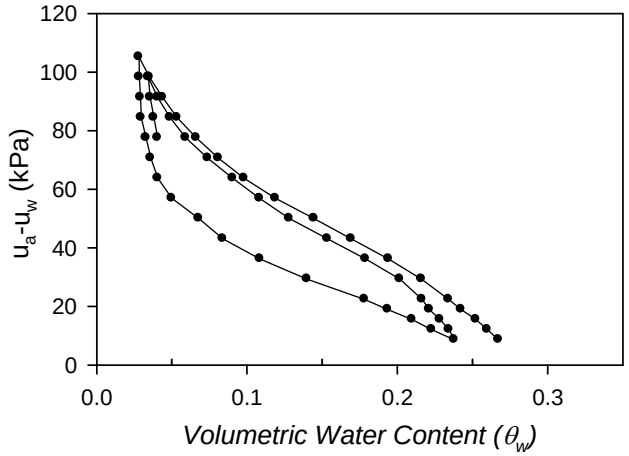

Figure 5.14 - SWCC for As-Compacted Sample at Net Normal Stress of 0 kPa

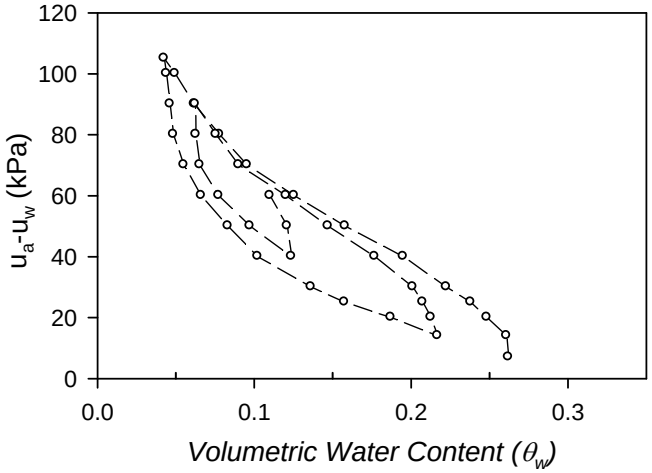

Figure 5.15- SWCC for As-Compacted Sample at Net Normal Stress of 150 kPa

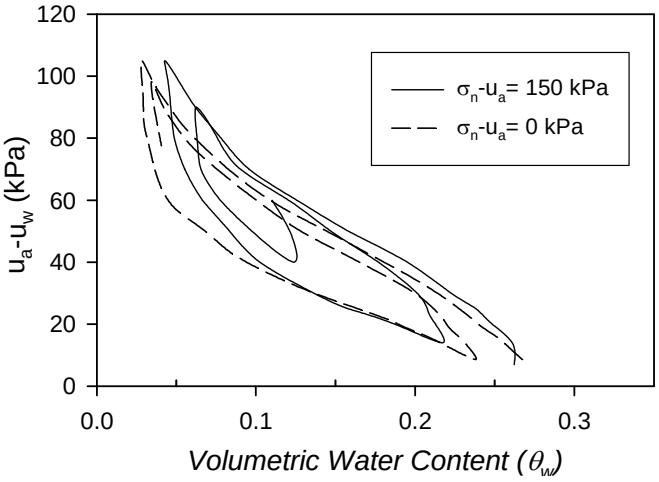

Figure 5.16- Comparison of SWCCs for As-Compacted Sample at Net Normal Stress of 0 and 150 kPa

Consolidation of the sample at net normal stress of 150 kPa indicates approximately 2% volumetric strain during incremental loading as shown in Figure 5.17. A plot of void ratio (e) versus suction during SWCC drying-wetting cycles is shown in Figure 5.18. This change in void ratio (corresponding to a volumetric strain of approximately 0.2 %) was determined from LVDT measurements of vertical deformation during SWCCs, and although it is very small, was included in the computation of volumetric water content. It is noted, that this small volume change due to suction was initially observed during early drying increments, but then ceased completely during further wetting/drying cycles.

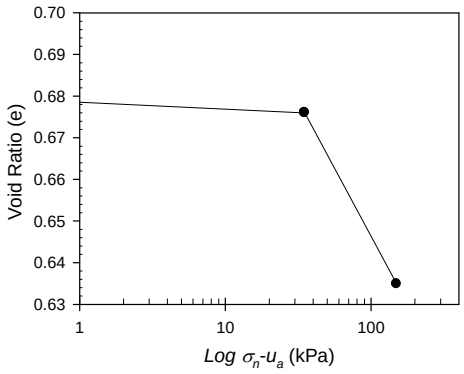

Figure 5.17- Void Ratio (e) versus Net Normal Stress of the SWCC Specimen at σ_n-u_a of 150 kPa

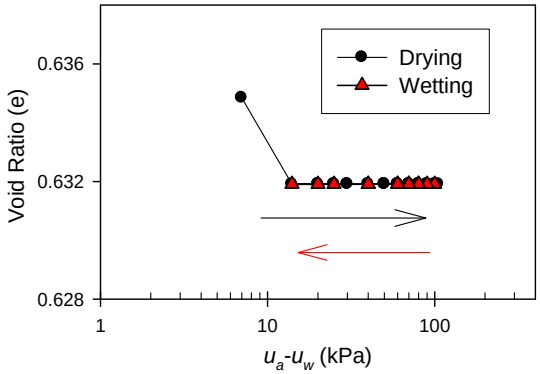

Figure 5.18 - Void Ratio versus Suction during SWCC Drying-Wetting Cycles

6. MODELING THE SOIL WATER CHARACTERISTIC CURVE

6.1 General

The SWCC has been extensively studied, and some early researchers proposed functional models to describe a single (primary drying) SWCC as follows:

Brooks and Corey (1964),

$$\theta = \theta_r + (\theta_s - \theta_r)(a \times \psi^n) \qquad \textbf{(6.1)}$$

Van Genuchten (1980),

$$\theta = \theta_r + \frac{(\theta_s - \theta_r)}{\left[1 + (a \times \psi^n)\right]^m} \qquad \textbf{(6.2)}$$

Fredlund and Xing (1994) ,

$$\theta = \theta_s \left[1 - \frac{\ln(1 + \psi/\psi_r)}{\ln(1 + 10^6/\psi_r)}\right] \left[\frac{1}{\left\{\ln\left[e + (\psi/a)^n\right]\right\}^m}\right] \qquad \textbf{(6.3)}$$

Feng and Fredlund (1999),

$$\theta = \frac{\theta_s + \theta_r \left(\frac{\psi}{a}\right)^m}{1 + (\frac{\psi}{a})^m} \qquad \textbf{(6.4)}$$

Where: θ = volumetric water content, θ_s = saturated volumetric water content, θ_r = residual volumetric water content, ψ = matric suction, ψ_r = matric suction at residual water content, *e* = base of natural logarithm = 2.71828, and *a, m, n* = are fitting parameters that describe the shape of the SWCC.

These models are essentially curve fitting equations, found through best fit of test data. Others have proposed models for hysteretic SWCCs such as Wheeler et al. (2003), Gallipoli et al. (2003), Yang et al. (2004), Wei and Dewoolkar 2006, Li (2007a&b), Kohgo (2008), Muraleetharan et al. (2008).

In this study the functional model by Fredlund and Xing (1994) and Feng and Fredlund (1999) was used to fit the primary drying and primary wetting curves as presented in Section 6.2. The resulting fit parameters were used for prediction of resilient modulus with suction.

On the other hand, SWCC tests (following the primary drying/wetting, secondary drying and scanning curves) obtained in this study for different stress histories (i.e. under different normal stresses) were used to validate the model by Muraleetharan et al. (2008) presented in Miller et al. (2008), as shown in Section 03.

6.2 Functional Form Models

The models, Equations 6.3 and 6.4, by Fredlund and Xing (1994) and Feng and Fredlund (1999) were used to fit the primary drying and primary wetting curves, respectively. Comparison between experimental and fitting model results are shown in Figures 6.1 through 6.7. The resulting fit parameters for each set of SWCC data (i.e. different net normal stresses, and different initial conditions) obtained in this study are shown in Table 6.1 and some of which (i.e. the one corresponding to the same initial conditions) were used to predict the resilient modulus of soil as presented in Section 8.

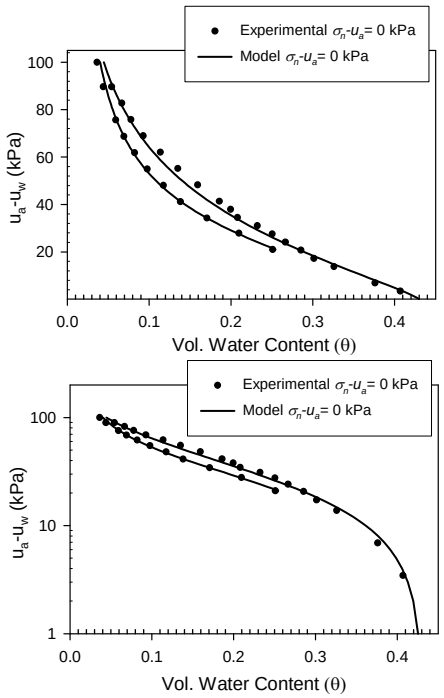

Figure 6.1 - Comparison of Model SWCC with Measured for Initially Saturated Tests at Net Normal Stress of 0 kPa

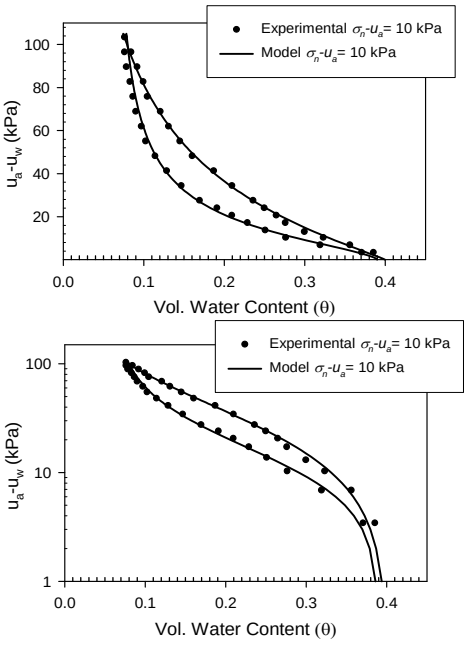

Figure 6.2- Comparison of Model SWCC with Measured for Initially Saturated Tests at Net Normal Stress of 10 kPa

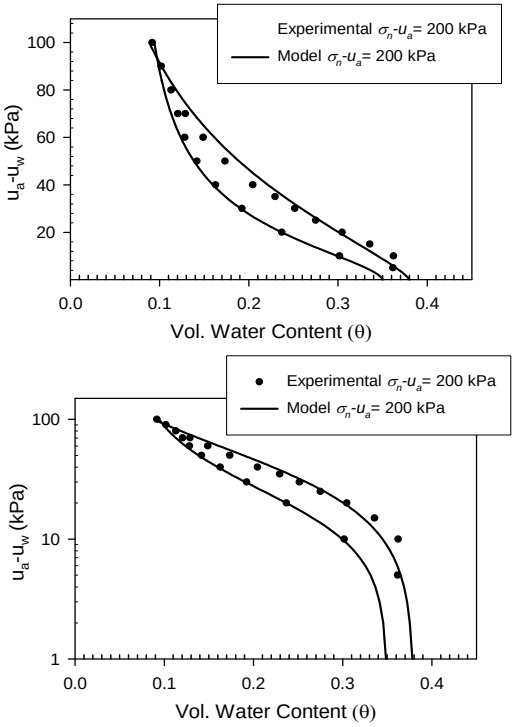

Figure 6.3- Comparison of Model SWCC with Measured for Initially Saturated Tests at Net Normal Stress of 200 kPa

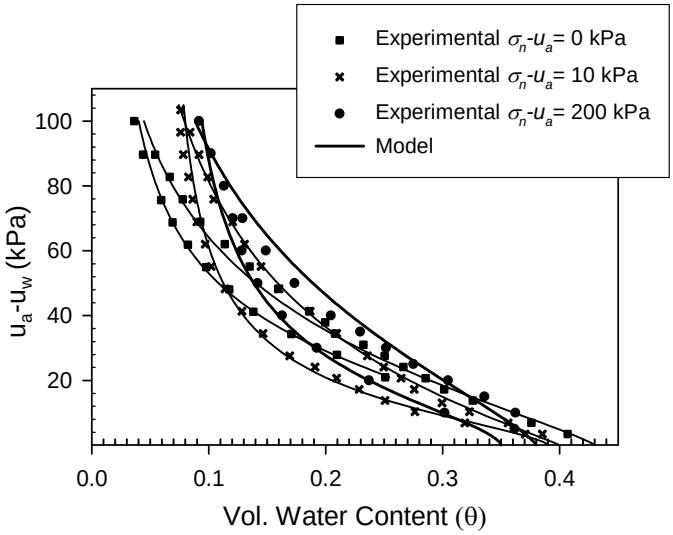

Figure 6.4 - Comparison of Model SWCC with Measured for Initially Saturated Tests at Net Normal Stresses of 0, 10 and 200 kPa

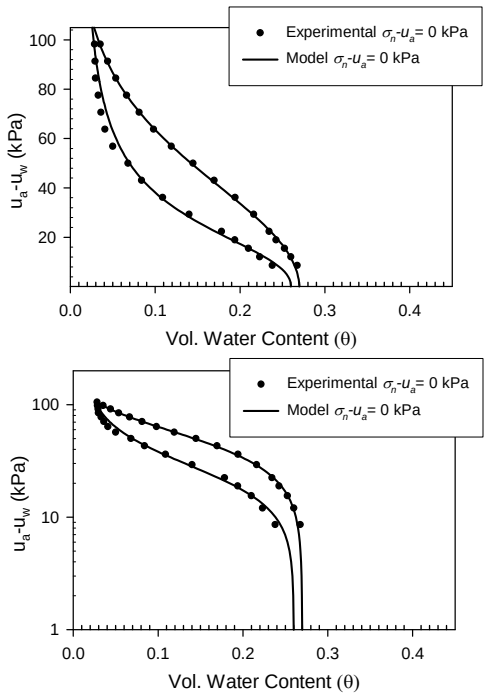

Figure 6.5 - Comparison of Model SWCC with Measured for As Compacted Tests at Net Normal Stress of 0 kPa

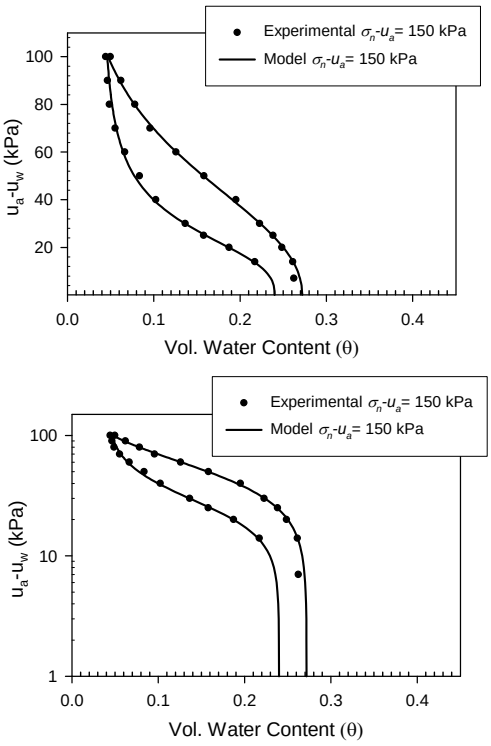

Figure 6.6- Comparison of Model SWCC with Measured for As Compacted Tests at Net Normal Stress of 150 kPa

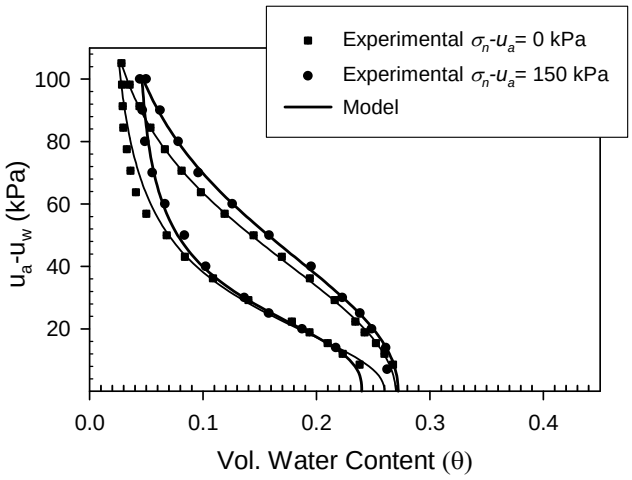

Figure 6.7- Comparison of Model SWCC with Measured for As Compacted Tests at Net Normal Stresses of 0 and 150 kPa

Table 6.1 - Fitting Parameters of the Functional Form Models for the Primary Drying and Wetting SWCC Results

Initial Condition	Net Vertical Stress (kPa)	Fredlund and Xing (1994)					Feng and Fredlund (1999)			
		a	m	n	Ψ_r (kPa)	θ_s	b_1	d_1	θ_r	θ_s
Saturated	0	110	8.90	1.230	200	0.430	31.64	2.05	0.010	0.360
Saturated	10	65.56	4.18	1.102	300	0.400	17.2	1.56	0.060	0.390
Saturated	200	100	5.30	1.300	1000	0.380	25.96	1.61	0.065	0.350
As Compacted	0	93.4	6.80	2.100	200	0.270	29.08	2.20	0.012	0.260
As Compacted	150	76.06	4.20	2.189	1000	0.272	29.288	2.68	0.039	0.24

6.3 Coupled Hydraulic-Mechanical Elastoplastic Constitutive Model

The hysteretic data (including primary, secondary and scanning curves) obtained for SWCCs starting from saturation under different stress histories (i.e. under different normal stresses) were modeled as shown below by Miller et al. (2008).

The constitutive model used combines an elastoplastic description of the SWCCs with an elastoplastic description of the stress-strain behavior of the solid skeleton (Muraleetharan et al. 2008). While the SWCCs are described

using a bounding surface elastoplastic model the stress-strain behavior is simulated using the classical plasticity theory. The theoretical descriptions of the model are detailed by Muraleetharan et al. (2008).

Briefly, Miller et al. (2008) used the intergranular stress and solid skeleton strains to describe the mechanical behavior, and used the matric suction and volumetric water content to describe the hydraulic behavior. The intergranular stress tensor σ^*_{ij} in soil mechanics sign convention (i.e., compressive stresses are positive) is given by:

$$\sigma^*_{ij} = (\sigma_{ij} - p^a \delta_{ij}) + n^w S \delta_{ij} \qquad \textbf{(6.5)}$$

Where: σ_{ij} = total stress tensor, $S\ (= p^a - p^w)$ = matric suction, p^a and p^w are pore air and pore water pressures, respectively, n^w = volumetric water content, and δ_{ij} is the Kronecker delta.

Motivated by the observation that all the scanning curves are bounded by the primary wetting curve and the secondary drying curve, Miller et al. (2008) chose the bounding surface plasticity theory originally proposed by Dafalias and Popov (1975, 1976) to describe the SWCCs as described by Muraleetharan et al. (2008). In addition, Equation (6.4) proposed by Feng and Fredlund (1999) is used to describe the bounding curves (the primary wetting curve and the secondary drying curve).

In order to describe the coupled hydraulic-mechanical behavior in one-dimensional problems, the SWCC model is coupled with an isotropic stress-strain model based on the classical plasticity theory in a manner similar to the one proposed by Wheeler et al. (2003). More details of the model are presented by Muraleetharan et al. (2008) and Miller et al. (2008)

For the soil used in this study, the parameters describing the SWCCs were first calibrated using the measured curves for 10 kPa net vertical stress shown in Figure 5.7. The measured SWCCs and predicted curves for calibration are shown in Figure 6.8 and used for all subsequent predictions.

The parameters that describe the coupled hydraulic-mechanical behavior can be obtained from an unloading-reloading portion (here using the initial portion of Figure 6.9) of a constant suction oedometer test and a wetting induced collapse test as shown in Figure 6.9. Predicted $S - n^w$ curves during wetting and portions of the bounding curves during the wetting process are shown in Figure 6.10.

After obtaining the calibrated model parameters, the SWCC for 200 kPa net vertical stress was predicted following a stress/suction change path that simulated the stress/suction change path for a portion of the experiment. Specifically, starting with as compacted conditions, loading and wetting paths as shown in Figure 6.9 were first simulated. Then the following wetting/drying cycles were simulated: start at zero suction and follow the secondary drying curve to near residual saturation at a suction of 70 kPa, wet back to a point along the primary wetting curve at a suction of 20 kPa, followed by a complete drying and wetting path (suction increase to 60 kPa then decrease back to 20 kPa) to establish a scanning curve loop. The measured and predicted portions of the SWCCs for 200 kPa net vertical stress are shown in Figure 6.11. The only parameter that needed adjustment was the residual saturation. A value of $n_{res}^{w} = 0.06$ was used to predict the behavior at 200 kPa net vertical stress. The comparison in Figure 6.11 demonstrates that the proposed model is well suited to capture the hysteretic nature of the SWCC and a reasonable agreement with experimental results was obtained. To further appreciate the potential of the model to capture the coupled mechanical-hydraulic behavior, the predicted SWCCs for net normal stress of 10 and 200 kPa are plotted with the experimental data as shown in Figures 6.12a and 6.12b. Predicted and experimental results for 10 and 200 kPa normal stress are also plotted together as shown in Figure 6.12c. In this figure it is apparent that the model is capturing some of the essential features demonstrated by the

experimental data. In particular, the shape and position of the model SWCCs for 10 and 200 kPa normal stress are similar to that exhibited by the experimental curves. That is, the model SWCC for a net normal stress of 200 kPa is slightly steeper and positioned slightly above the model SWCC for a normal stress of 10 kPa. However, the model does not show the slight difference in the air-entry value observed in the experimental results.

The limited experimental data on the hysteretic behavior between suction and water content available in the literature (i.e. SWCC) under different levels of externally applied stress (or at different void ratios) shows the importance of the experimental SWCC results obtained in this study for model validation as presented in this section.

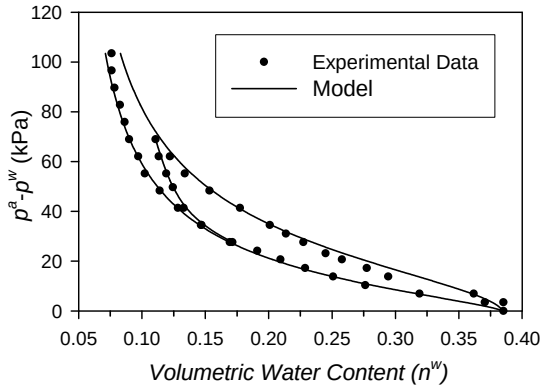

Figure 6.8- Measured SWCCs for a Normal Stress of 10 kPa and Calibrated Predicted Curves Obtained

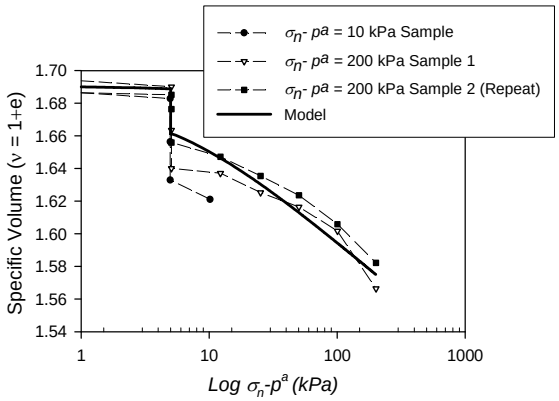

Figure 6.9 - Specific Volume versus Normal Stress during Compression for Three Similarly Prepared SWCC Test Specimens Superimposed with the Model Predictions Obtained during Calibration

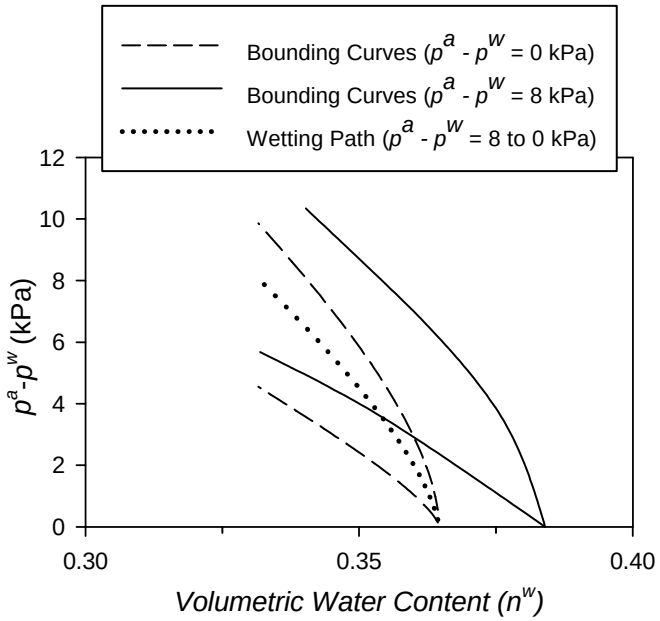

Figure 6.10 - Portions of the Wetting Path and the Bounding Curves when Suction Changes from 8 kPa to 0 kPa

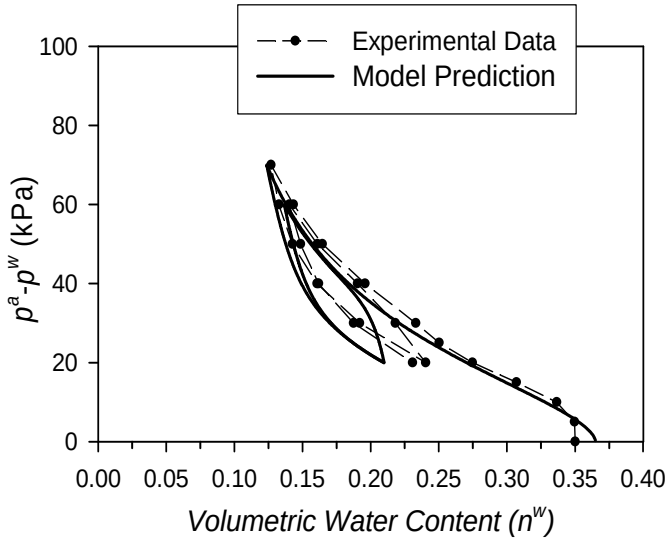

Figure 6.11- Measured and Predicted SWCCs for a Normal Stress of 200 kPa

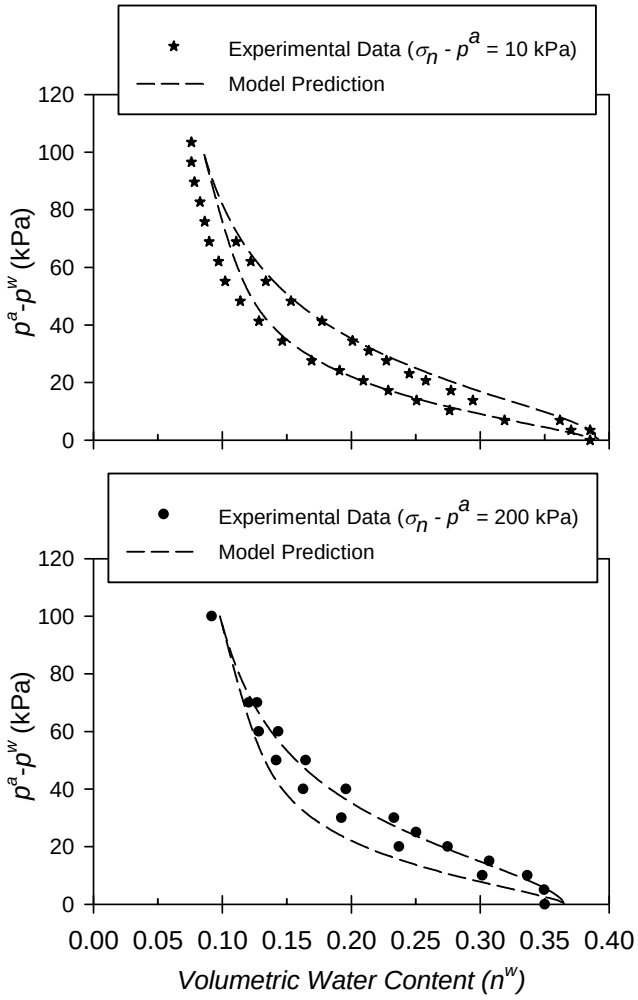

Figure 6.12- Comparison of Measured and Predicted SWCCs for Normal Stresses of 10 and 200 kPa

7. RESULTS AND DISCUSSION – RESILIENT MODULUS

7.1 Samples Continuously Tested for M_r along the Drying and Wetting Curves

7.1.1 Equilibrium of Matric Suction and Net Confining Stress

During the suction-controlled M_r tests, the change in moisture content for each desired suction value was recorded and plotted versus time, as shown in Figure 7.1. As can be seen in Figure 7.1, water flowed out of the sample during drying and then back into the sample during wetting. Suction was assumed to reach equilibrium when negligible change of water content was

observed. Figure 7.1 indicates that more than 3 months was needed to generate M_r tests for primary drying, primary wetting, and secondary drying for the manufactured soil used in this study.

The relationship between suction and gravimetric water content (at the end of suction equilibrium) was obtained during the M_r tests as shown in Figure 7.2. A comparison of this relationship with the SWCCs at different net confining stresses is shown in Figure 7.3. The relationship between suction and water content during the suction controlled resilient modulus tests in this study seems reasonably consistent with the SWCC results. That the SWCC from M_r testing is rotated slightly clockwise relative to the other curves may be due to the complex stress history of the test, which affects the void ratio of the soil specimen during testing. Also, M_r SWCC represents isotropic net normal stress while other SWCCs represent 1-D net normal stress states in the oedometer.

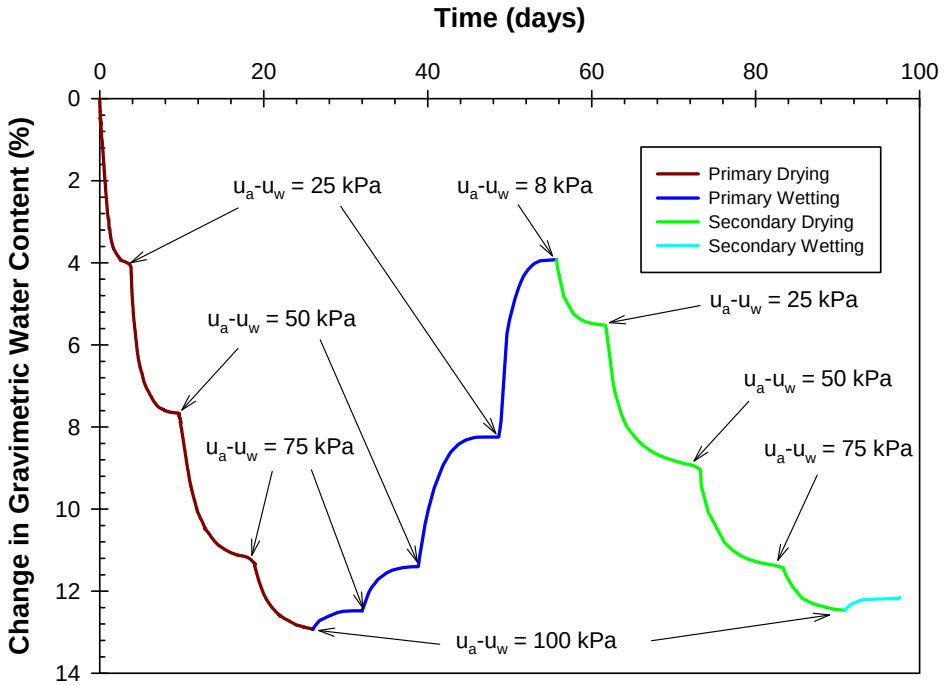

Figure 7.1- Water Content Change for Primary Drying, Wetting, Secondary Drying and Wetting

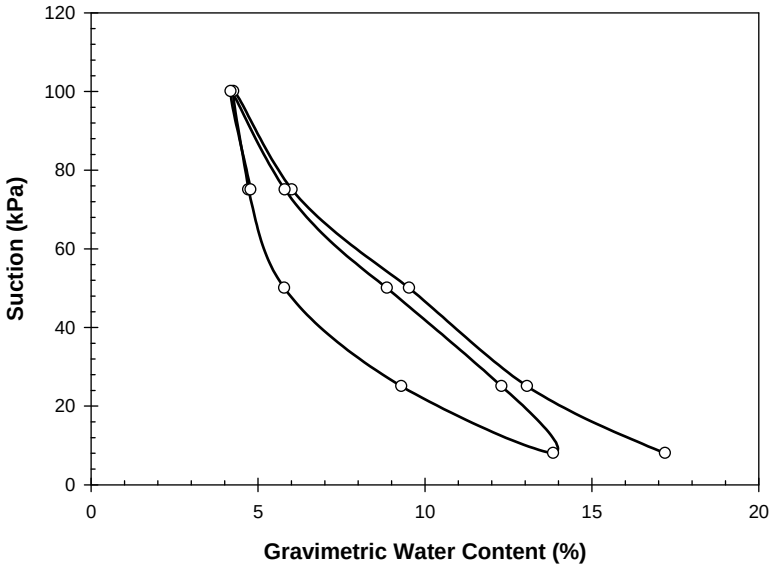

Figure 7.2 - Suction versus Gravimetric Water Content Obtained During M_r Suction Control Tests

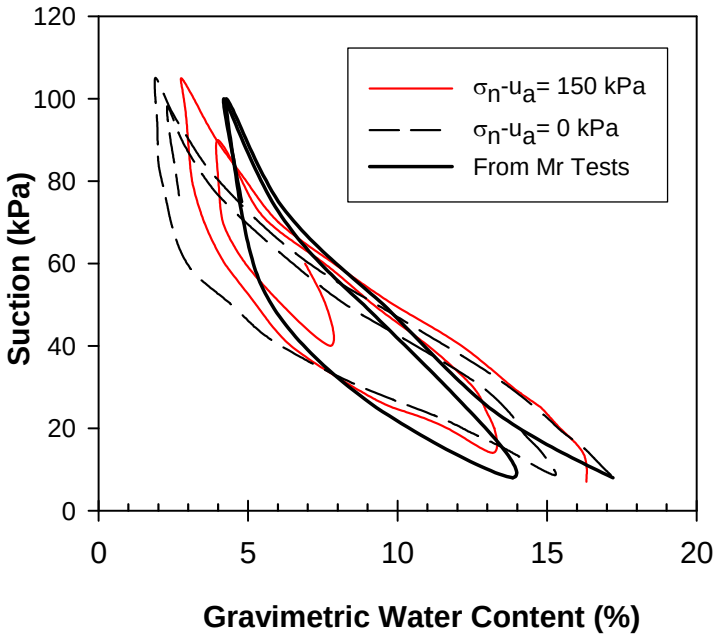

Figure 7.3 - Comparison of Soil-Water Characteristic Curves from M_r Suction Control Tests with SWCC at Net Normal Stresses of 0 kPa and 150 kPa

7.1.2 Effect of Suction Hysteresis on Resilient Modulus (M_r Characteristic Curve MRCC)

Figure 7.4 shows resilient modulus (M_r) versus deviator stress (σ_d), for various net confining stresses of 41 kPa (6 psi), 28 kPa (4 psi) and 14 kPa (2 psi) under different matric suction values (25, 50, 75 and 100 kPa) on the primary drying curve of the SWCC. In general, results (Figure 7.4) indicate that M_r increases slightly with increasing deviator stress. This increase is more pronounced at higher suction values (e.g. 100 kPa); this behavior was also observed by Yang et al. (2008) for residual lateritic and pulverized mudstone soils both classified as lean clayey (CL) soil.

In this study, the effect of suction hysteresis variations was evaluated on the M_r values determined at a bulk stress (θ) of approximately 154.6 kPa (22.5 psi) and at an octahedral stress (τ) of 14 kPa (2 psi) as suggested by SHRP Protocol P-46. The generalized universal model (Equation 2.2) adopted by the MEPDG was used for this purpose. In this model, the resilient modulus (M_r) is expressed as a function of bulk stress (θ) and octahedral stress (τ). Model parameters (k_1, k_2 and k_3) and M_r values at the aforementioned stresses, for primary drying (PD), primary wetting (PW), secondary drying (SD) and secondary wetting, (SW) are summarized in Table 7.1.

Figure 7.5 shows the M_r-(u_a-u_w) relationship, known as MRCC, at the aforementioned stress levels. Some important observations were made based on Figures 7.5 and 7.6, which are typical of the suction-controlled M_r test results at all stress levels:

1. Resilient Modulus increased with increased matric suction (drying), and decreased as suction decreased (wetting). The increase in resilient modulus was attributed to the fact that higher soil suction results in stiffening of the specimens, and thus higher resilient modulus. It seems that higher suction increases the integrity of soil structure (i.e., increasing rigidity of soil

skeleton). This behavior is consistent with the work of Yang et al. (*2008*), Gupta et al. (*2007*), Khoury and Zaman (*2004*), and Motan and Edil (*1982*).

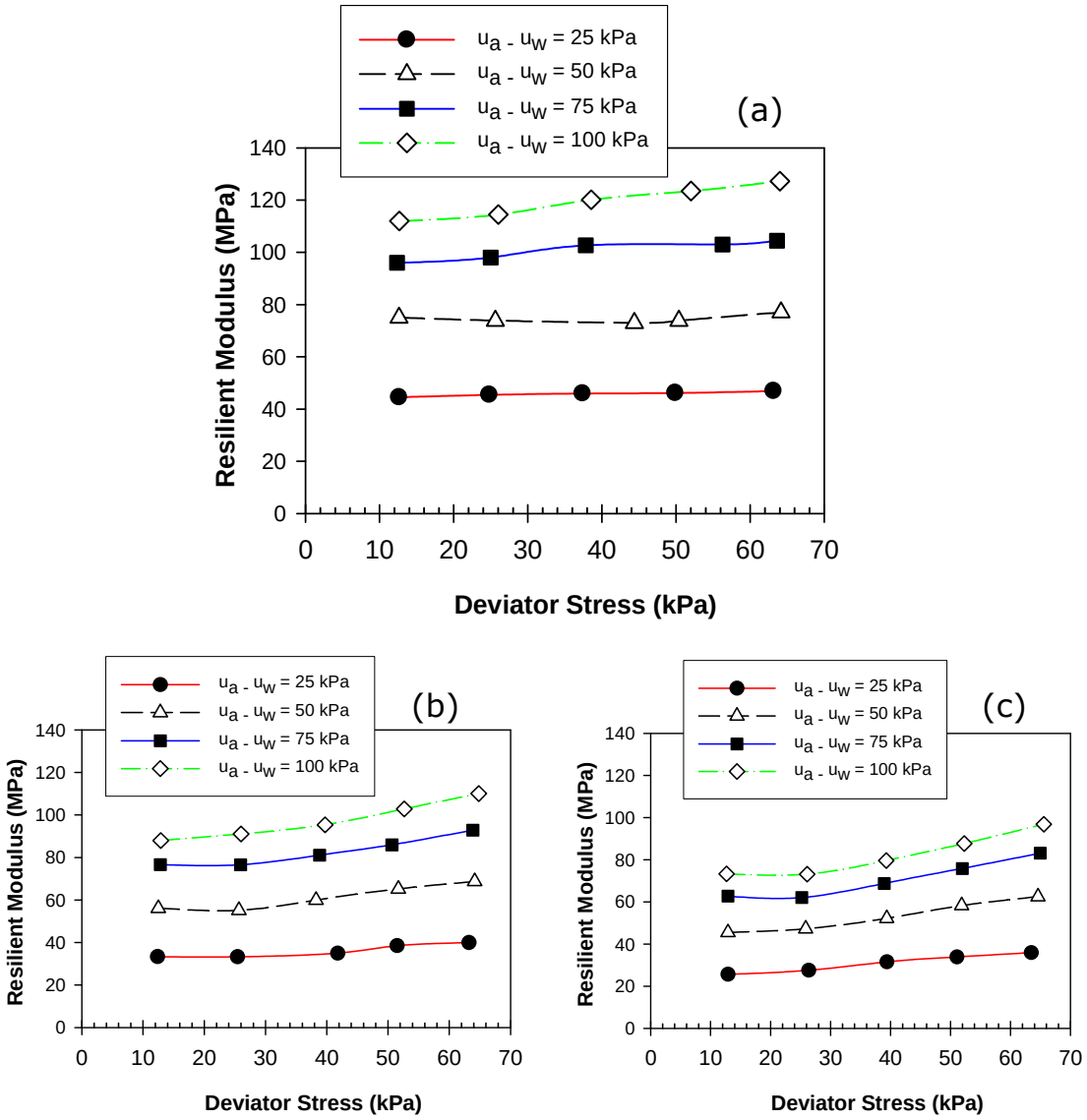

Figure 7.4 - Resilient Modulus versus Deviator Stress for Different Suction Values during Primary Drying at (a) Net Confining Stress of 41 kPa (6psi), (b) Net Confining Stress of 28 kPa (4psi) and (c) Net Confining Stress of 14 kPa (2psi)

Table 7.1 - A Summary of Model Parameters and M_r Values a Net Confining Stress of 41 kPa and Deviator Stress of 28 kPa

Condition	Suction (kPa)	w(%)	k_1	k_2	k_3	R^2	M_R
Primary Drying	8	17.2	235.5	0.4339	-0.1609	0.900	28.1
	25	13.1	356.5	0.5640	-0.3733	0.943	43.8
	50	9.6	590.9	0.4901	-0.2385	0.925	71.6
	75	6.1	797.9	0.5053	-0.2746	0.950	96.9
	100	4.3	927.4	0.5253	-0.2347	0.956	114.1
Primary Wetting	75	4.8	861.6	0.6194	-0.2373	0.963	110.3
	50	5.9	758.9	0.6659	-0.1984	0.943	99.5
	25	9.0	630.6	0.7197	-0.3777	0.955	82.8
Secondary Drying	25	11.0	535.3	0.6187	0.0828	0.955	71.2
	50	7.9	696.9	0.5729	0.1490	0.952	91.6
	75	5.7	887.5	0.4886	-0.0243	0.966	110.3
	100	4.4	1026.4	0.5523	-0.4020	0.952	125.2
Secondary Wetting	75	4.7	910.9	0.6125	-0.1831	0.942	117.0
	50	5.7	783.9	0.6316	-0.0431	0.9412	100.7
	25	7.6	629.3	0.6332	0.3092	0.9631	84.5

2. At a given suction value, M_r values along PD and SD curves were lower than the corresponding values on the PW curve. For example, the average M_r value on PD at a suction of 50 kPa was 74 MPa (10.73 ksi) compared to approximately 101 MPa (14.65 psi) on *PW*. It is an indication that the MRCC relationship of compacted subgrade, due to wetting and drying, is hysteretic.

The fact that the M_r tests were performed on the same sample at each target suction along the drying and the wetting curves raises a question as to the reason behind the higher M_r on the wetting than on the drying curves. Would that difference be attributed to suction hysteresis only, to cyclic stress loading history, or to a combination of both? To this end, selected tests were performed on virgin samples at target suctions without previous M_r tests as discussed in the next section (Section 7.2).

The M_r-(u_a-u_w) relationship, at a different stress level (i.e., for net confining stress of 14 kPa and deviator stress of 69 kPa, which is the worse

condition with highest deviator stress and lowest confining stress) is shown in Figure 7.6 superimposed with the MRCC at the previously mentioned stress level. Similar behavior of MRCC, discussed above, was observed at both stress levels. However, at a given suction as deviator stress increased and net confining stress decreased, M_r decreased resulting in a downward shift in MRCC (Figure 7.6).

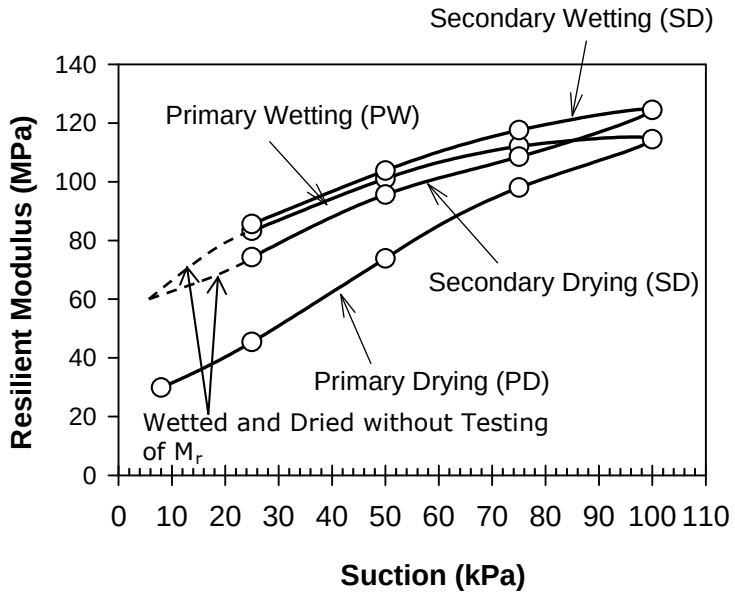

Figure 7.5 - Resilient Modulus Characteristic Curve (MRCC) at Net Confining Stress of 41 kPa (6psi) and Deviator Stress of 28 kPa (4psi)

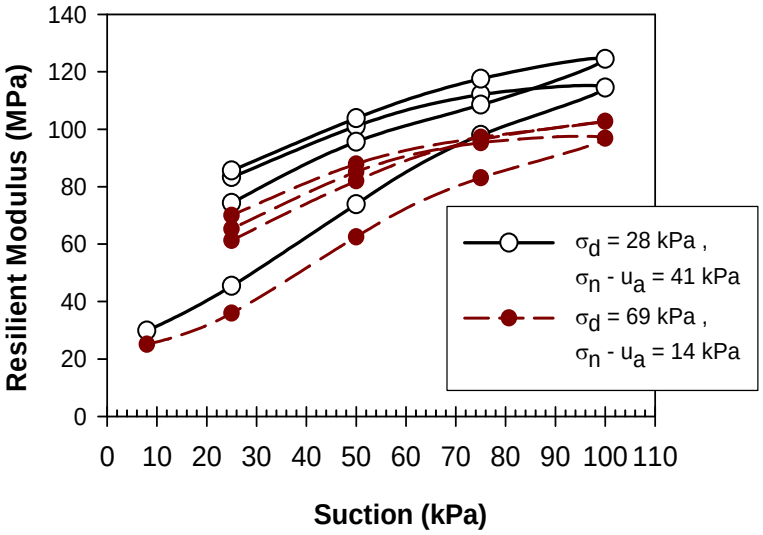

Figure 7.6 - Resilient Modulus Characteristic Curve (MRCC) for Two Different Stress Levels

One repeated M_r test was conducted following the same suction path to investigate experimental variability. Figure 7.7 shows the comparison of results from the two nominally identical tests. For the repeat test, only the primary drainage and a portion of the primary wetting curve were obtained because the system developed a leak that could not be repaired during testing. Nevertheless, the comparison of the MRCC curves was favorable. While the number of repeat tests was limited, the results for a duplicate test (of the primary drying and wetting paths) demonstrate that the MRCC was reproducible to reasonable accuracy.

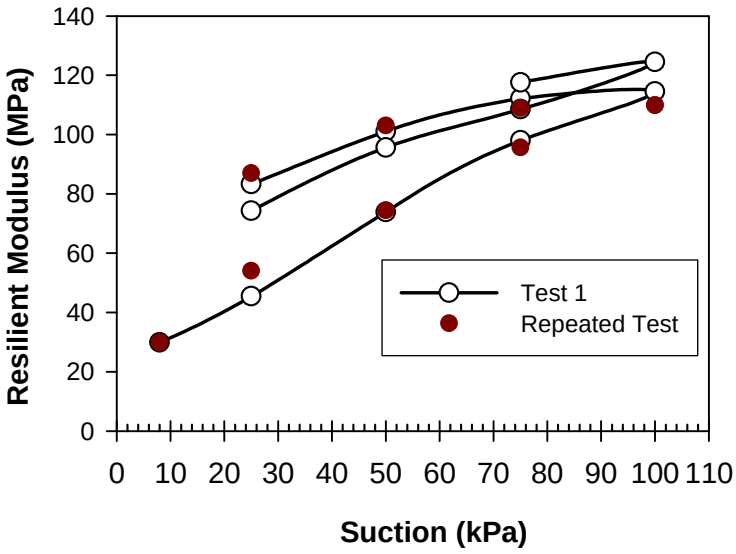

Figure 7.7 - Comparison of MRCC Results from Two Nominally Identical Tests at net confining stress of 41 kPa and deviator stress of 28 kPa

7.2 Test Results for Samples without Previous M_r Testing

Virgin samples were tested at different selected points on the SWCC without previous M_r testing. One sample was tested for M_r at suction of 50 kPa along the drying curve without previous M_r testing at lower suction values. A similar virgin sample was also prepared and subjected to drying then wetting (DW) and tested on the wetting curve at suction of 50 kPa, which is similar suction to that on the drying. Also similar virgin samples were tested at 25

kPa on the drying (D) and on the wetting (DW) curves without any previous M_r tests. Suction and net confining stress equilibrium and M_r results are presented below.

7.2.1 Equilibrium of Matric Suction and Net Confining Stress

The change in moisture content at the desired suction values was recorded and plotted versus time as shown in Figures 7.8 and 7.9 for each test. Comparison of results between tests at 50 kPa suction on the drying (D) and wetting (DW) is shown in Figure 7.8, while the results for (D) and (DW) tests at suction of 25 kPa are shown in Figure 7.9. From these figures it is observed that water flowed out of the sample during drying and then back into the sample during wetting. Suction was assumed to reach equilibrium when negligible change of water content was observed. Results indicate that approximately the same amount of water was drained out of sample in all tests at a specific suction (e.g., at suction of 50 kPa on the drying curve of Figure 7.8 and suction of 25 kPa on drying curve of Figure 7.9).

The relationship between suction and gravimetric water content (at the end of suction equilibrium) was obtained during the M_r test and shown together in Figure 7.10 along with results for samples previously tested for M_r. Figure 7.10**Error! Reference source not found.** indicates that water content changes due to suction applications for all tests are significantly comparable.

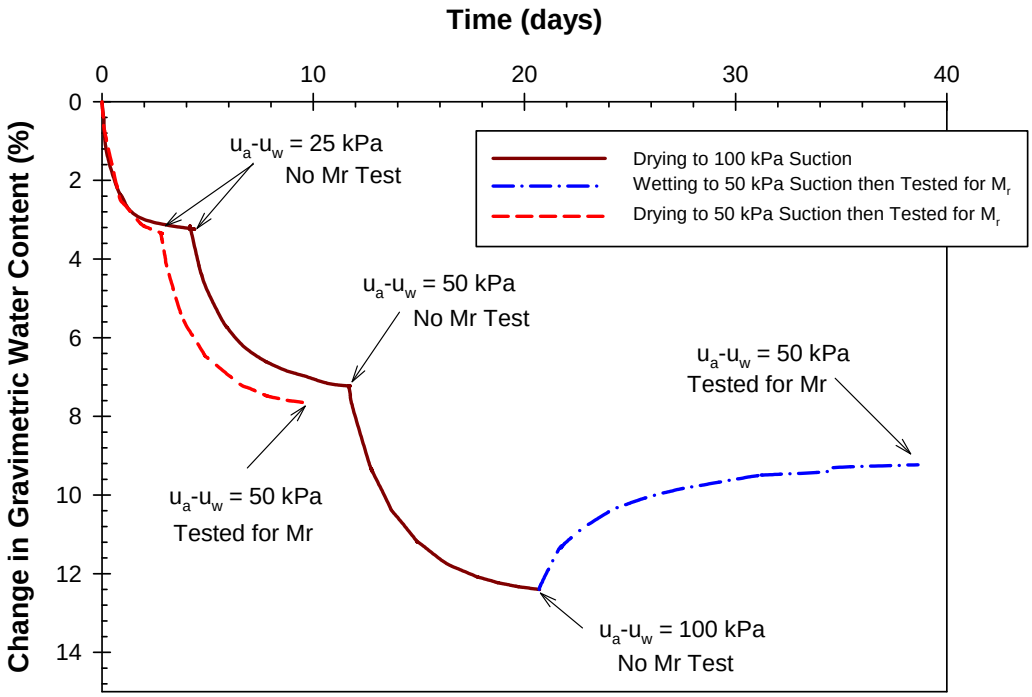

Figure 7.8 - Comparison of Water Content Change for both Samples on Drying Curve and Wetting after Drying at target Suction of 50 kPa

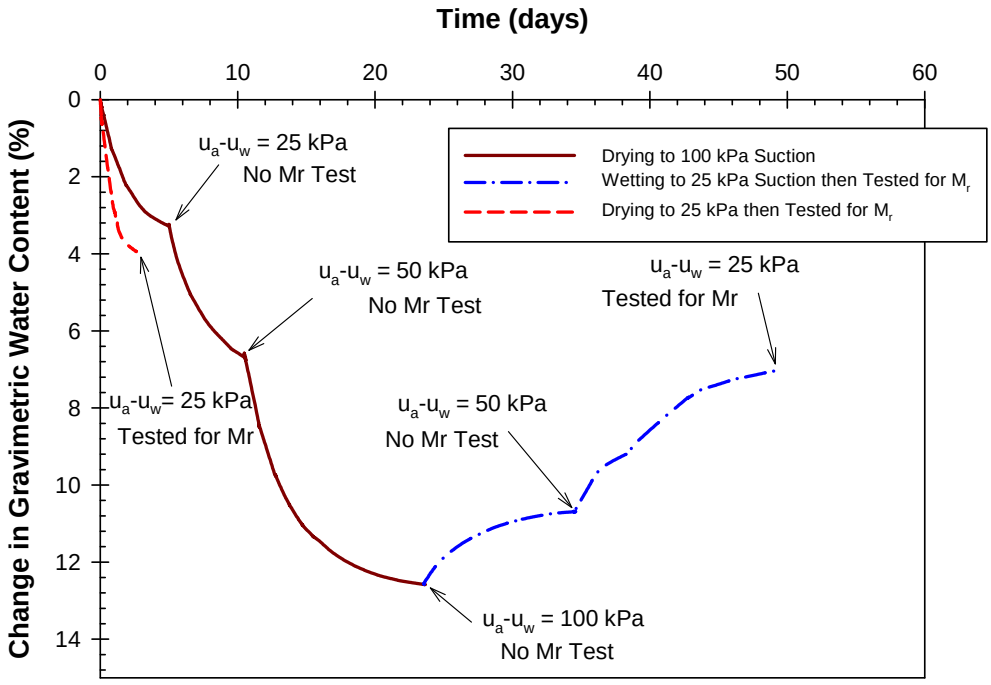

Figure 7.9 - Comparison of Water Content Change for both Samples on Drying Curve and Wetting after Drying at target Suction of 25 kPa

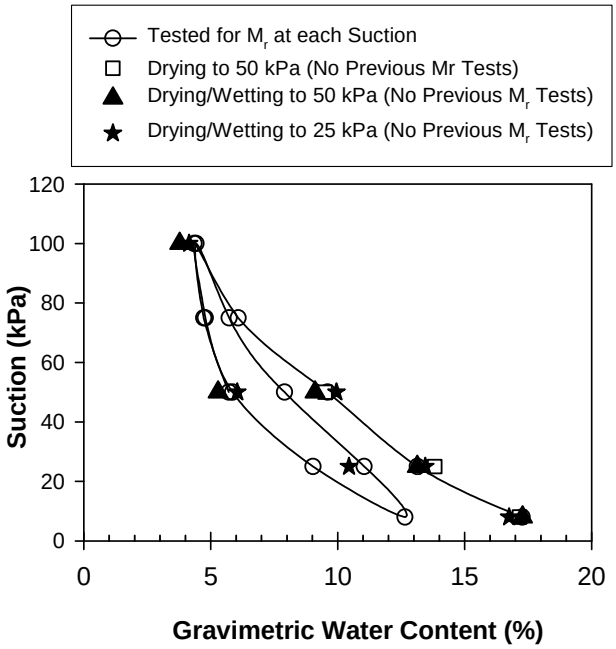

Figure 7.10 - Results from M_r Suction Control Tests with no Previous M_r Tests Compared to Results with Previous M_r Tests at each Suction Value

7.2.2 Resilient Modulus Results

This section presents results for the tests on virgin samples, which were conducted to check the effect of suction excluding the influence of previous M_r loading history on the results. The M_r values were determined using Equation (2.2) and presented here for a bulk stress of approximately 154.6 kPa (22.5 psi) and at an octahedral stress of 14 kPa (2 psi). Figures 7.11 and 7.12 show the M_r results versus deviator stress (σ_d), for a net confining stress of 41 kPa (6 psi) at matric suction values, on the primary drying (D) and wetting (DW) curve, of 25 and 50 kPa, respectively. In general, results for both drying and wetting tests in those figures indicate that M_r increases slightly and nonlinearly with increasing deviator stress. On the other hand, for all deviator stress values, M_r results on the wetting curves were higher than the values on the drying curves. The Model parameters and M_r values for the corresponding tests for primary drying (D), and primary wetting (DW) are presented in Table 7.2.

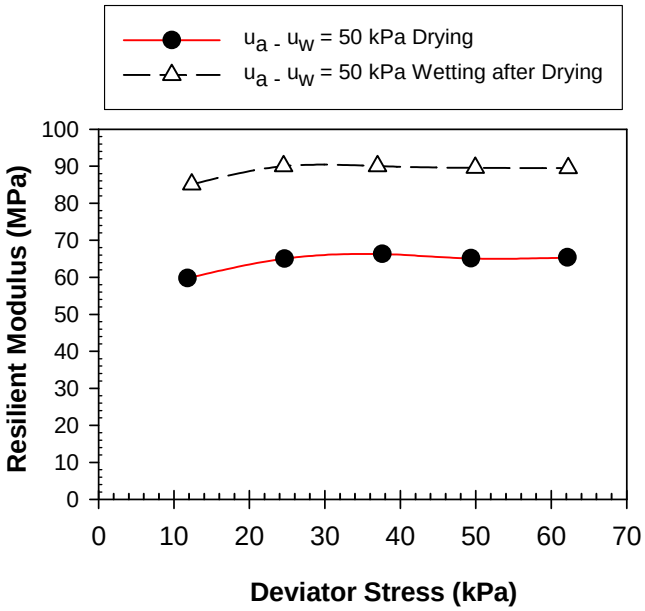

Figure 7.11 - Comparison of Resilient Modulus versus Deviator Stress at Net Confining Stress of 41 kPa for Samples not previously Tested for M_r at Suction of 50 kPa

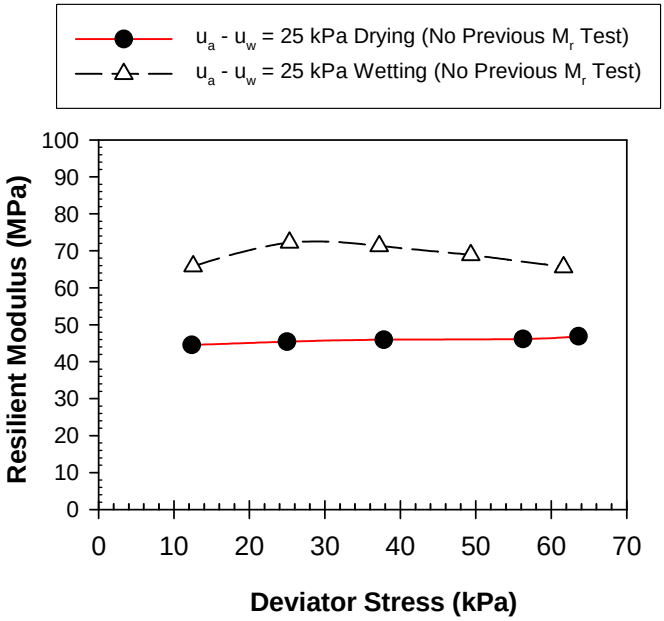

Figure 7.12 - Comparison of Resilient Modulus versus Deviator Stress at Net Confining Stress of 41 kPa for Samples not previously Tested for M_r at Suction of 25 kPa

Table 7.2 - A Summary of Model Parameters and M_r Values for Tests without Previous M_r

Condition	Suction (kPa)	w(%)	k_1	k_2	k_3	R^2	M_R
Primary Drying	50	9.4	535.2	0.4209	-0.3066	0.946	62.4
Primary Wetting	50	5.3	730.2	0.4818	-0.4105	0.938	86.2
	25	9.8	567.0	0.5921	-0.7960	0.926	66.9

7.3 Effect of Suction and Stress History on Resilient Modulus

Figure 7.13 presents the M_r-(u_a-u_w) relationship, known as MRCC, at a bulk stress of approximately 154.6 kPa (22.5 psi) and at an octahedral stress of 14 kPa (2 psi). This figure shows the M_r results from stage tests conducted continuously on a sample at each target suction superimposed with results from tests performed on similar virgin samples without previous M_r testing. As noted previously, data for continuous M_r tests in Figure 7.13 indicate that the MRCC relationship of compacted soil, due to wetting and drying, is hysteretic; i.e., M_r values on the wetting curves were higher than that on the drying curves.

Results from three virgin samples without previous (w o/p M_r) M_r testing compare favorably with the results from the stage tested samples (CM_r) at each suction value. This comparison shows that M_r is slightly lower for tests (w o/p M_r) than (CM_r) tests.

Possible reasons for higher M_r on primary wetting (PW) than the primary drying (PD) and secondary drying (SD) curves are discussed in the following paragraph. But before presenting these factors, a brief summary of some related studies on the effect of hysteresis on M_r is first presented.

As mentioned previously, no research has been found in the literature on the effect of suction hysteresis on M_r; some studies have been conducted on the effects of moisture hysteresis on M_r and different conclusions were drawn. For example, Khoury and Khoury (2009) and Khoury et al. (2009) observed that the M_r-moisture content relationship, for clayey soil, exhibited a hysteretic behavior due to the wetting and drying actions where M_r on the

drying curve seemed higher than that of the wetting curve. Other research studied the effect of suction hysteresis on the shear strength of unsaturated soils. Thu et al. (2006), Nishimura and Fredlund (2002), Han et al. (1995), among others, reported that the drying path showed higher shear strength compared to the wetting path (for silty and clayey soils). They suggested that this difference is related to the contact area of water in the soil (less water during wetting thus less contact area between water and particles) which affects the interparticle forces and results in lower shear strength for wetting. On the other hand, a study by Khoury and Miller (2010) on the effect of hysteresis on unsaturated steel interface shear strength, using the same soil in this study, revealed that shear strength values on the wetting curve were higher than the corresponding values on the drying curves. In a related study, Galage and Uchimura (2006) reported that the soil at wetting had higher shear strength as compared to the soil at drying under same suction, for sandy-silt soil. Shemsu et al. (2005) studied the cyclic suction loading influence on the shear strength of unsaturated soil. It was concluded that specimens that underwent cyclic suction loading showed higher peak shear strength. Noteworthy is that aforementioned studies showing higher shear strength for wetting than drying have been conducted on cohesionless soil (e.g. sandy-silt), similar to the soil used in this study; however, other studies that showed higher strength on drying than wetting were conducted on cohesive fine grained soils (e.g. silty and clayey soils).

Based on the literature the findings from this study, the MRCC relationship seems to be affected by the following factors: (1) cyclic suction loading on specimens (Figure 4.2 shows the loading patterns used in this study), (2) cyclic deviator stress loading history, (3) water-particle contact area and (4) soil type. However, results from the selective samples tested without previous M_r tests confirm that the possible cyclic stress loading history may have a minor effect on the results since: a) a slight difference in

M_r was observed on tests with and without previous M_r testing, and b) the secondary drying resulted in lower M_r values than those of the primary wetting. Therefore, the stiffening effect and the possible water content lubricant effect (at same suction), due to cyclic suction (i.e., hysteresis) may be the major factors resulting in the higher M_r for wetting compared to drying. It is worth to mention that this behavior (increased stiffness with cyclic suction) for small strain stiffness (G_o) was also reported by Vassallo et al. (2007) among others.

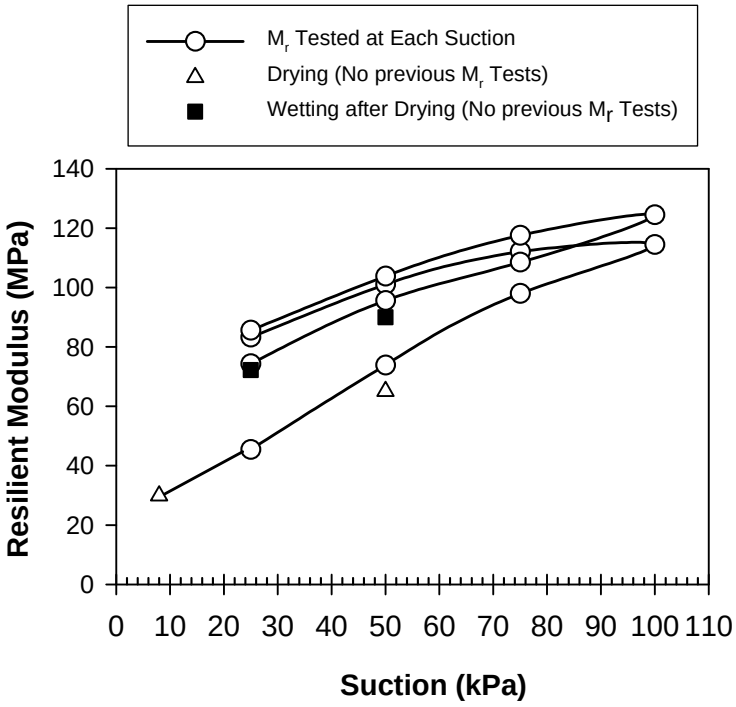

Figure 7.13 - Resilient Modulus Characteristic Curve (MRCC) at Net Confining Stress of 41 kPa and Deviator Stress of 28 kPa on Samples with and without previous M_r Tests

8. MODELING RESILIENT MODULUS

As previously discussed in Section 2.2, various research studies have been conducted to predict M_r values with suction. Recent relevant models were presented by Yang et al. (2005), Gupta et al. (2007) and Cary and Zapata (2010) most of which maybe be able to predict M_r values only at a specific

suction or due to moisture variations (e.g. Liang et al. 2007), but none can capture the effect of suction hysteresis (drying/wetting) on M_r. In addition, most of these models are based on regression analysis on specific types of soils. Therefore, in this study the results from suction-controlled M_r tests including drying and wetting (hysteresis) were used to develop models to predict M_r values due to drying and due to hysteresis (wetting after drying) based on the SWCC.

In this study, M_r results were plotted versus suction and defined the MRCC (Figure 8.1). Noteworthy to mention is that MRCC results were obtained from the same sample with M_r tests conducted along drying and wetting. This may best simulate the actual field conditions under seasonal and traffic loading variations, rather than conducting M_r at specific suction on different samples without previous M_r testing.

As previously discussed, M_r increased with increase of suction along the drying curve, a behavior modeled as shown in Equation (8.1), which is a modification of the universal model to account for variation of suction.

$$M_R = \left(k_1 p_a \times \frac{\theta_b}{p_a}^{k_2} \times (\frac{\tau}{p_a} + 1)^{k_3} \right) + (\psi - \psi_o) \left(\frac{\theta_d}{\theta_s} \right)^{\frac{m}{a}} \qquad \textbf{(8.1)}$$

where: the first part $\left(k_1 p_a \times \frac{\theta_b}{p_a}^{k_2} \times (\frac{\tau}{p_a} + 1)^{k_3} \right)$ represents the universal model equation, ψ = suction, ψ_o = low suction corresponding to the M_r test (e.g. wet of optimum), θ_d = volumetric water content along the drying curve, θ_s = initial volumetric water content (obtained from SWCCs), *m* and *a* are model parameters obtained from Fredlund and Xing (1994) fitting model (Equation 6.3) of SWCC.

The second part $(\psi - \psi_o) \left(\frac{\theta_d}{\theta_s} \right)^{\frac{m}{a}}$ of equation (8.1), aims at capturing the contribution of suction to the increase in M_r. By conducting an M_r test at any

low suction value (defined as ψ_o), the rest of the drying curve can be predicted using the proposed model, which relates to the SWCC. Thus, the initial suction (ψ_o) was subtracted from the suction term (ψ) in the equation; suction is multiplied by the ratio (θ_d/θ_s), which accounts for the change in water content with suction along the drying curve similar to the approach by Vanapalli et al. (1996) for the shear strength. Then, the use of this volumetric water content ratio was subjected to the power of (*m/a*), which represents the increase in suction with water content from the fitting equation for the SWCC. In fact, "*a*" is a soil parameter related to the AEV of the soil, and "*m*" is related to the residual water content portion of the SWCC curve. Thus, as parameter *"a"* increases or *"m"* decreases, the shape of SWCC above the air entry value (AEV) shifts upward (i.e. at specific water content or suction increase), which dictates stiffer behavior. This is also consistent in the proposed equation, a decrease in the ratio (*m/a*, i.e. decrease in *m* or increase in *a*) results in an increase of M_r, with the fact that ($\theta_d < \theta_s$).

To further appreciate the potential of the model to capture the effect of suction increase on M_r, the predicted results along the drying path are plotted together with the experimental data as shown in Figure 8.1. In this figure it is apparent that the model matches the experimental M_r results.

The model was further expanded to predict the M_r results due to hydraulic hysteresis (wetting after drying). The proposed model is shown as Equation (8.2), from which M_r hysteresis can be predicted by relating directly to the hysteretic behavior of the SWCC.

$$M_R = \left[\left(k_1 p_a \times \frac{\theta_b}{p_a}^{k_2} \times (\frac{\tau}{p_a} + 1)^{k_3} \right) + (\psi - \psi_o) \left(\frac{\theta_d}{\theta_s} \right)^{\frac{m}{a}} \right] \left(\frac{\theta_d}{\theta_w} \right) \qquad \textbf{(8.2)}$$

Where: θ_d = volumetric water content along the drying curve, θ_w = volumetric water content along the wetting curve corresponding to same

suction as for θ_d. The first part of the equation $\left[\left(k_1 p_a \times \frac{\theta_b}{p_a}^{k_2} \times (\frac{\tau}{p_a}+1)^{k_3}\right)+(\psi-\psi_o)\left(\frac{\theta_d}{\theta_s}\right)^{\frac{m}{a}}\right]$ represents the M_r prediction along the drying curve, which is multiplied by the term (θ_d/θ_w) to give the values of M_r on the wetting path. The proposed formulation (i.e. multiplying the drying results by the ratio θ_d/θ_w) seems to capture the effect of hysteresis. Predicted M_r values from the proposed Equation (8.2) compared to the experimental data at two different stress levels are shown in Figures 8.2 and 8.3, and indicate strong agreement between the results. Model parameters, k_1, k_2 and k_3 are summarized in Table 7.1, while parameters *m* and *a* are equal to 4.0 and 82.5, respectively.

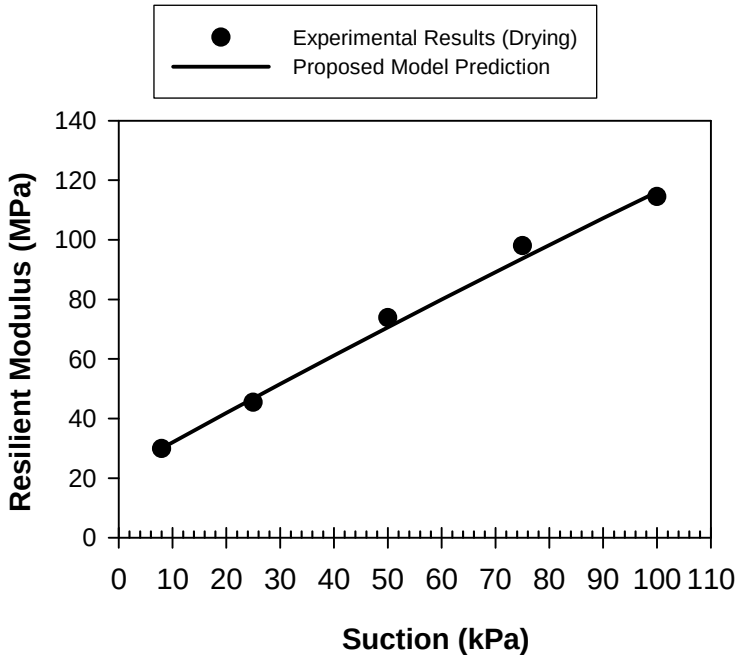

Figure 8.1 - Comparison of Predicted MRCC using the Proposed Model with the Experimental MRCC from Drying Tests

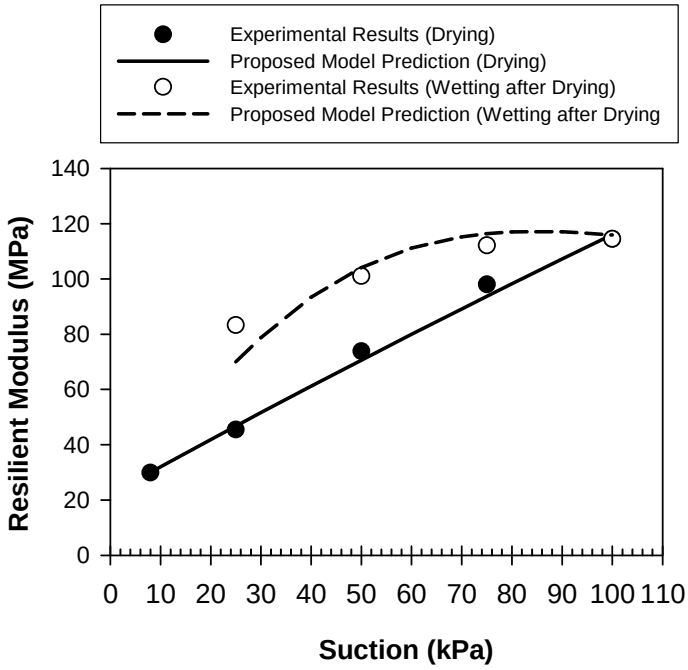

Figure 8.2 - Comparison of Predicted MRCC using the Proposed Model with the Experimental MRCC from both Drying and Wetting after Drying Tests at Net Confining Stress of 41 kPa and Deviator Stress of 28 kPa

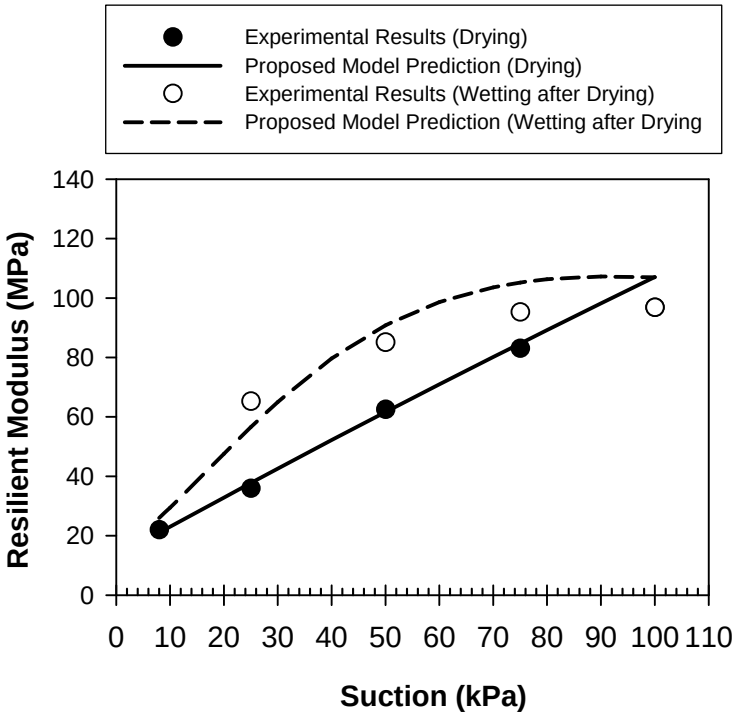

Figure 8.3 - Comparison of Predicted MRCC using the Proposed Model with the Experimental MRCC from both Drying and Wetting after Drying Tests at Net Confining Stress of 14 kPa and Deviator Stress of 68 kPa

9. CONCLUSIONS AND RECOMMENDATIONS

The primary of objective of this research was to study the effect of hydraulic hysteresis (i.e. SWCC suction hysteresis) on the Resilient Modulus (M_r) of fine-grained cohesionless soil. To this end, suction-controlled M_r tests were performed, on compacted samples, along the primary drying, primary wetting, secondary drying and secondary wetting paths. Two test types were performed to check the effect of cyclic deviatoric stress loading history on the results. The first set of M_r tests were performed on the same sample (stage-loaded) at each suction (i.e. 25, 50, 75, 100 kPa) value along all different SWCC paths. A relationship between resilient modulus (M_r) and matric suction was obtained and identified as the resilient modulus characteristic curve (MRCC). The second set of M_r tests were performed at selected suction on virgin samples without previous M_r tests to study the effect of cyclic deviator stress loading history on the results. In order to study the effect of hydraulic hysteresis on the M_r results, it is crucial to first understand the hysteretic behavior of the SWCC and its effect on M_r. Thus, laboratory tests of SWCCs under different stresses along the drying, wetting, secondary drying, and along scanning curves were performed and presented. Conclusions and recommendations for future research are summarized in the following sections.

9.1 Soil Water Characteristic Curve Conclusions

SWCC experimental tests were conducted in a custom-made one-dimensional testing cell to examine the coupled mechanical-hydraulic behavior of artificial unsaturated silty soil. Experimental techniques were developed and employed, which proved to be very valuable in the timely completion of testing. Some conclusions follow.

1) Use of an artificial soil composed of crushed silica and glass beads, having a grain size distribution similar to fine sandy silt, enabled a

significant number of SWCC tests to be conducted in a relatively short amount of time. The main advantage of this soil is that it has a relatively high hydraulic conductivity but similar suction compared to typical natural soils with similar gradations.

2) A new approach was developed to reduce SWCC testing time. A series of SWCC tests were performed on different sample heights (e.g., 1" and ¼"). Results indicated that significant time gains (i.e., testing time was reduced by 50 % when the sample height was reduced from 1" to ¼") were achieved using relatively thin samples without sacrificing accuracy with respect to volume change measurements.

3) Experimental results of SWCCs revealed that the air entry value tended to increase as the net normal stress increased, as expected given the decreased void ratio at higher net normal stress. The residual moisture content also increased with increases in net normal stress.

4) As the water contents approached residual saturation the slope of the SWCCs tended to change with increase in net normal stress. The volumetric water content corresponding to a net normal stress of 200 kPa was higher than on the corresponding curve for 10 kPa net normal stress at the same suction. The constitutive model reported by Miller et al. (2008) appeared to capture this behavior quite well.

5) The SWCC curve fitting models of Fredlund and Xing (1994) and Feng and Fredlund (1999) were found to fit very well the experimental data obtained during wetting and drying SWCC testing.

9.2 Resilient Modulus Conclusions

Laboratory testing of suction-controlled resilient modulus tests were conducted on unsaturated soils (fine grained artificial soil). The results

showed a relationship between resilient modulus and suction referred to as the M_R characteristic curve (MRCC). The conclusions and observations based on the results are summarized as follows:

1) Resilient modulus (M_R) slightly increased with increase in deviator stress (σ_d). This increase seems dependent on suction where a more pronounced increase is observed at higher suction values.
2) Resilient modulus tends to increase with an increase in matric suction. This increase was attributed to the fact that higher soil suction results in stiffening of the specimens.
3) The MRCC exhibited a hysteretic behavior similar to that of the SWCC. However, for a given suction, M_R values on MRCC on the wetting curve are higher than that on the drying curve for the coheshionless soil used.
4) Duplicate suction controlled M_R tests on the primary drying and wetting paths demonstrate that the MRCC is reproducible to reasonable accuracy.
5) Selected virgin samples (i.e. at specific suction of 25 and 50 kPa, on drying and wetting) were tested without previous M_r testing. Corresponding results compared favorably with the results from the stage-loaded samples tested continuously at each suction value. This indicates that the cyclic deviatoric stress loading history had a minor effect on the results.
6) It is believed that the suction stress history and the possible water content lubricant effect (at same suction), due to cyclic suction (i.e., hysteresis) may be the reason for higher M_r on wetting compared to drying. This observation for the cohesionless test soil used in this study is consistent with limited observations on the influence of suction hysteresis on cohesionless soils in the literature. However,

observations from the literature suggest that for cohesive soils, strength and stiffness is higher on wetting than on drying.

7) A model was proposed to predict M_r along the drying and wetting curves based on the SWCC. The proposed model provides reasonably good predictions of M_r due to hydraulic hysteresis (i.e. SWCC suction hysteresis, or cyclic suction loading) for all stress levels.

9.3 Recommendations

1) The present study used an artificial soil for testing. However, unsaturated natural soils are also very widespread throughout the world and the behavior of these natural soils may be different to that of compacted artificial soils (because of the different soil structures). Therefore, experimental research should be carried out to on different types of materials such as clayey natural soils. However, the experimental challenges (long equilibrium times, high suctions) with cohesive soils are likely to prohibit a study of similar scope to that described herein, given the state of technology at this point in time.
2) Compare the influence of hydraulic hysteresis on natural clayey soils to the results on the artificial soil obtained in this study. Develop a complete framework for analysis of the effect of hydraulic hysteresis on different type of soils (i.e., natural sands, silts and clays) for which the behavior is expected to be significantly different.
3) Regarding the first two recommendations, the challenges are monumental in experimentally observing the impact of hydraulic hysteresis on clayey soils. Test methods on fine-grained cohesive soils (e.g. clayey soils) require extremely long equilibrium times to produce changes in suction, which practically prohibits routine examination of the hydraulic hysteresis and its influence on resilient modulus. Research is needed to develop innovative test methods to overcome this problem. One such innovative method that the current principal

investigators will soon explore is a miniature suction controlled unsaturated triaxial apparatus compatible with very small samples. This research will pioneer advanced testing of unsaturated soils whereby suction controlled resilient modulus tests on fine grained soils will be practical. The equipment will not be limited to resilient modulus testing, but will be fully capable of conducting traditional large strain quasi-static shear tests on soils.

4) Use and validate the proposed M_r model from this study to predict M_r based on the experimental results obtained on natural soils.
5) Based on results from various soil types, formalize recommendations to consider suction hysteresis in the selection of subgrade resilient modulus used in pavement design.

9.4 Implementation/Technology Transfer

The results of this research are just the beginning of work that examines the importance of hysteresis (wetting/drying cycles) on the resilient modulus of unsaturated subgrade soils. As this body of work grows it is expected that this aspect of soil behavior will be incorporated into integrated climatic modeling of subgrade properties. This work along with a handful of other studies has set the stage for its eventual implementation. There is much work to be done, particularly on clayey subgrade soils. This work was presented at the TRB 2011 Annual Meeting and was well received. The accompanying paper manuscript was accepted for publication in the 2011 Transportation Research Record. It is difficult to get published in the TRB Journal, which indicates the value of this work by people knowledgeable about the topic.

10. REFERENCES

Adamson, A. W., (1990), "Physical Chemistry of Surfaces," 5th Edition, Wiley Interscience, New York.

American Association of State Highway and Transportation Officials, (AASHTO) (2007), http://www.mrr.dot.state.mn.us/pavement/PvmtDesign/designguide.asp, accessed February, 2008.

ASCE (2007), "Infrastructure Report Card 2005, Oklahoma, "http://www.asce.org/reportcard/2005/page.cfm?id=76, accessed February, 2008.

Barbour, S. L., (1998), "Nineteenth Canadian Geotechnical Colloquium: The Soil Water Characteristic Curve: a Historical Perspective," Canadian Geotechnical Journal, 35, pp. 873-894.

Bear, J., (1972), "Dynamics of Fluids in Porous Media," Dover Publications, Inc., New York.

Bishop, A.W., 1959, "The Principle of Effective Stress," *Teknisk Ukeblad*, Vol. 106, No. 39, pp. 859-863.

Brooks, R.H., and A.T. Corey., (1964), "Hydraulic properties of porous media. Hydrology Paper 3. Colorado State Univ., Fort Collins.

Cary, C. E., Zapata, C. E., (2010), "Resilient Modulus Testing for Unsaturated Unbound Materials," Transportation Research Board: Journal of Transportation Research Board, TRB, Washington D.C., August 2010.

Ceratti, G. A., Gehling, W. Y. Y., and Nunez, W. P. (2004), " Seasonal Variations of Subgrade Soil Resilient Modulus in Southern Brazil," Transportation Research Board: Journal of Transportation Research Board, No. 1874, TRB, Washington D.C., pp. 165-173.

Dafalias, Y.F. and E.P. Popov, (1975), "A model of nonlinearly hardening materials for complex loading," *Acta Mechanica*, *21*, pp. 173-192.

Dafalias, Y.F. and E.P. Popov, (1976), "Plastic internal variables formalism of cyclic plasticity," *Journal of Applied Mechanics*, *43*, pp. 645-651.

Drumm, E. C., and Desai, C. S., (1986), "Determination of Parameters for a Model for the Cyclic Behavior of Interfaces," *Earthquake Engineering and Structural Dynamics*. Vol. 14, pp.1-18.

Edris, E. V., Jr., and Lytton, R. L. (1976). "Dynamic properties of subgrade soils including environmental effects." *Texas Transportation Institute Rep. No. TTI-2-18-74-164-3*, Texas A&M Univ., College Station, Texas.

Feng, M. and D.G. Fredlund (1999), "Hysteretic influence associated with thermal conductivity sensor measurements," *Proceedings from Theory to the Practice of Unsaturated Soil Mechanics, in associated with 52nd Can. Geotech. Conference and Unsaturated Soil Group*, Regina.

Fredlund, D.G., and Xing, A., (1994), "Equations for the Soil Water Characteristic Curve," Canadian Geotechnical Journal, 31, pp. 521-532.

Gupta, S, Ranaivoson, A., Edil, T., Benson, C., and Sawangsuriya, A, (2007), "*Pavement Design Using Unsaturated Soil Technology,"* Minnesota Department of Transportation, St. Paul, Minnesota, pp. 1-104.

Han, K.K., Rahardjo, H., and Broms, B.B., (1995), "Effect of hysteresis on the shear strength of a residual soil," *Proceeding of the first international conference on unsaturated soils*, Paris, 2, pp. 499–504.

Ho, K.M.Y., Ng, C.W.W., Ho, K.K.S. and W.H. Tang (2006), "State-dependent Soil-water Characteristic Curves (SDSWCCs) of Weathered Soils," Proc. of UNSAT 2006, ASCE, pp. 1302-1313.

Galage, C. P. K., Uchimura, T., (2006), "Effects of Wetting and Drying on the Unsaturated Shear Strength of a Silty Sand Under Low Suction," *Proceedings of the Fourth International Conference of Unsaturated Soils*, ASCE, Carefree, Arizona, pp. 1247-1258.

Gallipoli, D., A. Gens, R. Sharma and J. Vaunat (2003), An elasto-plastic model for unsaturated soil incorporating the effects of suction and degree of saturation on mechanical behavior, *Géotechnique,53(1), 123-135.*

Karube, D. and K. Kawai (2001), "The role of pore water in the mechanical behavior of unsaturated soils," *Geotechnical and Geological Engineering,* 19, 211-241.

Khoury, N. K., Brooks, R., Zaman, M., Khoury, C. K., (2009), "Variations of Resilient Modulus of Sub-grade Soils with Post-Compaction Moisture Contents," *Transportation Research Record: Journal of the Transportation*

Research Board. Transportation Research Board of the National Academies, Washington D.C.

Khoury, C. K., Khoury, N. K., (2009), "The effect of Moisture Hysteresis on Resilient Modulus of Subgrade Soil," *Eighth International Conference on the Bearing Capacity of Roads, Railways, and Airfields*, Champaign, Illinois, USA.

Khoury, C. N., and Miller G. A. (2010), " Effect of Suction Hysteresis on the Shear Strength of Unsaturated Soil Interfaces, " Fifth International Conference on Unsaturated Soils, September 2010, Barcelona, Spain, in press.

Khoury, N. N., and Zaman, M., (2004), "Correlation Among Resilient Modulus, Moisture Variation, and Soil Suction for Subgrade Soils," *Transportation Research Record. 1874*, Transportation Research Board, Washington, D.C., 99–107.

Khoury, N. N., Zaman, M., Nevels, J. B., and Mann, J. (2003). "Effect of soil suction on resilient modulus of subgrade soil using the filter paper technique." *Proc., Transportation Research Board,* National Research Council, Washington, D.C.

Kohgo, Y., (2008), "A Hysteresis Model of Soil Water Retention Curves Based on Bounding Surface Concept," Soils and Foundations, 58 (5), pp. 633-640.

Kung, J. H. S., Lin, H. D., Yang, S. J. and Huang. W. H., (2006), "Resilient Modulus and Plastic Strain of Unsaturated Cohesive Subgrade Soils." The 4th International Conference on Unsaturated Soils, ASCE, Arizona, Vol. 1, pp. 541-552.

Larson, G., and Dempsey, B. J. (1997). "Integrated climatic model, Version 2.0." *Rep. No. DTFA MN/DOT 72114*, Univ. of Illinois at Urbana- Champaign and Newmark Civil Engineering Laboratory, Urbana, Ill.

Leong, E. C., Rahardjo, H., (1997), "Review of Soil Water Characteristic Curve Equations," *Journal of Geotechnical and Geoenvironmental Engineering*, ASCE, Vol. 123, No. 12, pp 1106-1117.

Li, X.S., (2007a), Thermodynamics-based constitutive framework for unsaturated soils 1: Theory, *Géotechnique*, *57(5)*, pp. 411-422.

Li, X.S., (2007b), "Thermodynamics-based Constitutive Framework for Unsaturated Soils 2: A Basic Triaxial Model," *Geotechnique*, *57(5)*, pp. 423-435.

Liang, R. Y., Rabab'ah, S., and Khasawneh, M., (2007), "Predicting Moisture Content-Dependent Resilient Modulus of Cohesive Soils Using Soil Suction Concept," Journal of Transportation Engineering, ASCE, Vol. 134, No. 1.

Lu, N. and W.J. Likos (2004), *Unsaturated Soil Mechanics*, Wiley, New York.

Marshal, T. J., Holmes, J. W., Rose, C. W., (1996), Soil Physics, third edition. Cambridge: Cambridge, University Press.

Miller, G. A., Khoury, C. N., Muraleetharan, K. K., Liu, C., and Kibbey, T. C. G. (2008), "Effects of Solid Deformations on Hysteretic Soil Water Characteristic Curves: Experiments and Simulations," *Water Resources Research Journal, 44, W00C06, doi:10.1029/2007WR006492.*

Motan, S. E., and Edil, T. B., (1982), "Repetitive-Load Behavior of Unsaturated Soils," *Transportation Research Record*, No. 872, Washington, D.C., pp. 41-48.

Muraleetharan, K.K., Liu, C., Wei, C.F., Kibbey, T.C.G. and Chen, L., (2008), "An elastoplastic framework for coupling hydraulic and mechanical behavior of unsaturated soils," *Int. J. Plasticity*, 25, 473-490.

Nishimura, T., and Fredlund, D. G., (2002), "Hysteresis Effects Resulting from Drying and Wetting under Relatively Dry Conditions," *Proceeding of the third international conference on Unsaturated soils*, Recife, Brazil, pp.301-305.

Oklahoma Transportation Center (OTC) (2007), "University Transportation Center Strategic Plan," U.S Department of Transportation, Oklahoma. http://www.oktc.org/OTCv3/OTC_Strategic_Plan/OTC%20Strategic%20Plan.htm.

Vanapalli, S.K., Fredlund, D.G., and Pufahl, D.E., (1999), "The Influence of Soil Structure and Stress History on the Soil Water Characteristic Curve of a Compacted Till," Geotechnique, 49, No. 2, pp. 143-159.

Pham, H. Q., Fredlund , D.G., and Barbour, S. L., (2005), "A Study of Hysteresis Models for Soil Water Characteristic Curves," Canadian Geotechnical Journal, 42, No. 6, pp. 1548-1568.

Romero, E., A. Gens, and A. Lloret (1999), Water permeability, water retention and microstructure of unsaturated compacted Boom clay, *Engineering Geology*, 54, 117–127.

Shemsu, K. A., Kiyama, S., Aoyama, S., Kobayashi, A., (2005), "Experimental Study of the Effect of Cyclic Suction Loading on Shearing Behavior of Collapsible Soils," *Proceedings of the International Symposium on Advanced Experimental Unsaturated Soil Mechanics*, Trento, Italy, pp. 235-241.

Sun, D.A., D.C. Sheng, H.B. Cui and S.W. Sloan, (2007), "A Density-dependent Elastoplastic Hydro-mechanical Model for Unsaturated Compacted Soils," *International Journal for Numerical and Analytical Methods in Geomechanics*. *31*, pp. 1257-1279.

Tarantino, A. and S. Tombolato (2005), "Coupling of hydraulic and mechanical behaviour in unsaturated compacted clay," *Géotechnique*, 55(4), 307–317.

Van Genuchten, (1980), "A closed form equation for predicting the hydraulic conductivity of unsaturated soils," Soil Science Society of America Journal, 44, pp. 892–898.

Vanapalli, S.K., Fredlund, D.G., and Pufahl, D.E., (2001), "Influence of Soil Structure and Stress History on the Soil Water Characteristics of a Compacted Till," Geotechnique, Discussion. Vol. LI, 6, pp. 573-576.

Vanapalli, S.K., Fredlund, D.G., Pufahl, D.E., and Clifton, A.W. (1996), "Model for the Prediction of Shear Strength with Respect to Soil Suction," Canadian Geotechnical Journal, 33, pp. 379-392.

Vassallo, R., Mancuso, C., Vinale, F., (2007), "Effects of net stress and suction history on the small strain stiffness of a compacted clayey silt," Canadian Geotechnical Journal, Vol. 44, pp. 447-462.

Yang, S. J. Huang. W. H., and Tai, Y. T. (2005). "Variation of Resilient Modulus with Soil Suction for Compacted Subgrade Soils." *Proc., Transportation Research Board* Annual Meeting, Washington, D.C.

Yang, S. R., Lin, H. D., Kung, J. H. S., Huang, W. H., (2008), "Suction-Controlled Laboratory Test on Resilient Modulus of Unsaturated Compacted Subgrade Soils," *Journal of Geotechnical and Geo-environmental Engineering*, Vol. 134, No. 9, pp. 1375-1384.

Thu, T. M., Rahardjo, H., and Leong, E. C., (2006), "Effects of Hysteresis on Shear Strength Envelopes from Constant Water Content and Consolidated Drained Triaxial Tests," *Proceedings of the Fourth International Conference of Unsaturated Soils*, ASCE, Carefree, Arizona, pp. 1212-1222.

Yuan, D. and Nazarian, S. Variation in Moduli of Base and Subgrade with Moisture, CD-ROM, Transportation Research Board of the National Academies, Washington D.C., 2003.

Wei, C. and M.M. Dewoolkar, (2006), "Formulation of Capillary Hysteresis with Internal State Variables," *Water Resources Research*, *42*, W07405.

Wheeler, S.J., R.S. Sharma and M.S.R. Buisson (2003), "Coupling of hydraulic hysteresis and stress-strain behavior in unsaturated soils," *Géotechnique*, *53(1)*, 41-53.

11. APPENDIX – SUMMARY OF RESILIENT MODULUS TEST RESULTS

11.1 Summary of M_r Results for Samples Continuously Tested for M_r along the Drying and Wetting Curves

Table 11.1- Summary of M_r Results at Suction of 8 kPa along the Primary Drying Curve

Column #	1	2	3	4	5	6	7	8	9	10	11	12	13
Parameter	Chamber Confining Pressure	Nominal Maximum Axial Stress	Actual Applied Max. Axial Load	Actual Applied Cyclic Load	Actual Applied Contact Load	Actual Applied Max. Axial Stress	Actual Applied Cyclic Stress	Actual Applied Contact Stress	Recov. Def. LVDT # 1 Reading	Recov. Def. LVDT # 2 Reading	Average Recov. Def. LVDT 1 & 2	Resilient Strain	Resilient Modulus
Designation	S3	Scyclic	Pmax	Pcyclic	Pcontact	Smax	Scyclic	Scontact	H1	H2	Havg	er	Mr
Unit	kPa	kPa	N	N	N	kPa	kPa	kPa	mm	mm	mm	mm/mm	MPa
Precision	—	—	—	—	—	—	—	—	—	—	—	—	—
Sequence 1	41	13.8	52.98	46.28	6.70	13.58	11.86	1.72	0.0596	0.0606	0.0601	0.00043	28
Sequence 2	41	27.6	107.16	95.56	11.60	27.46	24.49	2.97	0.1150	0.1168	0.1159	0.00082	30
Sequence 3	41	41.3	158.34	142.44	15.90	40.58	36.50	4.07	0.1704	0.1716	0.1710	0.00121	30
Sequence 4	41	55.1	214.72	192.72	22.00	55.03	49.39	5.64	0.2388	0.2408	0.2398	0.00170	29
Sequence 5	41	68.9	273.28	246.38	26.90	70.04	63.14	6.89	0.0360	0.3094	0.1727	0.00204	31
Sequence 6	28	13.8	54.78	49.88	4.90	14.04	12.78	1.26	0.0802	0.0818	0.0810	0.00057	22
Sequence 7	28	27.6	109.40	99.00	10.40	28.04	25.37	2.67	0.1600	0.1618	0.1609	0.00114	22
Sequence 8	28	41.3	163.72	146.62	17.10	41.96	37.58	4.38	0.2250	0.2252	0.2251	0.00159	24
Sequence 9	28	55.1	220.18	198.78	21.40	56.43	50.94	5.48	0.2880	0.2908	0.2894	0.00205	25
Sequence 10	28	68.9	276.62	248.52	28.10	70.89	63.69	7.20	0.3398	0.3422	0.3410	0.00242	26
Sequence 11	14	13.8	55.16	49.06	6.10	14.14	12.57	1.56	0.0924	0.0956	0.0940	0.00067	19
Sequence 12	14	27.6	109.16	97.56	11.60	27.98	25.00	2.97	0.1774	0.1812	0.1793	0.00127	20
Sequence 13	14	41.3	167.20	149.50	17.70	42.85	38.31	4.54	0.2526	0.2550	0.2538	0.00180	21
Sequence 14	14	55.1	217.66	195.06	22.60	55.78	49.99	5.79	0.3004	0.3040	0.3022	0.00214	23
Sequence 15	14	68.9	274.56	245.86	28.70	70.36	63.01	7.36	0.3564	0.3600	0.3582	0.00254	25
* Reported results are based on the average of the last 5 cycles of each load sequence													

Table 11.2- Summary of M_r Results at Suction of 25 kPa along the Primary Drying Curve

Column #	1	2	3	4	5	6	7	8	9	10	11	12	13
Parameter	Chamber Confining Pressure	Nominal Maximum Axial Stress	Actual Applied Max. Axial Load	Actual Applied Cyclic Load	Actual Applied Contact Load	Actual Applied Max. Axial Stress	Actual Applied Cyclic Stress	Actual Applied Contact Stress	Recov. Def. LVDT # 1 Reading	Recov. Def. LVDT # 2 Reading	Average Recov. Def. LVDT 1 & 2	Resilient Strain	Resilient Modulus
Designation	S3	Scyclic	Pmax	Pcyclic	Pcontact	Smax	Scyclic	Scontact	H1	H2	Havg	er	Mr
Unit	kPa	kPa	N	N	N	kPa	kPa	kPa	mm	mm	mm	mm/mm	MPa
Precision	—	—	—	—	—	—	—	—	—	—	—	—	—
Sequence 1	41	13.8	55.42	49.32	6.10	14.20	12.64	1.56	0.0414	0.0388	0.0401	0.00028	45
Sequence 2	41	27.6	107.76	96.76	11.00	27.62	24.80	2.82	0.0780	0.0762	0.0771	0.00055	45
Sequence 3	41	41.3	162.50	146.00	16.50	41.65	37.42	4.23	0.1178	0.1122	0.1150	0.00081	46
Sequence 4	41	55.1	216.70	194.70	22.00	55.54	49.90	5.64	0.1560	0.1494	0.1527	0.00108	46
Sequence 5	41	68.9	273.40	246.50	26.90	70.07	63.17	6.89	0.1934	0.1872	0.1903	0.00135	47
Sequence 6	28	13.8	53.70	48.20	5.50	13.76	12.35	1.41	0.0532	0.0514	0.0523	0.00037	33
Sequence 7	28	27.6	111.34	99.14	12.20	28.53	25.41	3.13	0.1094	0.1060	0.1077	0.00076	33
Sequence 8	28	41.3	168.58	163.08	5.50	43.20	41.79	1.41	0.1524	0.1474	0.1499	0.00119	35
Sequence 9	28	55.1	223.52	200.92	22.60	57.28	51.49	5.79	0.1916	0.1858	0.1887	0.00134	39
Sequence 10	28	68.9	274.78	246.68	28.10	70.42	63.22	7.20	0.2268	0.2200	0.2234	0.00158	40
Sequence 11	14	13.8	55.78	50.28	5.50	14.30	12.89	1.41	0.0716	0.0702	0.0709	0.00050	26
Sequence 12	14	27.6	113.26	102.86	10.40	29.03	26.36	2.67	0.1372	0.1330	0.1351	0.00096	28
Sequence 13	14	41.3	169.58	153.68	15.90	43.46	39.38	4.07	0.1788	0.1738	0.1763	0.00125	32
Sequence 14	14	55.1	221.30	199.30	22.00	56.71	51.08	5.64	0.2162	0.2092	0.2127	0.00151	34
Sequence 15	14	68.9	275.78	247.68	28.10	70.68	63.48	7.20	0.2546	0.2448	0.2497	0.00177	36
* Reported results are based on the average of the last 5 cycles of each load sequence													

Table 11.3- Summary of M_r Results at Suction of 50 kPa along the Primary Drying Curve

Column #	1	2	3	4	5	6	7	8	9	10	11	12	13
Parameter	Chamber Confining Pressure	Nominal Maximum Axial Stress	Actual Applied Max. Axial Load	Actual Applied Cyclic Load	Actual Applied Contact Load	Actual Applied Max. Axial Stress	Actual Applied Cyclic Stress	Actual Applied Contact Stress	Recov. Def. LVDT # 1 Reading	Recov. Def. LVDT # 2 Reading	Average Recov. Def. LVDT 1 & 2	Resilient Strain	Resilient Modulus
Designation	S3	Scyclic	Pmax	Pcyclic	Pcontact	Smax	Scyclic	Scontact	H1	H2	Havg	er	Mr
Unit	kPa	kPa	N	N	N	kPa	kPa	kPa	mm	mm	mm	mm/mm	MPa
Precision	—	—	—	—	—	—	—	—	—	—	—	—	—
Sequence 1	41	13.8	56.56	49.26	7.30	14.50	12.62	1.87	0.0330	0.0320	0.0325	0.00023	75
Sequence 2	41	27.6	112.18	99.98	12.20	28.75	25.62	3.13	0.0500	0.0480	0.0490	0.00035	74
Sequence 3	41	41.3	190.90	173.20	17.70	48.92	44.39	4.54	0.0882	0.0836	0.0859	0.00061	73
Sequence 4	41	55.1	220.42	196.62	23.80	56.49	50.39	6.10	0.0988	0.0940	0.0964	0.00068	74
Sequence 5	41	68.9	277.82	250.32	27.50	71.20	64.15	7.05	0.1210	0.1142	0.1176	0.00083	77
Sequence 6	28	13.8	54.78	48.68	6.10	14.04	12.48	1.56	0.0314	0.0314	0.0314	0.00022	56
Sequence 7	28	27.6	112.30	100.10	12.20	28.78	25.65	3.13	0.0664	0.0650	0.0657	0.00047	55
Sequence 8	28	41.3	165.76	149.26	16.50	42.48	38.25	4.23	0.0912	0.0890	0.0901	0.00064	60
Sequence 9	28	55.1	223.64	201.64	22.00	57.31	51.68	5.64	0.1144	0.1094	0.1119	0.00079	65
Sequence 10	28	68.9	277.82	250.32	27.50	71.20	64.15	7.05	0.1350	0.1286	0.1318	0.00093	69
Sequence 11	14	13.8	57.02	50.32	6.70	14.61	12.90	1.72	0.0396	0.0404	0.0400	0.0003	46
Sequence 12	14	27.6	113.02	100.82	12.20	28.96	25.84	3.13	0.0780	0.0764	0.0772	0.0005	47
Sequence 13	14	41.3	171.26	153.56	17.70	43.89	39.35	4.54	0.1088	0.1042	0.1065	0.0008	52
Sequence 14	14	55.1	224.96	202.36	22.60	57.65	51.86	5.79	0.1282	0.1232	0.1257	0.0009	58
Sequence 15	14	68.9	280.18	252.08	28.10	71.80	64.60	7.20	0.1500	0.1420	0.1460	0.0010	62
* Reported results are based on the average of the last 5 cycles of each load sequence													

Table 11.4- Summary of M_r Results at Suction of 75 kPa along the Primary Drying Curve

Column #	1	2	3	4	5	6	7	8	9	10	11	12	13
Parameter	Chamber Confining Pressure	Nominal Maximum Axial Stress	Actual Applied Max. Axial Load	Actual Applied Cyclic Load	Actual Applied Contact Load	Actual Applied Max. Axial Stress	Actual Applied Cyclic Stress	Actual Applied Contact Stress	Recov. Def. LVDT # 1 Reading	Recov. Def. LVDT # 2 Reading	Average Recov. Def. LVDT 1 & 2	Resilient Strain	Resilient Modulus
Designation	S3	Scyclic	Pmax	Pcyclic	Pcontact	Smax	Scyclic	Scontact	H1	H2	Havg	er	Mr
Unit	kPa	kPa	N	N	N	kPa	kPa	kPa	mm	mm	mm	mm/mm	MPa
Precision	—	—	—	—	—	—	—	—	—	—	—	—	—
Sequence 1	41	13.8	54.90	48.20	6.70	14.07	12.35	1.72	0.0436	0.0370	0.0403	0.00013	96
Sequence 2	41	27.6	108.50	97.50	11.00	27.81	24.99	2.82	0.0400	0.0320	0.0360	0.00025	98
Sequence 3	41	41.3	164.08	147.58	16.50	42.05	37.82	4.23	0.0570	0.0470	0.0520	0.00037	103
Sequence 4	41	55.1	242.78	219.58	23.20	62.22	56.27	5.95	0.0838	0.0706	0.0772	0.00055	103
Sequence 5	41	68.9	278.18	248.28	29.90	71.29	63.63	7.66	0.0930	0.0790	0.0860	0.00061	104
Sequence 6	28	13.8	54.90	50.00	4.90	14.07	12.81	1.26	0.0252	0.0220	0.0236	0.00017	77
Sequence 7	28	27.6	111.58	101.18	10.40	28.60	25.93	2.67	0.0514	0.0442	0.0478	0.00034	77
Sequence 8	28	41.3	168.58	151.48	17.10	43.20	38.82	4.38	0.0722	0.0630	0.0676	0.00048	81
Sequence 9	28	55.1	221.44	197.64	23.80	56.75	50.65	6.10	0.0888	0.0776	0.0832	0.00059	86
Sequence 10	28	68.9	277.82	249.12	28.70	71.20	63.84	7.36	0.1038	0.0904	0.0971	0.00069	93
Sequence 11	14	13.8	55.18	50.28	4.90	14.14	12.89	1.26	0.0304	0.0276	0.0290	0.00021	63
Sequence 12	14	27.6	110.62	98.42	12.20	28.35	25.22	3.13	0.0610	0.0538	0.0574	0.00041	62
Sequence 13	14	41.3	169.10	152.00	17.10	43.34	38.95	4.38	0.0850	0.0750	0.0800	0.00057	69
Sequence 14	14	55.1	226.56	202.76	23.80	58.06	51.96	6.10	0.1030	0.0904	0.0967	0.00068	76
Sequence 15	14	68.9	282.24	253.54	28.70	72.33	64.98	7.36	0.1174	0.1034	0.1104	0.00078	83
* Reported results are based on the average of the last 5 cycles of each load sequence													

Table 11.5- Summary of M_r Results at Suction of 100 kPa along the Primary Drying Curve

Column #	1	2	3	4	5	6	7	8	9	10	11	12	13
Parameter	Chamber Confining Pressure	Nominal Maximum Axial Stress	Actual Applied Max. Axial Load	Actual Applied Cyclic Load	Actual Applied Contact Load	Actual Applied Max. Axial Stress	Actual Applied Cyclic Stress	Actual Applied Contact Stress	Recov. Def. LVDT # 1 Reading	Recov. Def. LVDT # 2 Reading	Average Recov. Def. LVDT 1 & 2	Resilient Strain	Resilient Modulus
Designation	S3	Scyclic	Pmax	Pcyclic	Pcontact	Smax	Scyclic	Scontact	H1	H2	Havg	er	Mr
Unit	kPa	kPa	N	N	N	kPa	kPa	kPa	mm	mm	mm	mm/mm	MPa
Precision	—	—	—	—	—	—	—	—	—	—	—	—	—
Sequence 1	41	13.8	56.68	49.38	7.30	14.53	12.66	1.87	0.0418	0.0360	0.0389	0.00011	112
Sequence 2	41	27.6	113.14	101.54	11.60	29.00	26.02	2.97	0.0346	0.0296	0.0321	0.00023	114
Sequence 3	41	41.3	168.08	150.38	17.70	43.08	38.54	4.54	0.0486	0.0420	0.0453	0.00032	120
Sequence 4	41	55.1	226.18	202.98	23.20	57.97	52.02	5.95	0.0630	0.0560	0.0595	0.00042	123
Sequence 5	41	68.9	278.42	249.72	28.70	71.35	64.00	7.36	0.0750	0.0670	0.0710	0.00050	127
Sequence 6	28	13.8	57.04	50.34	6.70	14.62	12.90	1.72	0.0220	0.0194	0.0207	0.00015	88
Sequence 7	28	27.6	113.02	101.42	11.60	28.96	25.99	2.97	0.0430	0.0376	0.0403	0.00029	91
Sequence 8	28	41.3	172.10	155.00	17.10	44.11	39.72	4.38	0.0620	0.0556	0.0588	0.00042	95
Sequence 9	28	55.1	228.66	205.46	23.20	58.60	52.66	5.95	0.0756	0.0690	0.0723	0.00051	103
Sequence 10	28	68.9	281.04	252.94	28.10	72.02	64.82	7.20	0.0870	0.0794	0.0832	0.00059	110
Sequence 11	14	13.8	54.30	49.40	4.90	13.92	12.66	1.26	0.0252	0.0236	0.0244	0.00017	73
Sequence 12	14	27.6	113.50	101.90	11.60	29.09	26.11	2.97	0.0532	0.0476	0.0504	0.00036	73
Sequence 13	14	41.3	170.42	153.32	17.10	43.68	39.29	4.38	0.0740	0.0654	0.0697	0.00049	80
Sequence 14	14	55.1	227.82	204.02	23.80	58.39	52.29	6.10	0.0882	0.0802	0.0842	0.00060	88
Sequence 15	14	68.9	283.32	255.82	27.50	72.61	65.56	7.05	0.0986	0.0926	0.0956	0.00068	97
* Reported results are based on the average of the last 5 cycles of each load sequence													

Table 11.6- Summary of M_r Results at Suction of 75 kPa along the Primary Wetting Curve

Column #	1	2	3	4	5	6	7	8	9	10	11	12	13
Parameter	Chamber Confining Pressure	Nominal Maximum Axial Stress	Actual Applied Max. Axial Load	Actual Applied Cyclic Load	Actual Applied Contact Load	Actual Applied Max. Axial Stress	Actual Applied Cyclic Stress	Actual Applied Contact Stress	Recov. Def. LVDT # 1 Reading	Recov. Def. LVDT # 2 Reading	Average Recov. Def. LVDT 1 & 2	Resilient Strain	Resilient Modulus
Designation	S3	Scyclic	Pmax	Pcyclic	Pcontact	Smax	Scyclic	Scontact	H1	H2	Havg	er	Mr
Unit	kPa	kPa	N	N	N	kPa	kPa	kPa	mm	mm	mm	mm/mm	MPa
Precision	—	—	—	—	—	—	—	—	—	—	—	—	—
Sequence 1	41	13.8	57.38	51.88	5.50	14.71	13.30	1.41	0.0488	0.0418	0.0453	0.00012	110
Sequence 2	41	27.6	110.14	99.14	11.00	28.23	25.41	2.82	0.0350	0.0290	0.0320	0.00023	112
Sequence 3	41	41.3	168.34	150.04	18.30	43.14	38.45	4.69	0.0500	0.0440	0.0470	0.00033	116
Sequence 4	41	55.1	223.38	200.18	23.20	57.25	51.30	5.95	0.0650	0.0566	0.0608	0.00043	119
Sequence 5	41	68.9	277.46	248.76	28.70	71.11	63.75	7.36	0.0778	0.0684	0.0731	0.00052	123
Sequence 6	28	13.8	57.16	50.46	6.70	14.65	12.93	1.72	0.0232	0.0204	0.0218	0.00015	84
Sequence 7	28	27.6	115.38	103.18	12.20	29.57	26.44	3.13	0.0478	0.0420	0.0449	0.00032	83
Sequence 8	28	41.3	168.96	151.86	17.10	43.30	38.92	4.38	0.0650	0.0584	0.0617	0.00044	89
Sequence 9	28	55.1	224.60	202.00	22.60	57.56	51.77	5.79	0.0788	0.0710	0.0749	0.00053	98
Sequence 10	28	68.9	283.20	255.10	28.10	72.58	65.38	7.20	0.0910	0.0830	0.0870	0.00062	106
Sequence 11	14	13.8	54.90	48.80	6.10	14.07	12.51	1.56	0.0292	0.0270	0.0281	0.00020	63
Sequence 12	14	27.6	111.94	99.74	12.20	28.69	25.56	3.13	0.0586	0.0532	0.0559	0.00040	65
Sequence 13	14	41.3	170.54	154.04	16.50	43.71	39.48	4.23	0.0800	0.0730	0.0765	0.00054	73
Sequence 14	14	55.1	225.68	201.88	23.80	57.84	51.74	6.10	0.0938	0.0858	0.0898	0.00064	81
Sequence 15	14	68.9	279.14	251.04	28.10	71.54	64.34	7.20	0.1040	0.0950	0.0995	0.00068	95
* Reported results are based on the average of the last 5 cycles of each load sequence													

Table 11.7- Summary of M_r Results at Suction of 50 kPa along the Primary Wetting Curve

Column #	1	2	3	4	5	6	7	8	9	10	11	12	13
Parameter	Chamber Confining Pressure	Nominal Maximum Axial Stress	Actual Applied Max. Axial Load	Actual Applied Cyclic Load	Actual Applied Contact Load	Actual Applied Max. Axial Stress	Actual Applied Cyclic Stress	Actual Applied Contact Stress	Recov. Def. LVDT # 1 Reading	Recov. Def. LVDT # 2 Reading	Average Recov. Def. LVDT 1 & 2	Resilient Strain	Resilient Modulus
Designation	S3	Scyclic	Pmax	Pcyclic	Pcontact	Smax	Scyclic	Scontact	H1	H2	Havg	er	Mr
Unit	kPa	kPa	N	N	N	kPa	kPa	kPa	mm	mm	mm	mm/mm	MPa
Precision	—	—	—	—	—	—	—	—	—	—	—	—	—
Sequence 1	41	13.8	54.90	50.00	4.90	14.07	12.81	1.26	0.0280	0.0240	0.0260	0.00013	102
Sequence 2	41	27.6	111.10	98.30	12.80	28.47	25.19	3.28	0.0374	0.0330	0.0352	0.00025	101
Sequence 3	41	41.3	164.32	147.22	17.10	42.11	37.73	4.38	0.0540	0.0480	0.0510	0.00036	104
Sequence 4	41	55.1	222.30	198.50	23.80	56.97	50.87	6.10	0.0690	0.0624	0.0657	0.00047	109
Sequence 5	41	68.9	279.80	251.10	28.70	71.71	64.35	7.36	0.0830	0.0752	0.0791	0.00056	115
Sequence 6	28	13.8	55.54	49.44	6.10	14.23	12.67	1.56	0.0270	0.0232	0.0251	0.00018	71
Sequence 7	28	27.6	112.18	99.98	12.20	28.75	25.62	3.13	0.0530	0.0486	0.0508	0.00036	71
Sequence 8	28	41.3	167.34	149.64	17.70	42.89	38.35	4.54	0.0718	0.0656	0.0687	0.00049	79
Sequence 9	28	55.1	221.06	198.46	22.60	56.65	50.86	5.79	0.0856	0.0790	0.0823	0.00058	87
Sequence 10	28	68.9	279.64	250.34	29.30	71.67	64.16	7.51	0.0990	0.0920	0.0955	0.00068	95
Sequence 11	14	13.8	57.04	52.14	4.90	14.62	13.36	1.26	0.0352	0.0322	0.0337	0.00024	56
Sequence 12	14	27.6	113.26	100.46	12.80	29.03	25.75	3.28	0.0672	0.0622	0.0647	0.00046	56
Sequence 13	14	41.3	166.12	149.62	16.50	42.57	38.34	4.23	0.0882	0.0818	0.0850	0.00060	64
Sequence 14	14	55.1	223.28	199.48	23.80	57.22	51.12	6.10	0.1028	0.0960	0.0994	0.00070	73
Sequence 15	14	68.9	278.30	250.20	28.10	71.32	64.12	7.20	0.1134	0.1072	0.1103	0.00075	85
* Reported results are based on the average of the last 5 cycles of each load sequence													

Table 11.8- Summary of M_r Results at Suction of 25 kPa along the Primary Wetting Curve

Column #	1	2	3	4	5	6	7	8	9	10	11	12	13
Parameter	Chamber Confining Pressure	Nominal Maximum Axial Stress	Actual Applied Max. Axial Load	Actual Applied Cyclic Load	Actual Applied Contact Load	Actual Applied Max. Axial Stress	Actual Applied Cyclic Stress	Actual Applied Contact Stress	Recov. Def. LVDT # 1 Reading	Recov. Def. LVDT # 2 Reading	Average Recov. Def. LVDT 1 & 2	Resilient Strain	Resilient Modulus
Designation	S3	Scyclic	Pmax	Pcyclic	Pcontact	Smax	Scyclic	Scontact	H1	H2	Havg	er	Mr
Unit	kPa	kPa	N	N	N	kPa	kPa	kPa	mm	mm	mm	mm/mm	MPa
Precision	—	—	—	—	—	—	—	—	—	—	—	—	—
Sequence 1	41	13.8	55.52	50.02	5.50	14.23	12.82	1.41	0.0334	0.0292	0.0313	0.00015	85
Sequence 2	41	27.6	107.76	96.16	11.60	27.62	24.64	2.97	0.0458	0.0378	0.0418	0.00030	83
Sequence 3	41	41.3	165.64	147.34	18.30	42.45	37.76	4.69	0.0660	0.0570	0.0615	0.00044	87
Sequence 4	41	55.1	222.04	198.24	23.80	56.90	50.80	6.10	0.0862	0.0746	0.0804	0.00057	89
Sequence 5	41	68.9	275.42	246.12	29.30	70.58	63.08	7.51	0.1026	0.0892	0.0959	0.00068	93
Sequence 6	28	13.8	53.58	48.08	5.50	13.73	12.32	1.41	0.0320	0.0280	0.0300	0.00021	58
Sequence 7	28	27.6	109.12	98.12	11.00	27.97	25.15	2.82	0.0638	0.0570	0.0604	0.00043	59
Sequence 8	28	41.3	167.34	150.84	16.50	42.89	38.66	4.23	0.0884	0.0806	0.0845	0.00060	65
Sequence 9	28	55.1	221.18	197.38	23.80	56.68	50.58	6.10	0.1064	0.0948	0.1006	0.00071	71
Sequence 10	28	68.9	303.18	273.88	29.30	77.70	70.19	7.51	0.1360	0.1200	0.1280	0.00091	77
Sequence 11	14	13.8	53.46	47.96	5.50	13.70	12.29	1.41	0.0414	0.0386	0.0400	0.00028	43
Sequence 12	14	27.6	111.70	100.70	11.00	28.63	25.81	2.82	0.0846	0.0780	0.0813	0.00058	45
Sequence 13	14	41.3	168.60	150.30	18.30	43.21	38.52	4.69	0.1110	0.1020	0.1065	0.00075	51
Sequence 14	14	55.1	223.16	199.96	23.20	57.19	51.25	5.95	0.1280	0.1164	0.1222	0.00087	59
Sequence 15	14	68.9	276.50	248.40	28.10	70.86	63.66	7.20	0.1448	0.1306	0.1377	0.00098	65
* Reported results are based on the average of the last 5 cycles of each load sequence													

Table 11.9- Summary of M_r Results at Suction of 25 kPa along the Secondary Drying Curve

Column #	1	2	3	4	5	6	7	8	9	10	11	12	13
Parameter	Chamber Confining Pressure	Nominal Maximum Axial Stress	Actual Applied Max. Axial Load	Actual Applied Cyclic Load	Actual Applied Contact Load	Actual Applied Max. Axial Stress	Actual Applied Cyclic Stress	Actual Applied Contact Stress	Recov. Def. LVDT # 1 Reading	Recov. Def. LVDT # 2 Reading	Average Recov. Def. LVDT 1 & 2	Resilient Strain	Resilient Modulus
Designation	S3	Scyclic	Pmax	Pcyclic	Pcontact	Smax	Scyclic	Scontact	H1	H2	Havg	er	Mr
Unit	kPa	kPa	N	N	N	kPa	kPa	kPa	mm	mm	mm	mm/mm	MPa
Precision	—	—	—	—	—	—	—	—	—	—	—	—	—
Sequence 1	41	13.8	53.10	48.20	4.90	13.61	12.35	1.26	0.0262	0.0228	0.0245	0.00017	71
Sequence 2	41	27.6	111.58	100.58	11.00	28.60	25.78	2.82	0.0520	0.0460	0.0490	0.00035	74
Sequence 3	41	41.3	196.98	179.88	17.10	50.48	46.10	4.38	0.0890	0.0784	0.0837	0.00059	78
Sequence 4	41	55.1	221.32	198.72	22.60	56.72	50.93	5.79	0.0960	0.0850	0.0905	0.00064	79
Sequence 5	41	68.9	270.40	242.30	28.10	69.30	62.10	7.20	0.1130	0.0994	0.1062	0.00075	83
Sequence 6	28	13.8	54.78	48.68	6.10	14.04	12.48	1.56	0.0376	0.0338	0.0357	0.00025	49
Sequence 7	28	27.6	110.14	99.14	11.00	28.23	25.41	2.82	0.0700	0.0634	0.0667	0.00047	54
Sequence 8	28	41.3	166.72	147.82	18.90	42.73	37.88	4.84	0.0950	0.0866	0.0908	0.00064	59
Sequence 9	28	55.1	221.82	199.22	22.60	56.85	51.06	5.79	0.1150	0.1040	0.1095	0.00078	66
Sequence 10	28	68.9	277.94	249.24	28.70	71.23	63.87	7.36	0.1330	0.1200	0.1265	0.00090	71
Sequence 11	14	13.8	55.28	50.38	4.90	14.17	12.91	1.26	0.0468	0.0436	0.0452	0.00032	40
Sequence 12	14	27.6	112.54	100.34	12.20	28.84	25.72	3.13	0.0906	0.0836	0.0871	0.00062	42
Sequence 13	14	41.3	166.24	147.94	18.30	42.60	37.91	4.69	0.1154	0.1054	0.1104	0.00078	48
Sequence 14	14	55.1	221.58	199.58	22.00	56.79	51.15	5.64	0.1330	0.1220	0.1275	0.00090	57
Sequence 15	14	68.9	273.30	244.00	29.30	70.04	62.53	7.51	0.1510	0.1372	0.1441	0.00102	61
* Reported results are based on the average of the last 5 cycles of each load sequence													

Table 11.10- Summary of M_r Results at Suction of 50 kPa along the Secondary Drying Curve

Column #	1	2	3	4	5	6	7	8	9	10	11	12	13
Parameter	Chamber Confining Pressure	Nominal Maximum Axial Stress	Actual Applied Max. Axial Load	Actual Applied Cyclic Load	Actual Applied Contact Load	Actual Applied Max. Axial Stress	Actual Applied Cyclic Stress	Actual Applied Contact Stress	Recov. Def. LVDT # 1 Reading	Recov. Def. LVDT # 2 Reading	Average Recov. Def. LVDT 1 & 2	Resilient Strain	Resilient Modulus
Designation	S3	Scyclic	Pmax	Pcyclic	Pcontact	Smax	Scyclic	Scontact	H1	H2	Havg	er	Mr
Unit	kPa	kPa	N	N	N	kPa	kPa	kPa	mm	mm	mm	mm/mm	MPa
Precision	—	—	—	—	—	—	—	—	—	—	—	—	—
Sequence 1	41	13.8	54.30	48.80	5.50	13.92	12.51	1.41	0.0204	0.0180	0.0192	0.00014	92
Sequence 2	41	27.6	111.82	99.62	12.20	28.66	25.53	3.13	0.0402	0.0352	0.0377	0.00027	96
Sequence 3	41	41.3	165.88	146.98	18.90	42.51	37.67	4.84	0.0590	0.0510	0.0550	0.00039	97
Sequence 4	41	55.1	221.92	197.52	24.40	56.87	50.62	6.25	0.0750	0.0650	0.0700	0.00050	102
Sequence 5	41	68.9	275.66	245.76	29.90	70.65	62.98	7.66	0.0890	0.0790	0.0840	0.00059	106
Sequence 6	28	13.8	53.94	48.44	5.50	13.82	12.41	1.41	0.0282	0.0270	0.0276	0.00020	64
Sequence 7	28	27.6	115.24	103.04	12.20	29.53	26.41	3.13	0.0558	0.0500	0.0529	0.00037	70
Sequence 8	28	41.3	169.44	152.94	16.50	43.42	39.20	4.23	0.0732	0.0652	0.0692	0.00049	80
Sequence 9	28	55.1	223.04	200.44	22.60	57.16	51.37	5.79	0.0890	0.0800	0.0845	0.00060	86
Sequence 10	28	68.9	277.58	249.48	28.10	71.14	63.94	7.20	0.1030	0.0920	0.0975	0.00069	93
Sequence 11	14	13.8	55.80	48.50	7.30	14.30	12.43	1.87	0.0340	0.0318	0.0329	0.00023	53
Sequence 12	14	27.6	112.42	100.22	12.20	28.81	25.68	3.13	0.0668	0.0606	0.0637	0.00045	57
Sequence 13	14	41.3	167.10	148.80	18.30	42.82	38.13	4.69	0.0874	0.0802	0.0838	0.00059	64
Sequence 14	14	55.1	224.48	201.28	23.20	57.53	51.58	5.95	0.1030	0.0938	0.0984	0.00070	74
Sequence 15	14	68.9	275.66	247.56	28.10	70.65	63.44	7.20	0.1144	0.1042	0.1093	0.00077	82
* Reported results are based on the average of the last 5 cycles of each load sequence													

Table 11.11- Summary of M_r Results at Suction of 100 kPa along the Secondary Drying Curve

Column #	1	2	3	4	5	6	7	8	9	10	11	12	13
Parameter	Chamber Confining Pressure	Nominal Maximum Axial Stress	Actual Applied Max. Axial Load	Actual Applied Cyclic Load	Actual Applied Contact Load	Actual Applied Max. Axial Stress	Actual Applied Cyclic Stress	Actual Applied Contact Stress	Recov. Def. LVDT # 1 Reading	Recov. Def. LVDT # 2 Reading	Average Recov. Def. LVDT 1 & 2	Resilient Strain	Resilient Modulus
Designation	S3	Scyclic	Pmax	Pcyclic	Pcontact	Smax	Scyclic	Scontact	H1	H2	Havg	er	Mr
Unit	kPa	kPa	N	N	N	kPa	kPa	kPa	mm	mm	mm	mm/mm	MPa
Precision	—	—	—	—	—	—	—	—	—	—	—	—	—
Sequence 1	41	13.8	55.90	49.80	6.10	14.33	12.76	1.56	0.0494	0.0394	0.0444	0.00010	125
Sequence 2	41	27.6	111.70	100.10	11.60	28.63	25.65	2.97	0.0320	0.0262	0.0291	0.00021	124
Sequence 3	41	41.3	164.44	146.74	17.70	42.14	37.61	4.54	0.0460	0.0380	0.0420	0.00030	126
Sequence 4	41	55.1	222.20	199.00	23.20	56.95	51.00	5.95	0.0600	0.0490	0.0545	0.00039	132
Sequence 5	41	68.9	280.42	252.32	28.10	71.87	64.66	7.20	0.0730	0.0600	0.0665	0.00047	137
Sequence 6	28	13.8	56.04	51.14	4.90	14.36	13.11	1.26	0.0198	0.0170	0.0184	0.00013	101
Sequence 7	28	27.6	111.70	99.50	12.20	28.63	25.50	3.13	0.0400	0.0344	0.0372	0.00026	97
Sequence 8	28	41.3	169.70	152.60	17.10	43.49	39.11	4.38	0.0580	0.0486	0.0533	0.00038	104
Sequence 9	28	55.1	226.30	201.90	24.40	58.00	51.74	6.25	0.0720	0.0608	0.0664	0.00047	110
Sequence 10	28	68.9	281.28	251.98	29.30	72.09	64.58	7.51	0.0830	0.0696	0.0763	0.00054	120
Sequence 11	14	13.8	52.98	47.48	5.50	13.58	12.17	1.41	0.0240	0.0200	0.0220	0.00016	78
Sequence 12	14	27.6	112.66	100.46	12.20	28.87	25.75	3.13	0.0500	0.0440	0.0470	0.00033	77
Sequence 13	14	41.3	168.60	151.50	17.10	43.21	38.83	4.38	0.0710	0.0600	0.0655	0.00046	84
Sequence 14	14	55.1	222.80	200.20	22.60	57.10	51.31	5.79	0.0842	0.0714	0.0778	0.00055	93
Sequence 15	14	68.9	277.34	249.24	28.10	71.08	63.87	7.20	0.0954	0.0802	0.0878	0.00062	103
* Reported results are based on the average of the last 5 cycles of each load sequence													

Table 11.12- Summary of M_r Results at Suction of 75 kPa along the Secondary Wetting Curve

Column #	1	2	3	4	5	6	7	8	9	10	11	12	13
Parameter	Chamber Confining Pressure	Nominal Maximum Axial Stress	Actual Applied Max. Axial Load	Actual Applied Cyclic Load	Actual Applied Contact Load	Actual Applied Max. Axial Stress	Actual Applied Cyclic Stress	Actual Applied Contact Stress	Recov. Def. LVDT # 1 Reading	Recov. Def. LVDT # 2 Reading	Average Recov. Def. LVDT 1 & 2	Resilient Strain	Resilient Modulus
Designation	S3	Scyclic	Pmax	Pcyclic	Pcontact	Smax	Scyclic	Scontact	H1	H2	Havg	er	Mr
Unit	kPa	kPa	N	N	N	kPa	kPa	kPa	mm	mm	mm	mm/mm	MPa
Precision	—	—	—	—	—	—	—	—	—	—	—	—	—
Sequence 1	41	13.8	56.30	49.60	6.70	14.43	12.71	1.72	0.0252	0.0230	0.0241	0.00011	120
Sequence 2	41	27.6	111.58	98.78	12.80	28.60	25.32	3.28	0.0328	0.0280	0.0304	0.00022	118
Sequence 3	41	41.3	164.68	145.78	18.90	42.20	37.36	4.84	0.0464	0.0402	0.0433	0.00031	122
Sequence 4	41	55.1	219.34	195.54	23.80	56.21	50.11	6.10	0.0598	0.0510	0.0554	0.00039	128
Sequence 5	41	68.9	271.12	241.82	29.30	69.48	61.97	7.51	0.0708	0.0610	0.0659	0.00047	133
Sequence 6	28	13.8	54.66	47.96	6.70	14.01	12.29	1.72	0.0220	0.0200	0.0210	0.00015	83
Sequence 7	28	27.6	107.52	96.52	11.00	27.56	24.74	2.82	0.0420	0.0370	0.0395	0.00028	88
Sequence 8	28	41.3	163.60	145.30	18.30	41.93	37.24	4.69	0.0594	0.0520	0.0557	0.00039	94
Sequence 9	28	55.1	218.26	195.66	22.60	55.94	50.14	5.79	0.0726	0.0636	0.0681	0.00048	104
Sequence 10	28	68.9	269.68	240.98	28.70	69.11	61.76	7.36	0.0826	0.0718	0.0772	0.00055	113
Sequence 11	14	13.8	53.58	48.08	5.50	13.73	12.32	1.41	0.0262	0.0240	0.0251	0.00018	69
Sequence 12	14	27.6	108.50	98.10	10.40	27.81	25.14	2.67	0.0540	0.0490	0.0515	0.00036	69
Sequence 13	14	41.3	164.68	146.38	18.30	42.20	37.51	4.69	0.0726	0.0660	0.0693	0.00049	76
Sequence 14	14	55.1	218.38	195.18	23.20	55.97	50.02	5.95	0.0858	0.0764	0.0811	0.00057	87
Sequence 15	14	68.9	270.88	241.58	29.30	69.42	61.91	7.51	0.0958	0.0842	0.0900	0.00064	97
* Reported results are based on the average of the last 5 cycles of each load sequence													

Table 11.13- Summary of M_r Results at Suction of 50 kPa along the Secondary Wetting Curve

Column #	1	2	3	4	5	6	7	8	9	10	11	12	13
Parameter	Chamber Confining Pressure	Nominal Maximum Axial Stress	Actual Applied Max. Axial Load	Actual Applied Cyclic Load	Actual Applied Contact Load	Actual Applied Max. Axial Stress	Actual Applied Cyclic Stress	Actual Applied Contact Stress	Recov. Def. LVDT # 1 Reading	Recov. Def. LVDT # 2 Reading	Average Recov. Def. LVDT 1 & 2	Resilient Strain	Resilient Modulus
Designation	S3	Scyclic	Pmax	Pcyclic	Pcontact	Smax	Scyclic	Scontact	H1	H2	Havg	er	Mr
Unit	kPa	kPa	N	N	N	kPa	kPa	kPa	mm	mm	mm	mm/mm	MPa
Precision	—	—	—	—	—	—	—	—	—	—	—	—	—
Sequence 1	41	13.8	47.74	41.64	6.10	12.23	10.67	1.56	0.0220	0.0182	0.0201	0.00010	103
Sequence 2	41	27.6	110.62	97.82	12.80	28.35	25.07	3.28	0.0368	0.0314	0.0341	0.00024	104
Sequence 3	41	41.3	161.86	144.76	17.10	41.48	37.10	4.38	0.0520	0.0440	0.0480	0.00034	109
Sequence 4	41	55.1	218.02	194.22	23.80	55.87	49.77	6.10	0.0660	0.0568	0.0614	0.00043	114
Sequence 5	41	68.9	270.64	241.34	29.30	69.36	61.85	7.51	0.0770	0.0660	0.0715	0.00051	122
Sequence 6	28	13.8	53.10	47.00	6.10	13.61	12.05	1.56	0.0250	0.0208	0.0229	0.00016	74
Sequence 7	28	27.6	106.56	94.96	11.60	27.31	24.34	2.97	0.0492	0.0426	0.0459	0.00033	75
Sequence 8	28	41.3	161.48	144.38	17.10	41.38	37.00	4.38	0.0680	0.0580	0.0630	0.00045	83
Sequence 9	28	55.1	214.24	193.44	20.80	54.91	49.57	5.33	0.0832	0.0724	0.0778	0.00055	90
Sequence 10	28	68.9	268.04	239.94	28.10	68.69	61.49	7.20	0.0908	0.0792	0.0850	0.00060	102
Sequence 11	14	13.8	53.22	47.72	5.50	13.64	12.23	1.41	0.0310	0.0276	0.0293	0.00021	59
Sequence 12	14	27.6	109.66	99.26	10.40	28.10	25.44	2.67	0.0626	0.0562	0.0594	0.00042	60
Sequence 13	14	41.3	161.70	145.20	16.50	41.44	37.21	4.23	0.0828	0.0744	0.0786	0.00056	67
Sequence 14	14	55.1	217.18	193.38	23.80	55.66	49.56	6.10	0.0960	0.0844	0.0902	0.00064	78
Sequence 15	14	68.9	268.84	241.34	27.50	68.90	61.85	7.05	0.1050	0.0938	0.0994	0.00070	88
* Reported results are based on the average of the last 5 cycles of each load sequence													

Table 11.14- Summary of M_r Results at Suction of 25 kPa along the Secondary Wetting Curve

Column #	1	2	3	4	5	6	7	8	9	10	11	12	13
Parameter	Chamber Confining Pressure	Nominal Maximum Axial Stress	Actual Applied Max. Axial Load	Actual Applied Cyclic Load	Actual Applied Contact Load	Actual Applied Max. Axial Stress	Actual Applied Cyclic Stress	Actual Applied Contact Stress	Recov. Def. LVDT # 1 Reading	Recov. Def. LVDT # 2 Reading	Average Recov. Def. LVDT 1 & 2	Resilient Strain	Resilient Modulus
Designation	S3	Scyclic	Pmax	Pcyclic	Pcontact	Smax	Scyclic	Scontact	H1	H2	Havg	er	Mr
Unit	kPa	kPa	N	N	N	kPa	kPa	kPa	mm	mm	mm	mm/mm	MPa
Precision	—	—	—	—	—	—	—	—	—	—	—	—	—
Sequence 1	41	13.8	53.58	46.88	6.70	13.73	12.01	1.72	0.0414	0.0348	0.0381	0.00014	84
Sequence 2	41	27.6	111.22	98.42	12.80	28.50	25.22	3.28	0.0446	0.0386	0.0416	0.00029	86
Sequence 3	41	41.3	162.76	145.06	17.70	41.71	37.18	4.54	0.0600	0.0520	0.0560	0.00040	94
Sequence 4	41	55.1	216.70	192.90	23.80	55.54	49.44	6.10	0.0750	0.0640	0.0695	0.00049	100
Sequence 5	41	68.9	273.92	244.62	29.30	70.20	62.69	7.51	0.0890	0.0768	0.0829	0.00059	107
Sequence 6	28	13.8	54.06	48.56	5.50	13.85	12.44	1.41	0.0302	0.0262	0.0282	0.00020	62
Sequence 7	28	27.6	107.64	96.04	11.60	27.59	24.61	2.97	0.0580	0.0518	0.0549	0.00039	63
Sequence 8	28	41.3	162.72	145.02	17.70	41.70	37.17	4.54	0.0784	0.0684	0.0734	0.00052	71
Sequence 9	28	55.1	214.60	192.60	22.00	55.00	49.36	5.64	0.0920	0.0800	0.0860	0.00061	81
Sequence 10	28	68.9	271.12	242.42	28.70	69.48	62.13	7.36	0.1048	0.0920	0.0984	0.00070	89
Sequence 11	14	13.8	54.18	48.08	6.10	13.89	12.32	1.56	0.0384	0.0346	0.0365	0.00026	48
Sequence 12	14	27.6	110.14	97.94	12.20	28.23	25.10	3.13	0.0742	0.0680	0.0711	0.00050	50
Sequence 13	14	41.3	161.36	144.86	16.50	41.35	37.12	4.23	0.0952	0.0858	0.0905	0.00064	58
Sequence 14	14	55.1	221.18	197.98	23.20	56.68	50.74	5.95	0.1104	0.0982	0.1043	0.00074	69
Sequence 15	14	68.9	268.44	238.54	29.90	68.80	61.13	7.66	0.1200	0.1068	0.1134	0.00087	70
* Reported results are based on the average of the last 5 cycles of each load sequence													

11.2 Test Results Summary for Virgin Samples without Previous M_r Testing

Table 11.15- Summary of M_r Results at Suction of 50 kPa along the Primary Drying Curve (without Previous M_r Testing)

Column #	1	2	3	4	5	6	7	8	9	10	11	12	13
Parameter	Chamber Confining Pressure	Nominal Maximum Axial Stress	Actual Applied Max. Axial Load	Actual Applied Cyclic Load	Actual Applied Contact Load	Actual Applied Max. Axial Stress	Actual Applied Cyclic Stress	Actual Applied Contact Stress	Recov. Def. LVDT # 1 Reading	Recov. Def. LVDT # 2 Reading	Average Recov. Def. LVDT 1 & 2	Resilient Strain	Resilient Modulus
Designation	S3	Scyclic	Pmax	Pcyclic	Pcontact	Smax	Scyclic	Scontact	H1	H2	Havg	er	Mr
Unit	kPa	kPa	N	N	N	kPa	kPa	kPa	mm	mm	mm	mm/mm	MPa
Precision	—	—	—	—	—	—	—	—	—	—	—	—	—
Sequence 1	41	13.8	51.54	46.04	5.50	13.21	11.80	1.41	0.0294	0.0264	0.0279	0.00020	60
Sequence 2	41	27.6	108.36	96.16	12.20	27.77	24.64	3.13	0.0570	0.0500	0.0535	0.00038	65
Sequence 3	41	41.3	163.84	146.74	17.10	41.99	37.61	4.38	0.0850	0.0752	0.0801	0.00057	66
Sequence 4	41	55.1	216.46	192.66	23.80	55.47	49.37	6.10	0.1128	0.1014	0.1071	0.00076	65
Sequence 5	41	68.9	270.64	242.54	28.10	69.36	62.16	7.20	0.1404	0.1284	0.1344	0.00095	65
Sequence 6	28	13.8	54.78	48.08	6.70	14.04	12.32	1.72	0.0354	0.0322	0.0338	0.00024	51
Sequence 7	28	27.6	108.50	97.50	11.00	27.81	24.99	2.82	0.0722	0.0660	0.0691	0.00049	51
Sequence 8	28	41.3	163.82	145.52	18.30	41.98	37.29	4.69	0.1028	0.0946	0.0987	0.00070	53
Sequence 9	28	55.1	220.46	197.26	23.20	56.50	50.55	5.95	0.1300	0.1204	0.1252	0.00089	57
Sequence 10	28	68.9	269.68	240.98	28.70	69.11	61.76	7.36	0.1546	0.1448	0.1497	0.00106	58
Sequence 11	14	13.8	52.98	47.48	5.50	13.58	12.17	1.41	0.0406	0.0388	0.0397	0.00028	43
Sequence 12	14	27.6	109.38	98.98	10.40	28.03	25.37	2.67	0.0844	0.0800	0.0822	0.00058	44
Sequence 13	14	41.3	163.96	146.26	17.70	42.02	37.48	4.54	0.1166	0.1094	0.1130	0.00080	47
Sequence 14	14	55.1	219.58	196.98	22.60	56.27	50.48	5.79	0.1432	0.1354	0.1393	0.00099	51
Sequence 15	14	68.9	269.92	241.82	28.10	69.17	61.97	7.20	0.1720	0.1638	0.1679	0.00119	52
* Reported results are based on the average of the last 5 cycles of each load sequence													

Table 11.16- Summary of M_r Results at Suction of 50 kPa along the Primary Wetting Curve (without Previous M_r Testing)

Column #	1	2	3	4	5	6	7	8	9	10	11	12	13
Parameter	Chamber Confining Pressure	Nominal Maximum Axial Stress	Actual Applied Max. Axial Load	Actual Applied Cyclic Load	Actual Applied Contact Load	Actual Applied Max. Axial Stress	Actual Applied Cyclic Stress	Actual Applied Contact Stress	Recov. Def. LVDT # 1 Reading	Recov. Def. LVDT # 2 Reading	Average Recov. Def. LVDT 1 & 2	Resilient Strain	Resilient Modulus
Designation	S3	Scyclic	Pmax	Pcyclic	Pcontact	Smax	Scyclic	Scontact	H1	H2	Havg	er	Mr
Unit	kPa	kPa	N	N	N	kPa	kPa	kPa	mm	mm	mm	mm/mm	MPa
Precision	—	—	—	—	—	—	—	—	—	—	—	—	—
Sequence 1	41	13.8	54.30	48.20	6.10	13.92	12.35	1.56	0.0210	0.0200	0.0205	0.00015	85
Sequence 2	41	27.6	107.28	95.68	11.60	27.49	24.52	2.97	0.0400	0.0394	0.0397	0.00027	90
Sequence 3	41	41.3	161.36	144.26	17.10	41.35	36.97	4.38	0.0590	0.0570	0.0580	0.00041	90
Sequence 4	41	55.1	218.62	194.82	23.80	56.03	49.93	6.10	0.0804	0.0770	0.0787	0.00056	90
Sequence 5	41	68.9	271.60	242.90	28.70	69.61	62.25	7.36	0.1010	0.0954	0.0982	0.00070	90
Sequence 6	28	13.8	55.02	48.32	6.70	14.10	12.38	1.72	0.0250	0.0246	0.0248	0.00018	71
Sequence 7	28	27.6	108.36	96.16	12.20	27.77	24.64	3.13	0.0518	0.0508	0.0513	0.00036	68
Sequence 8	28	41.3	162.64	145.54	17.10	41.68	37.30	4.38	0.0754	0.0722	0.0738	0.00052	71
Sequence 9	28	55.1	213.96	191.36	22.60	54.83	49.04	5.79	0.0930	0.0890	0.0910	0.00064	76
Sequence 10	28	68.9	272.44	243.74	28.70	69.82	62.47	7.36	0.1140	0.1078	0.1109	0.00079	80
Sequence 11	14	13.8	54.30	48.20	6.10	13.92	12.35	1.56	0.0310	0.0304	0.0307	0.00022	57
Sequence 12	14	27.6	106.92	94.72	12.20	27.40	24.27	3.13	0.0624	0.0602	0.0613	0.00043	56
Sequence 13	14	41.3	163.96	146.26	17.70	42.02	37.48	4.54	0.0872	0.0838	0.0855	0.00061	62
Sequence 14	14	55.1	216.70	194.10	22.60	55.54	49.74	5.79	0.1052	0.1010	0.1031	0.00073	68
Sequence 15	14	68.9	271.48	244.58	26.90	69.57	62.68	6.89	0.1258	0.1194	0.1226	0.00087	72
* Reported results are based on the average of the last 5 cycles of each load sequence													

Table 11.17- Summary of M_r Results at Suction of 25 kPa along the Primary Wetting Curve (without Previous M_r Testing)

Column #	1	2	3	4	5	6	7	8	9	10	11	12	13
Parameter	Chamber Confining Pressure	Nominal Maximum Axial Stress	Actual Applied Max. Axial Load	Actual Applied Cyclic Load	Actual Applied Contact Load	Actual Applied Max. Axial Stress	Actual Applied Cyclic Stress	Actual Applied Contact Stress	Recov. Def. LVDT # 1 Reading	Recov. Def. LVDT # 2 Reading	Average Recov. Def. LVDT 1 & 2	Resilient Strain	Resilient Modulus
Designation	S3	Scyclic	Pmax	Pcyclic	Pcontact	Smax	Scyclic	Scontact	H1	H2	Havg	er	Mr
Unit	kPa	kPa	N	N	N	kPa	kPa	kPa	mm	mm	mm	mm/mm	MPa
Precision	—	—	—	—	—	—	—	—	—	—	—	—	—
Sequence 1	41	13.8	55.04	48.94	6.10	14.11	12.54	1.56	0.0280	0.0258	0.0269	0.00019	66
Sequence 2	41	27.6	110.98	98.78	12.20	28.44	25.32	3.13	0.0510	0.0480	0.0495	0.00035	72
Sequence 3	41	41.3	163.48	145.18	18.30	41.90	37.21	4.69	0.0764	0.0710	0.0737	0.00052	71
Sequence 4	41	55.1	215.72	192.52	23.20	55.28	49.34	5.95	0.1044	0.0980	0.1012	0.00072	69
Sequence 5	41	68.9	269.80	240.50	29.30	69.14	61.64	7.51	0.1362	0.1292	0.1327	0.00094	66
Sequence 6	28	13.8	53.46	47.96	5.50	13.70	12.29	1.41	0.0352	0.0326	0.0339	0.00024	51
Sequence 7	28	27.6	108.24	97.24	11.00	27.74	24.92	2.82	0.0718	0.0690	0.0704	0.00050	50
Sequence 8	28	41.3	163.12	146.02	17.10	41.80	37.42	4.38	0.1032	0.0998	0.1015	0.00072	52
Sequence 9	28	55.1	218.02	195.42	22.60	55.87	50.08	5.79	0.1290	0.1246	0.1268	0.00090	56
Sequence 10	28	68.9	272.08	244.58	27.50	69.73	62.68	7.05	0.1568	0.1508	0.1538	0.00109	58
Sequence 11	14	13.8	53.34	48.44	4.90	13.67	12.41	1.26	0.0440	0.0424	0.0432	0.00031	41
Sequence 12	14	27.6	108.12	95.92	12.20	27.71	24.58	3.13	0.0888	0.0854	0.0871	0.00062	40
Sequence 13	14	41.3	164.92	148.42	16.50	42.27	38.04	4.23	0.1200	0.1170	0.1185	0.00084	45
Sequence 14	14	55.1	220.56	197.36	23.20	56.52	50.58	5.95	0.1490	0.1436	0.1463	0.00104	49
Sequence 15	14	68.9	275.30	247.80	27.50	70.55	63.51	7.05	0.1830	0.1764	0.1797	0.00127	50
* Reported results are based on the average of the last 5 cycles of each load sequence													